On the interplay among non-covalent interactions and activity of 4-aminoquinoline antimalarials: A crystallographic and spectroscopic study

***Leonardo Lo Presti*, Silvia Rizzato, Pietro Sacchi, Giovanni Macetti, Laura Loconte, Fabio Beghi, Lucia Silvestrini**

leonardo.lopresti@unimi.it

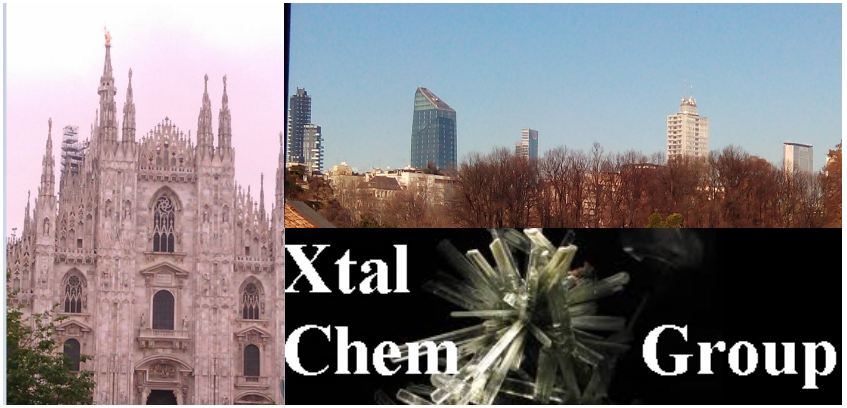

Malaria

Malaria is probably the topmost parasitic disease, with thousands of deaths per year, especially in undeveloped tropical countries

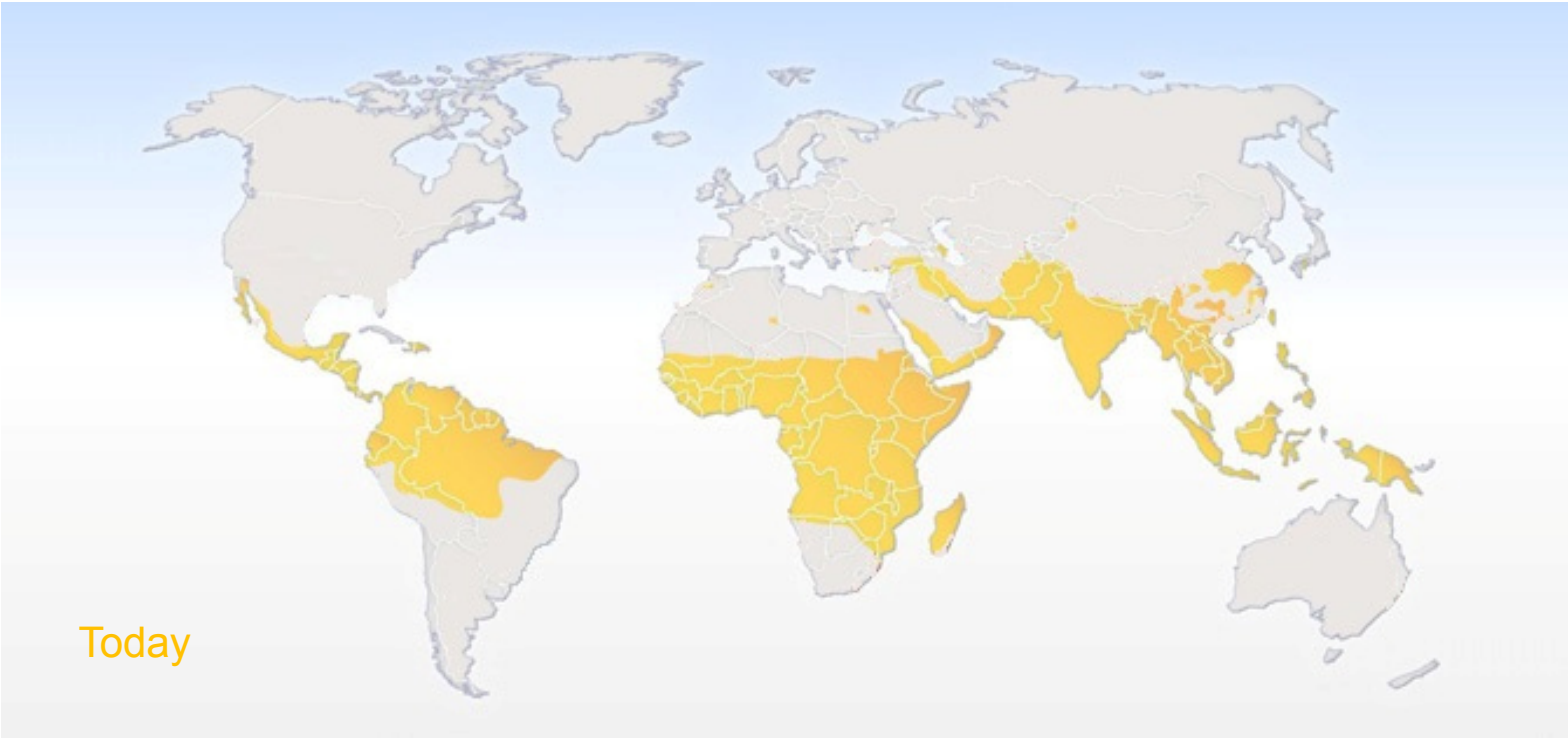

Yellow: regions of endemic disease

Malaria

Malaria is probably the topmost parasitic disease, with thousands of deaths per year, especially in undeveloped tropical countries

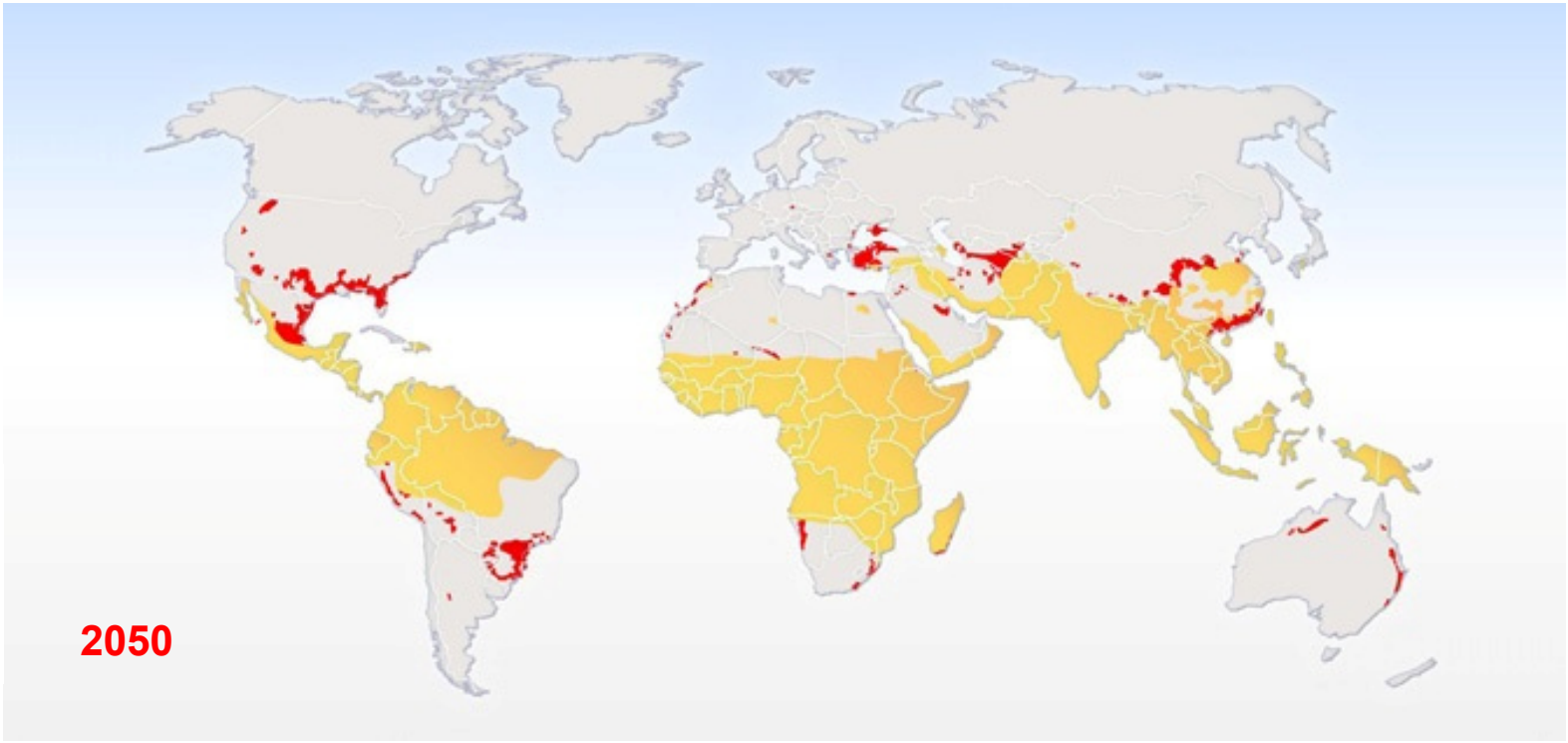

Siraj *et al*. *Science*, **2014**, *343*, 1154
Rogers, *Science*, **2000**, *289*,1763

Global warming is expected to increase the malaria spreading throughout temperate climates

Malaria

Malaria is probably the topmost parasitic disease, with thousands of deaths per year, especially in undeveloped tropical countries

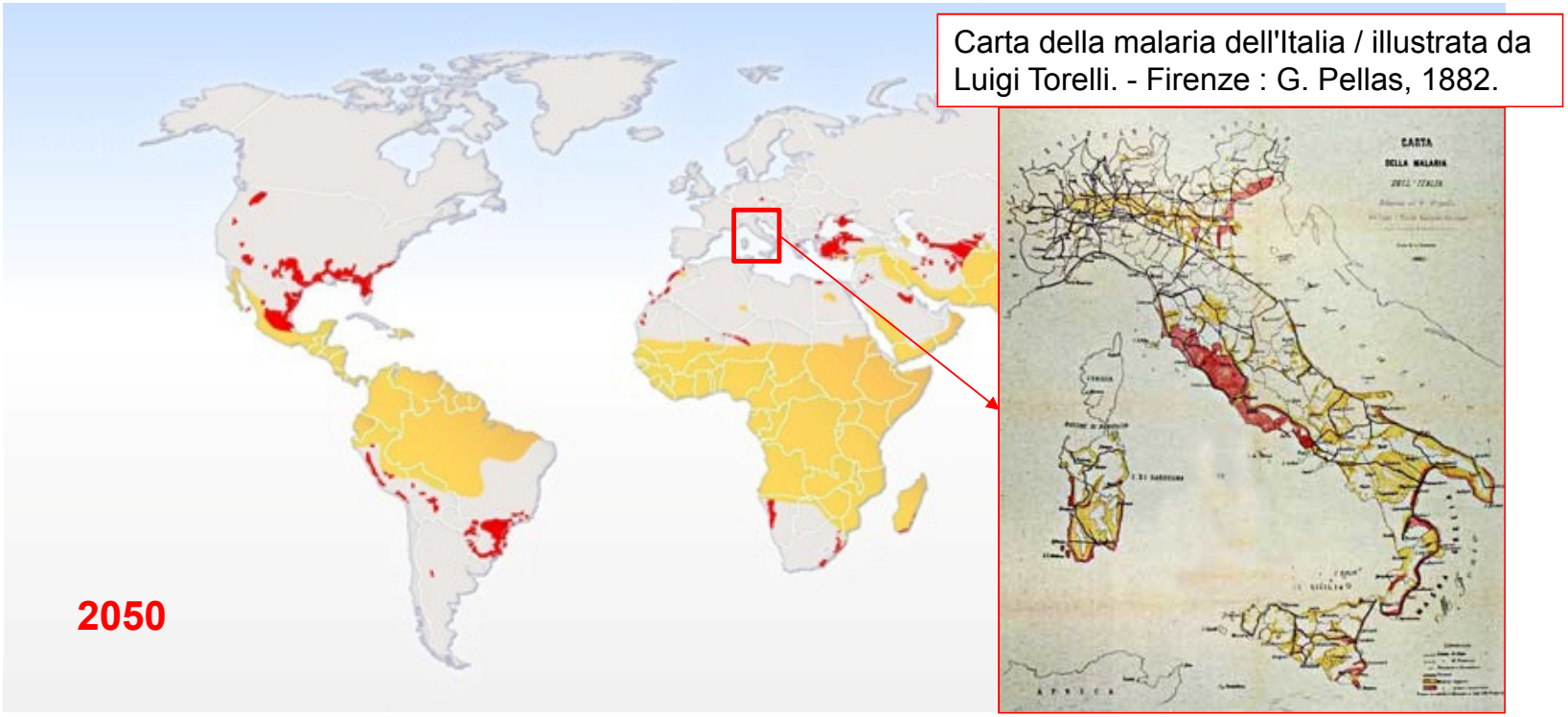

Siraj *et al*. *Science*, **2014**, *343*, 1154
Rogers, *Science*, **2000**, *289*,1763

Global warming is expected to increase the malaria spreading throughout temperate climates

Plasmodium life cycle

P. falciparum, gametocyte form,
electron micrograph
~ 4 μm in length

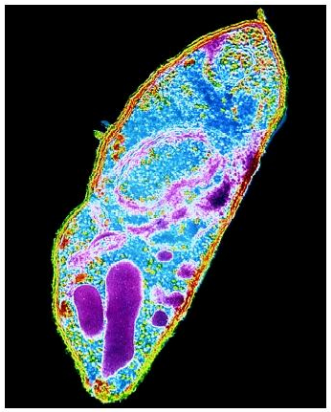

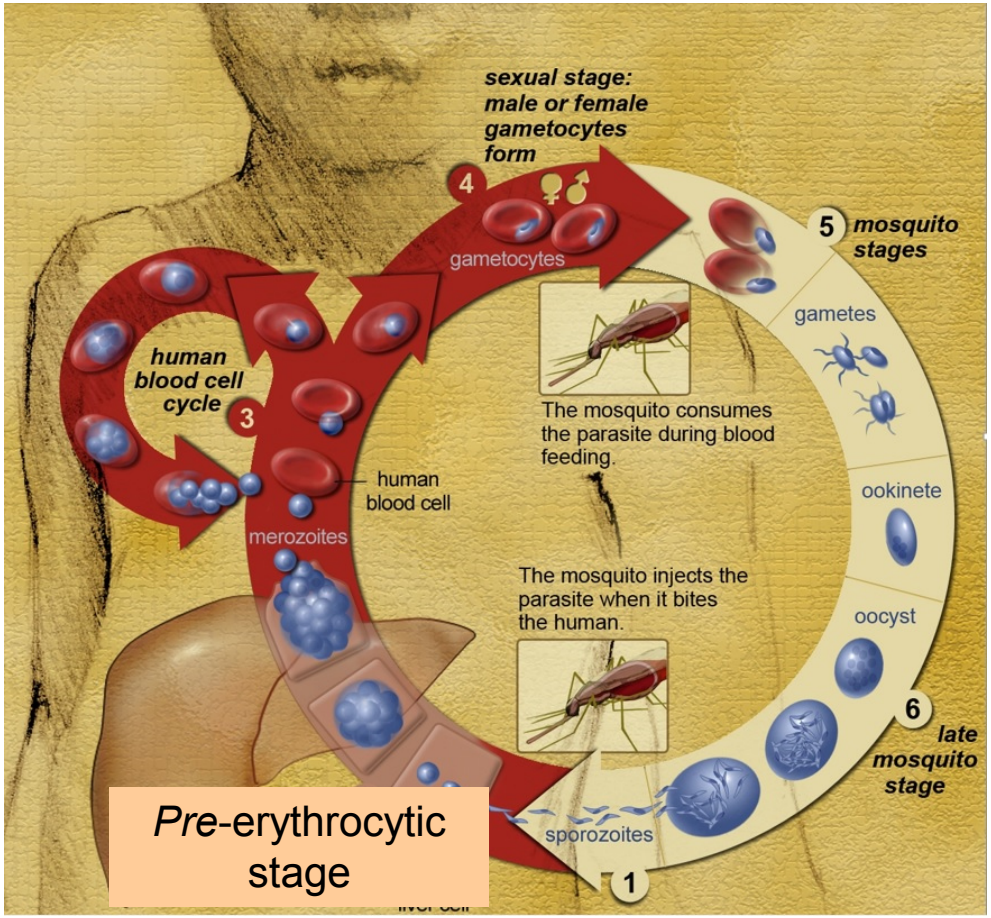

CDC
http://www.cdc.gov/malaria/

Plasmodium life cycle

P. falciparum, gametocyte form,
electron micrograph
~ 4 μm in length

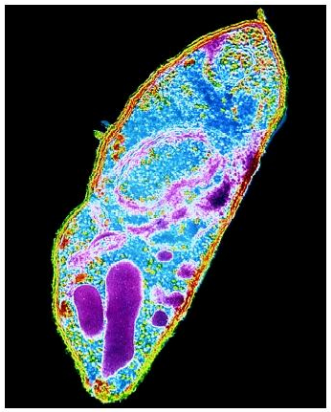

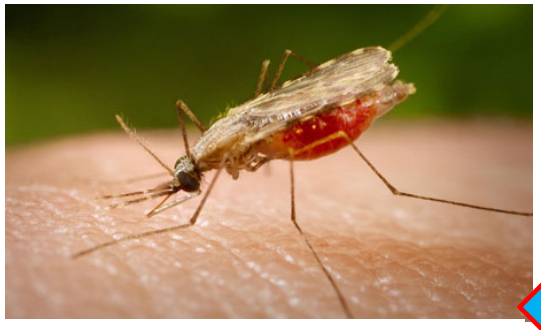

Anopheles mosquito

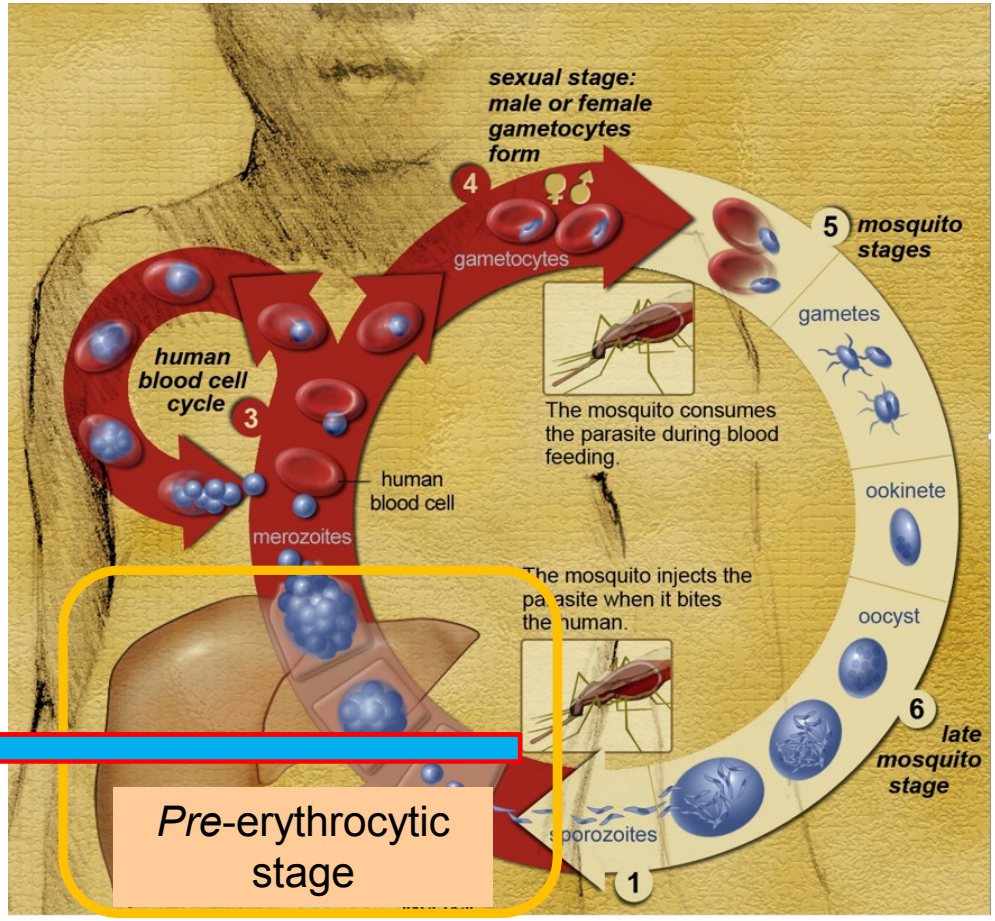

CDC
http://www.cdc.gov/malaria/

Plasmodium life cycle

P. falciparum, gametocyte form, electron micrograph ~ 4 μm in length

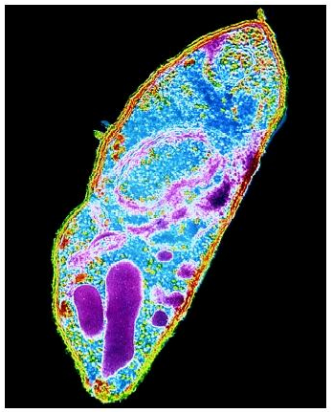

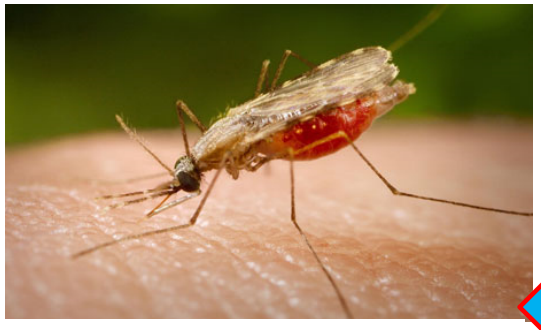

Anopheles mosquito

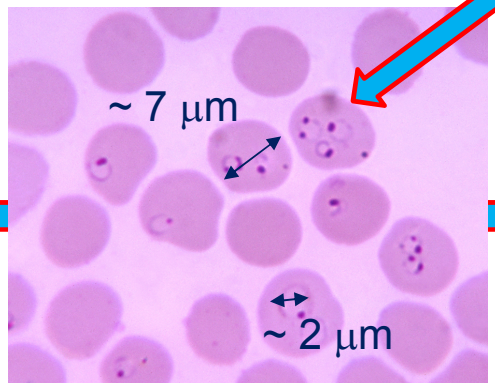

P. falciparum, ring form in infected red blood cells

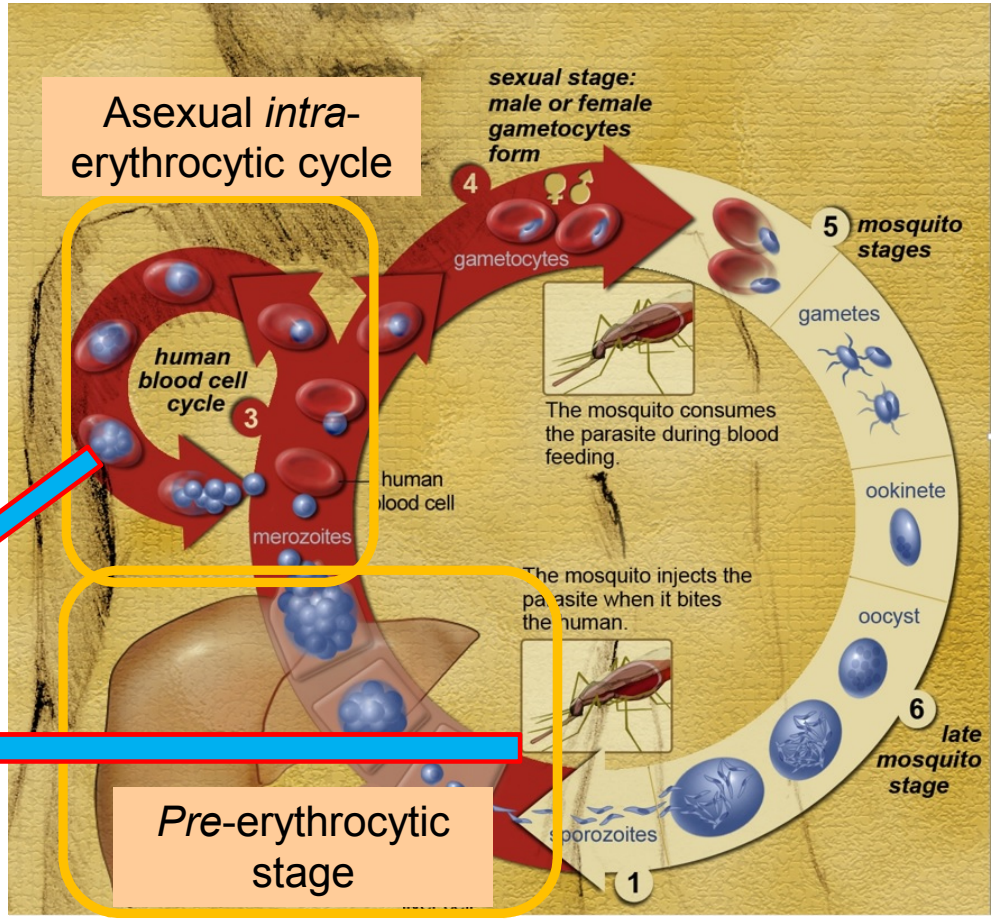

CDC
http://www.cdc.gov/malaria/

Parasite metabolism: Hb digestion

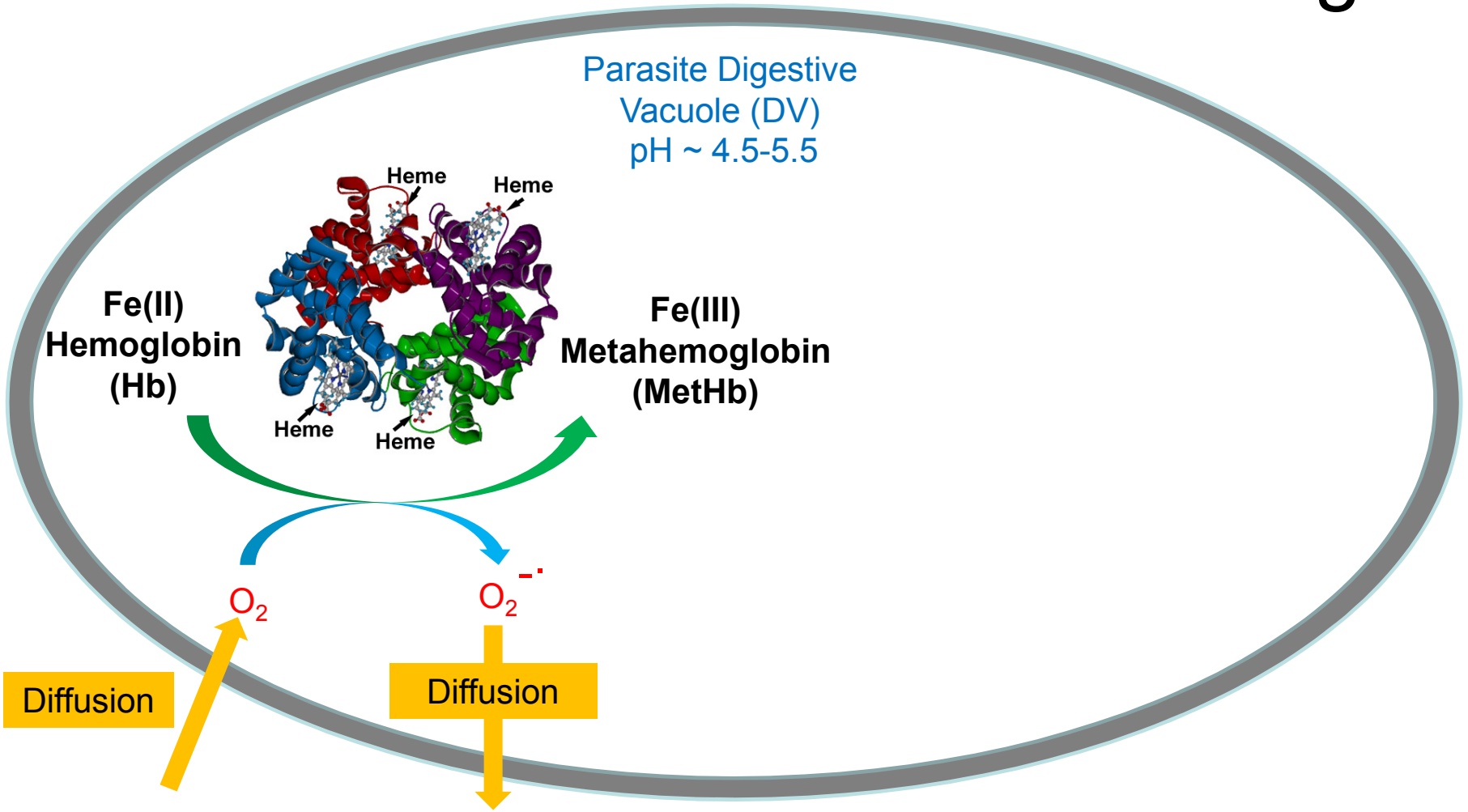

Parasite metabolism: Hb digestion

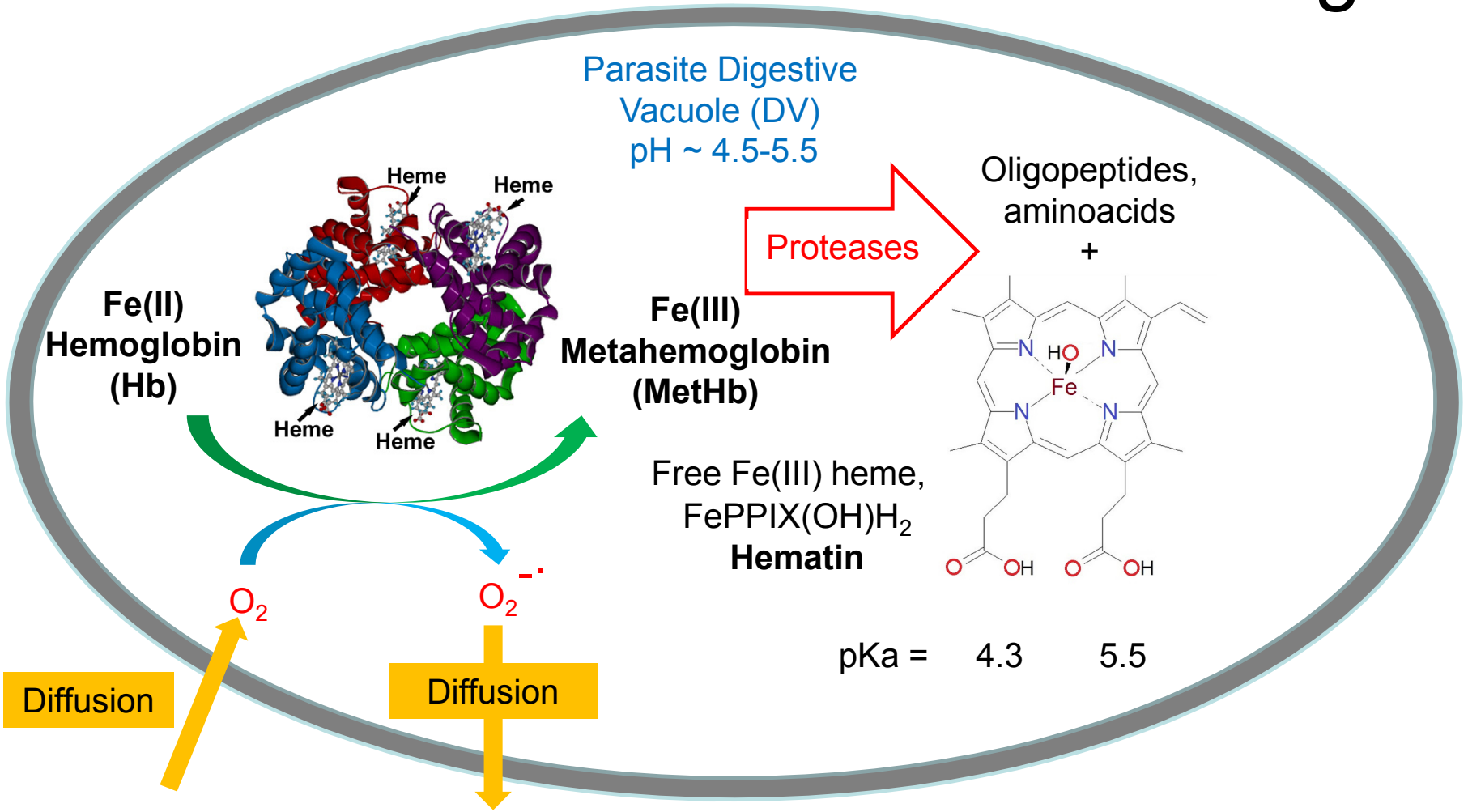

Parasite metabolism: Hb digestion

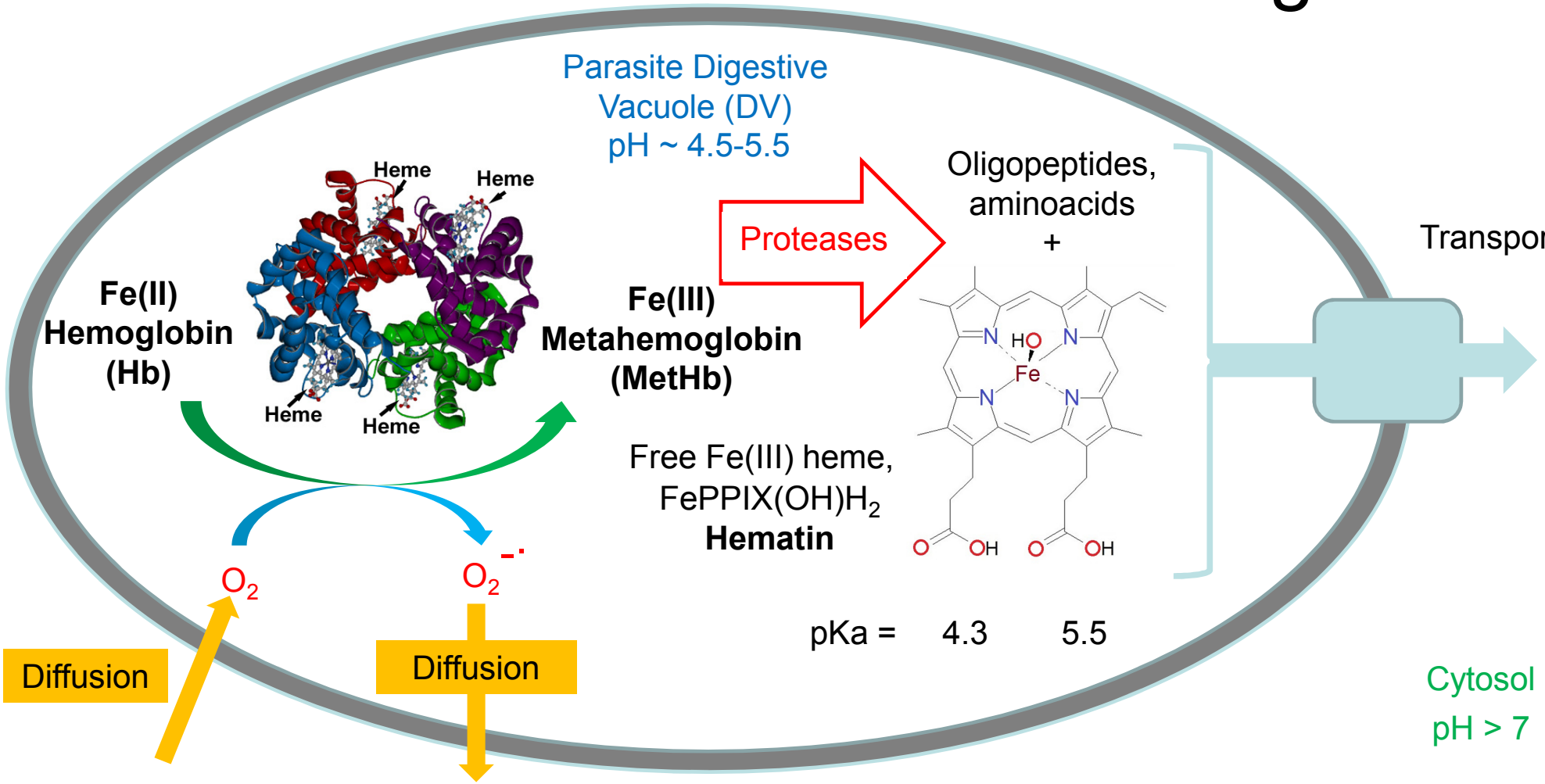

Possible weaknesses?

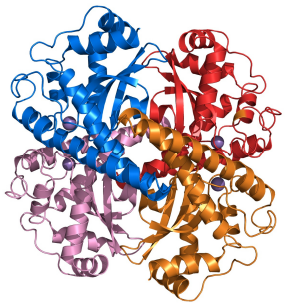

Superoxide dismutase

Fenton cycle

$O_2^{-\cdot}$

O_2 Harmless

H_2O_2

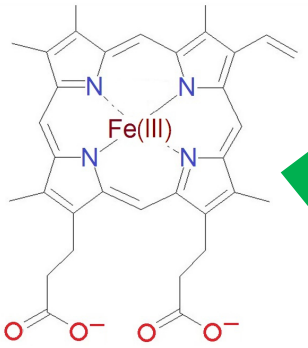

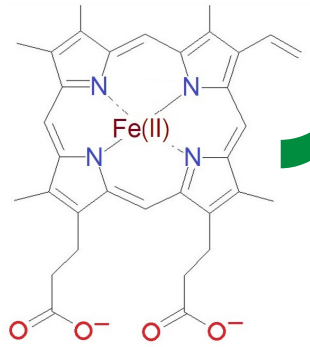

Harmless

$\cdot OH + OH^-$

H_2O_2

Potential cause of cellular oxidative stress

Cytosol

pH > 7

Muller Mol. Microbiol., **2004**, *53*, 1291

Heme detoxification

Parasite Digestive Vacuole (DV)

pH ~ 4.5-5.5

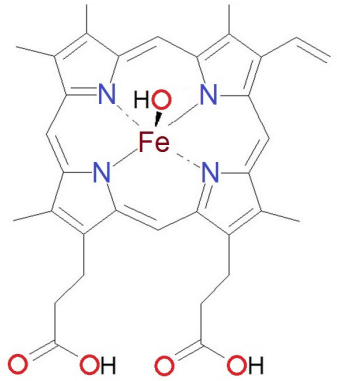

$FePPIX(OH)H_2$

Cytosol

pH > 7

Pagola *et al. Nature*, **2000**, *404*, 307

Heme detoxification

Parasite Digestive Vacuole (DV)

pH ~ 4.5-5.5

2 H_2O

2 x

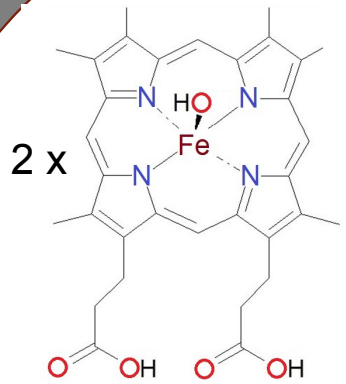

FePPIX(OH)H_2

Dimerization

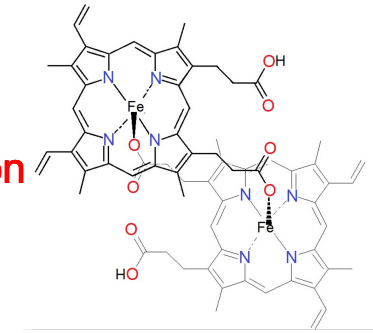

FePPIX(FePPIXH)H

Cytosol

pH > 7

Pagola *et al. Nature*, **2000**, *404*, 307

Heme detoxificati

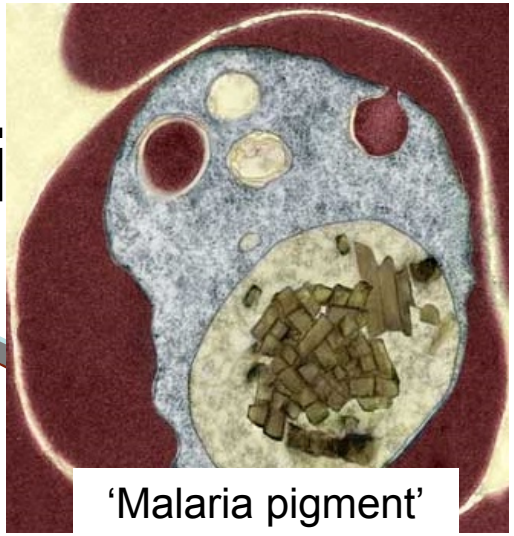

'Malaria pigment'

Parasite Digestive Vacuole (DV)

pH ~ 4.5-5.5

2 H_2O

2 x

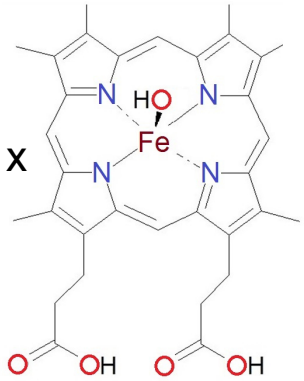

FePPIX(OH)H_2

Dimerization

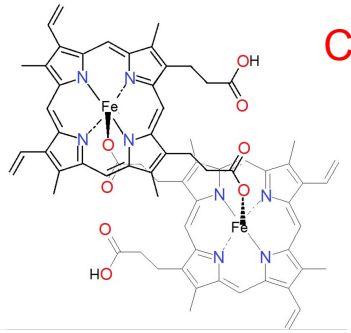

FePPIX(FePPIXH)H

Crystallization

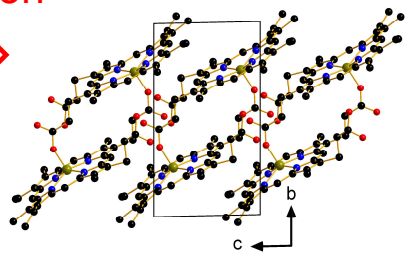

Hemozoin (natural)

β-Hematin (synthetic)

P $\bar{1}$

Lipidic nanodroplets

Cytosol

pH > 7

Pagola *et al. Nature*, **2000**, *404*, 307

Heme detoxificati

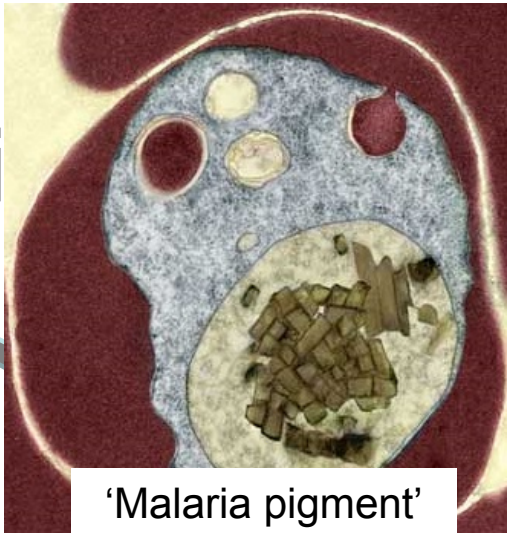

Parasite Digestive Vacuole (DV)

pH ~ 4.5-5.5

2 H_2O

2 x

Dimerization

Crystallization

$FePPIX(OH)H_2$

$FePPIX(FePPIX_{-H})H$

Hemozoin (natural)

β-Hematin (synthetic)

P $\bar{1}$

R–NH

N

Aminoquinoline drugs

Cytosol

pH > 7

Pagola *et al. Nature*, **2000**, *404*, 307

Aminoquinoline drugs

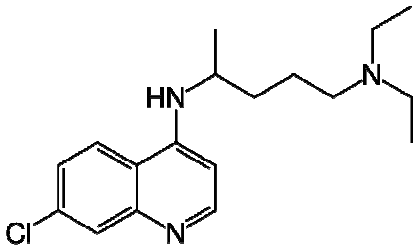

Chloroquine, CQ

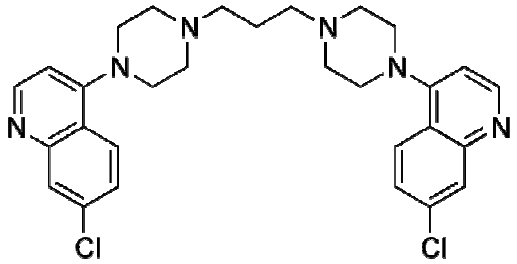

Piperaquine, PQ

Aminoquinoline drugs

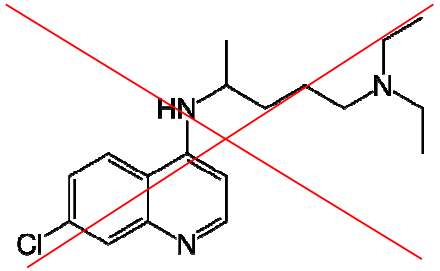

Chloroquine, CQ

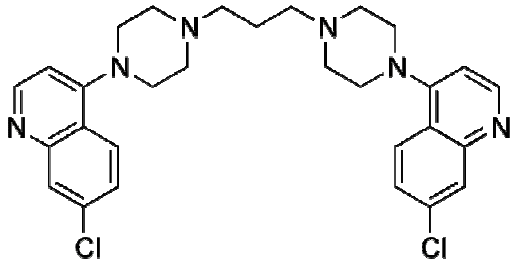

Piperaquine, PQ

P. Falciparum has developed resistance against most formerly effective antimalarials

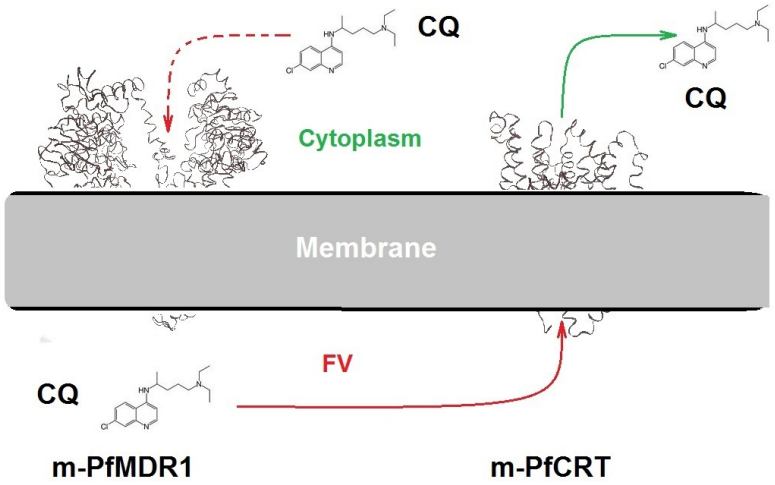

Aminoquinoline drugs

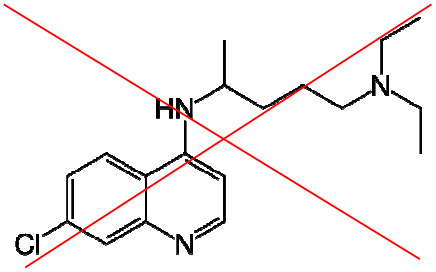

Chloroquine, CQ

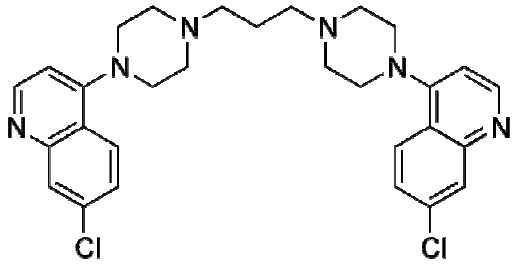

Piperaquine, PQ

P. Falciparum has developed resistance against most formerly effective antimalarials

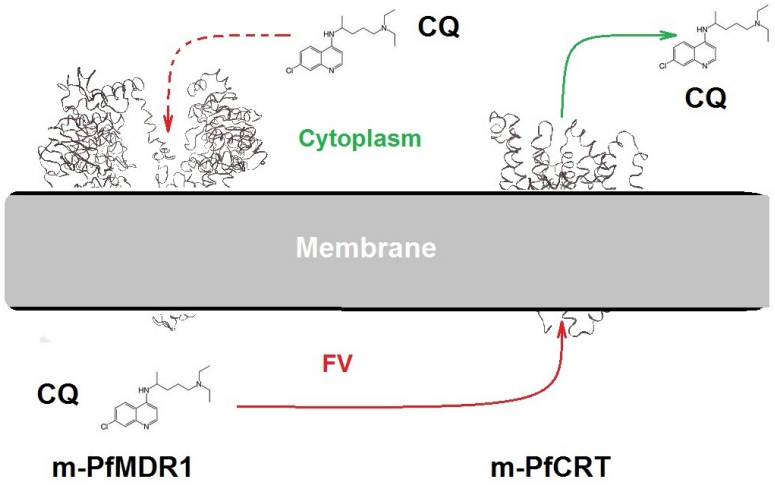

Crucial point: Understanding the drug:heme recognition process at the molecular level

NEW ACTIVE MOLECULES ARE REQUIRED

Methods (self-recognition)

Single-crystal X-ray diffraction experiments

- **CQ** · 2($\mathbf{H_2PO_4^-}$) · 2(H_2O) salt, 103(3) K
- **PQ** · 4$\mathbf{H_2PO_4^-}$ · 4(H_2O) salt, 150(2) K
- 2 [**PQ** · 4($\mathbf{NO_3^-}$)] · 2($H_3O^+ \cdot NO_3^-$) · 2(H_2O) salt, 180(2) K
- **PQ** · 4Br^- · ($H_3O^+ \cdot$**Br**$^-$) · 3(H_2O) salt, 120(2) K

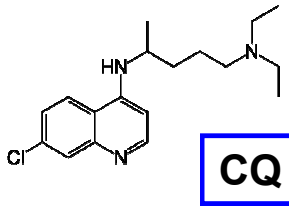

CQ

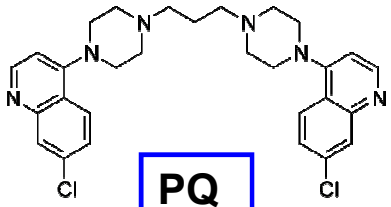

PQ

Solid-state structures reveal the **allegedly dominant** non-covalent interactions

Methods (self-recognition)

Single-crystal X-ray diffraction experiments

- **CQ** · 2(**$H_2PO_4^-$**) · 2(H_2O) salt, 103(3) K
- **PQ** · 4**$H_2PO_4^-$** · 4(H_2O) salt, 150(2) K
- 2 [**PQ** · 4(**NO_3^-**)] · 2($H_3O^+ \cdot NO_3^-$) · 2(H_2O) salt, 180(2) K
- **PQ** · 4Br^- · ($H_3O^+ \cdot$**Br^-**) · 3(H_2O) salt, 120(2) K

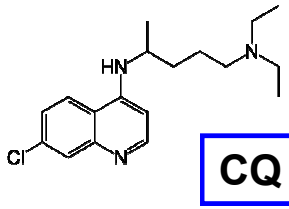

CQ

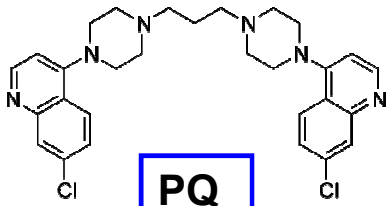

PQ

low-T high-resolution diffraction

Experimental structure

Solid-state structures reveal the **allegedly dominant** non-covalent interactions

Methods (self-recognition)

Single-crystal X-ray diffraction experiments

- **CQ** · 2($\mathbf{H_2PO_4^-}$) · 2(H_2O) salt, 103(3) K
- **PQ** · 4$\mathbf{H_2PO_4^-}$ · 4(H_2O) salt, 150(2) K
- 2 [**PQ** · 4($\mathbf{NO_3^-}$)] · 2($H_3O^+ \cdot NO_3^-$) · 2(H_2O) salt, 180(2) K
- **PQ** · 4Br^- · ($H_3O^+ \cdot$**Br**$^-$) · 3(H_2O) salt, 120(2) K

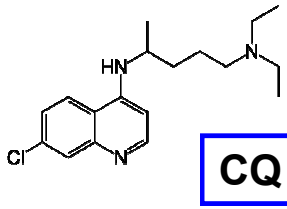

CQ

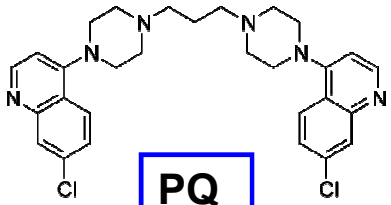

PQ

low-T high-resolution diffraction

Experimental structure

CRYSTAL14

Quantum model of the crystal

Solid-state structures reveal the **allegedly dominant** non-covalent interactions

a computational tool for solid state chemistry and physics

CRYSTAL

Methods: drug-substrate recognition

UV-Vis spectroscopy

- pH = 5.0, 1:1 H_2O:DMSO, [**CQ**]= 5 mM; [Hematin]= 5 mM

Methods: drug-substrate recognition

UV-Vis spectroscopy

• pH = 5.0, 1:1 H_2O:DMSO, [**CQ**]= 5 mM; [Hematin]= 5 mM

EXAFS spectroscopy

BM26A beamline,
ESRF, Grenoble (FR)

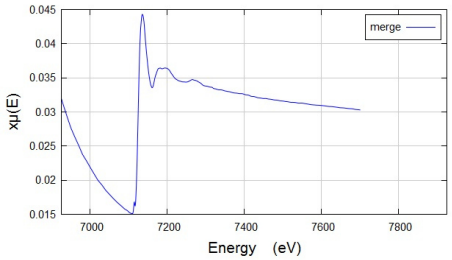

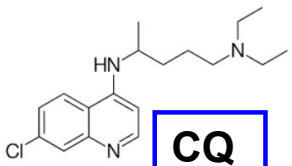

CQ

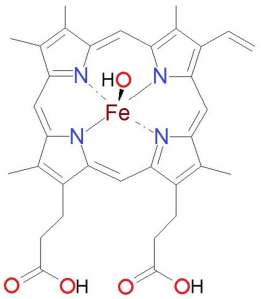

Hematin

- Data collected in **fluorescence mode**
- 6.9-7.7 keV, across Fe Kα edge (7.11 keV)
- 2 repeated measures of 3-4 freshly prepared solutions
- Data acquired at **RT**

Methods: drug-substrate recognition

UV-Vis spectroscopy

• pH = 5.0, 1:1 H_2O:DMSO, [**CQ**]= 5 mM; [Hematin]= 5 mM

EXAFS spectroscopy

BM26A beamline,
ESRF, Grenoble (FR)

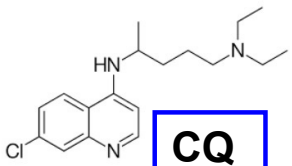

CQ

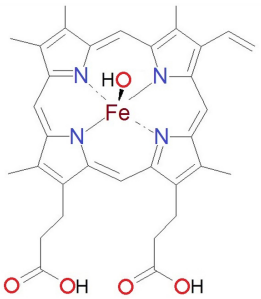

Hematin

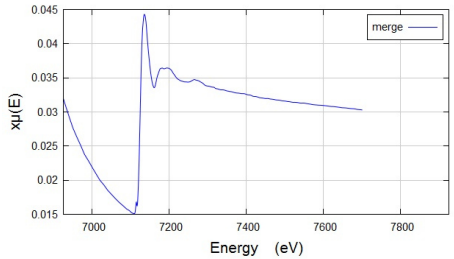

• Data collected in **fluorescence mode**
• 6.9-7.7 keV, across Fe Kα edge (7.11 keV)
• 2 repeated measures of 3-4 freshly prepared solutions
• Data acquired at **RT**

DFT simulations

• (U)B3LYP:6-311G(p,d) theory level, gas phase
• Dispersion-corrected functionals (Grimme)

UV-vis results

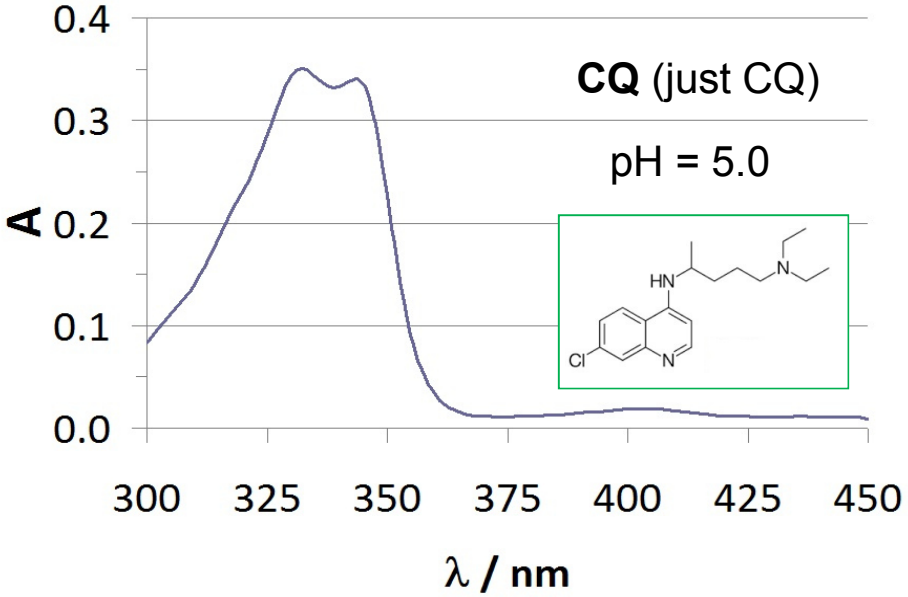

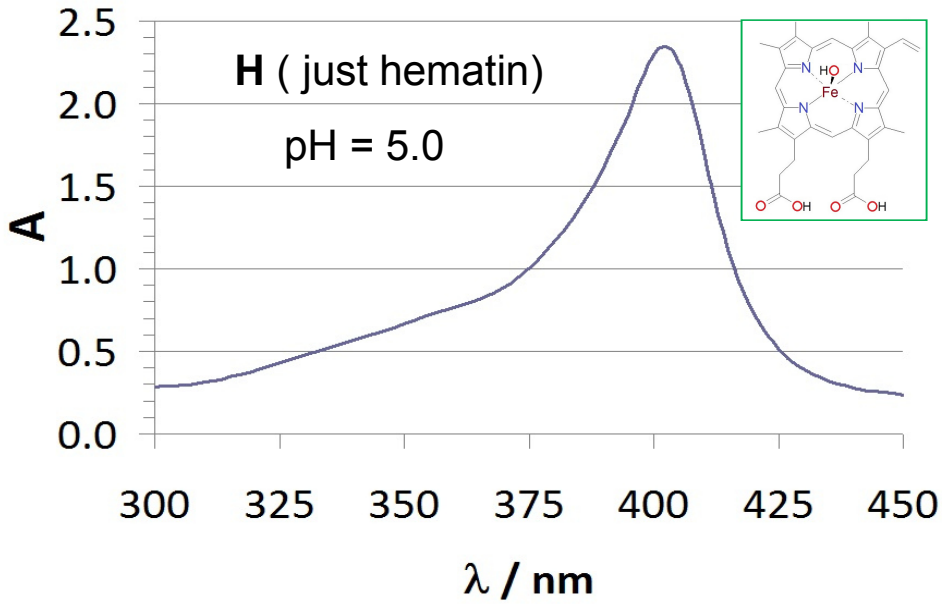

UV-vis results

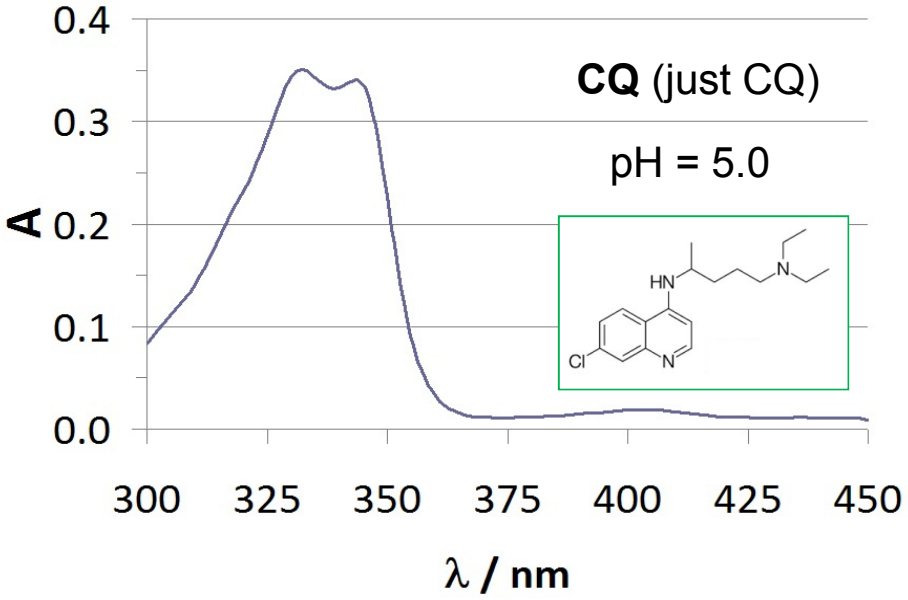

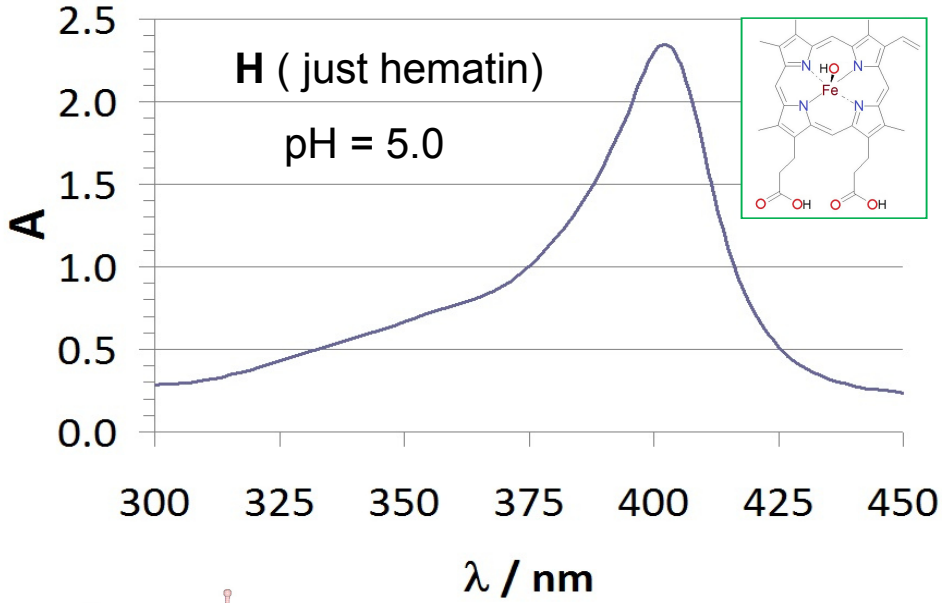

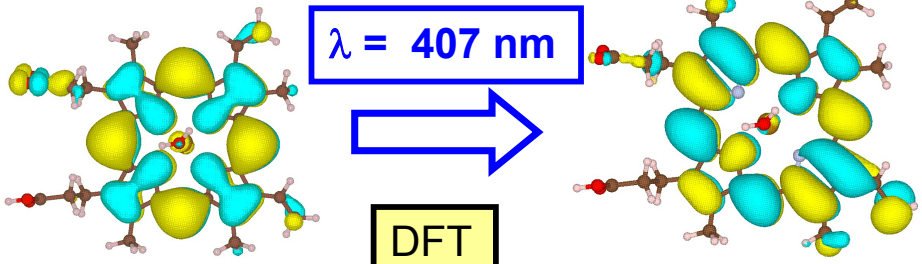

λ = 407 nm

DFT

HOMO-3, α

LUMO+1, α

Characteristic **Soret band** of the FePPIX system

UV-vis results

pH = 5.0

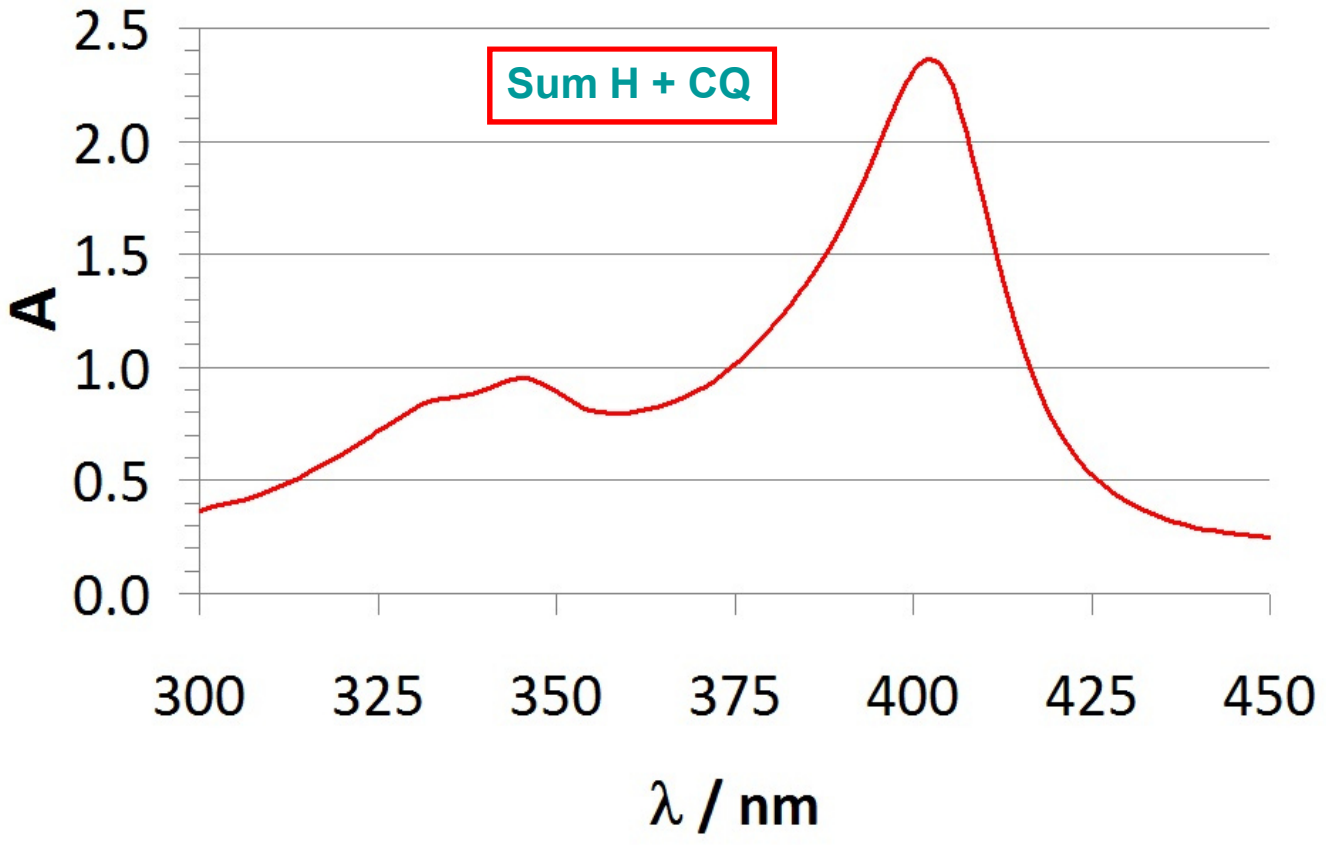

UV-vis results

pH = 5.0

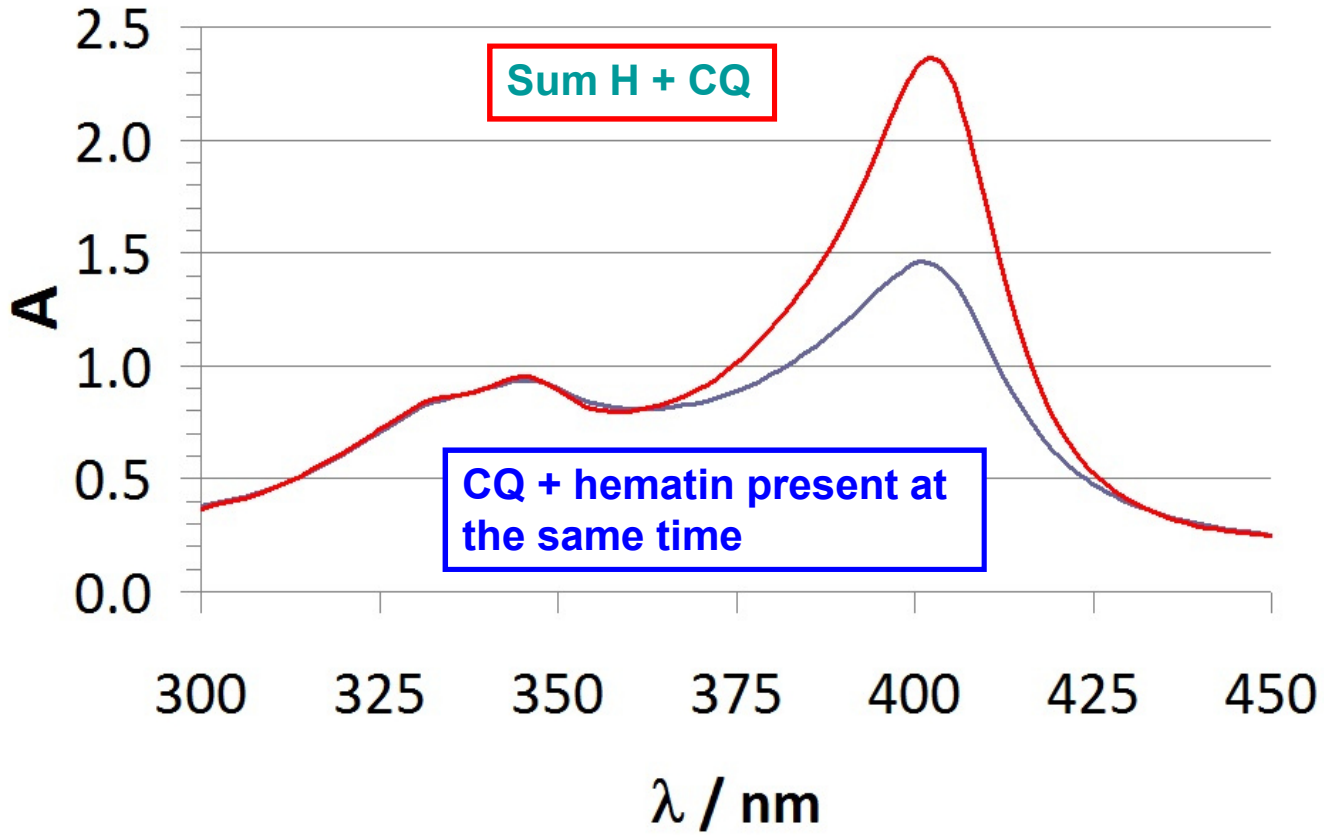

UV-vis results

pH = 5.0

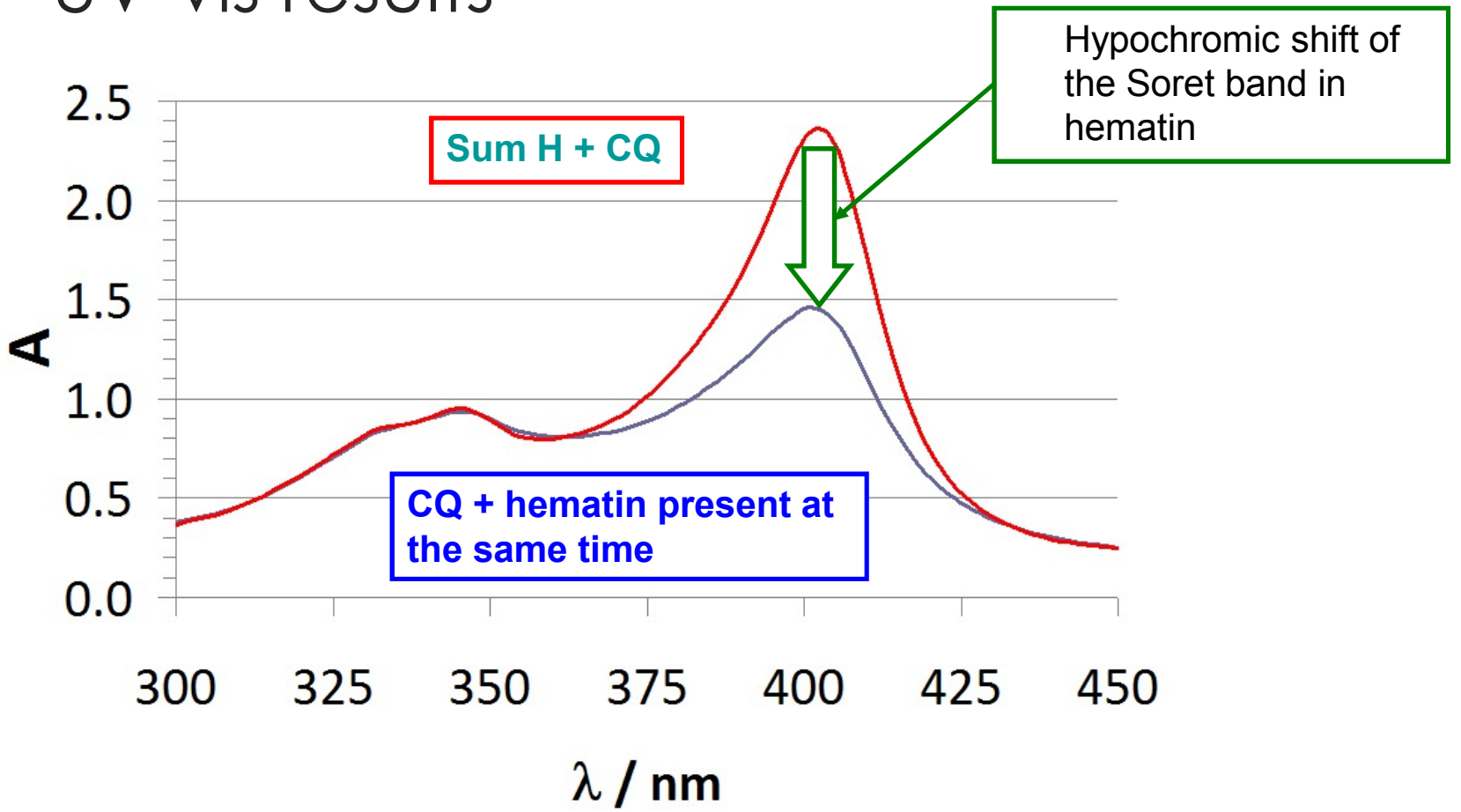

UV-vis results

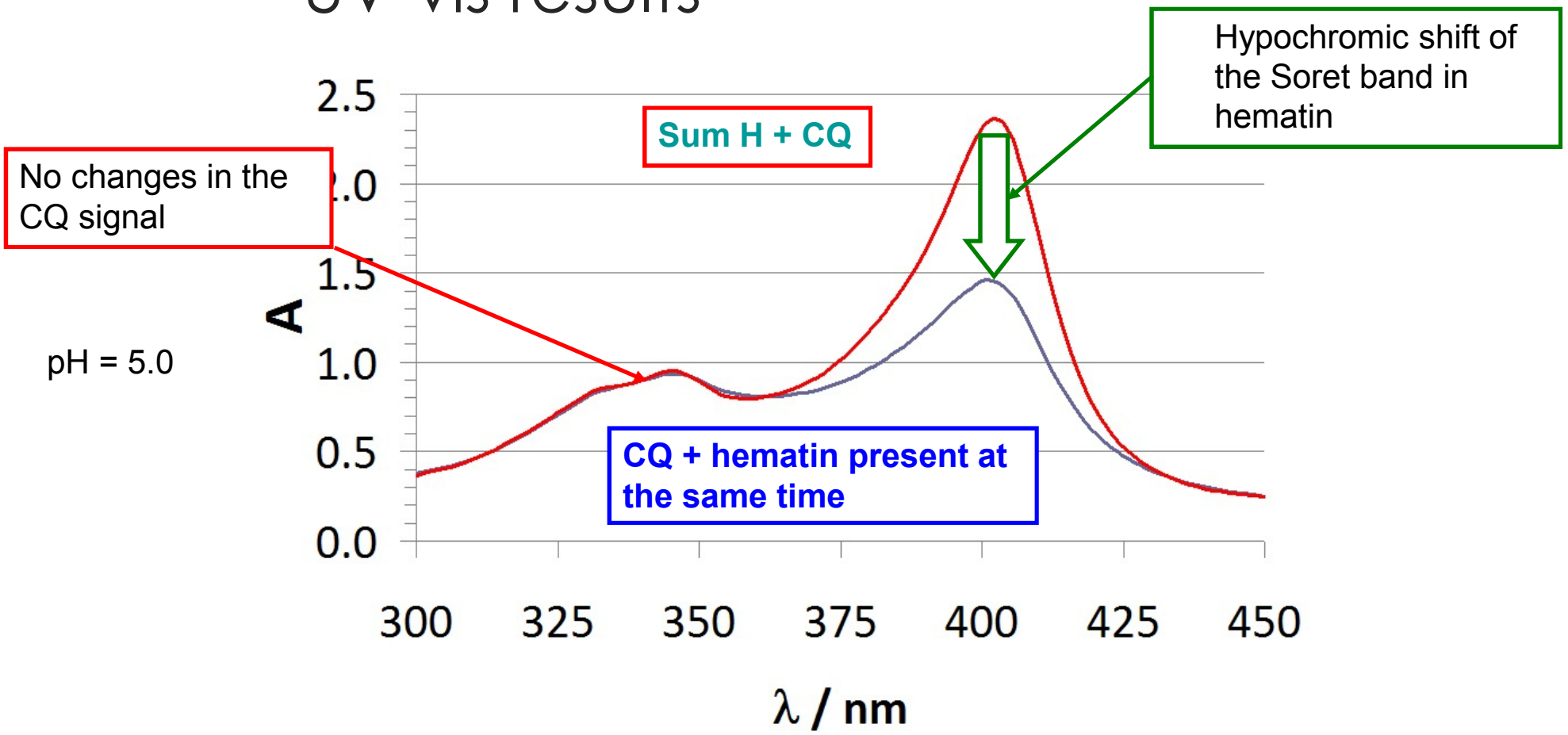

UV-vis results

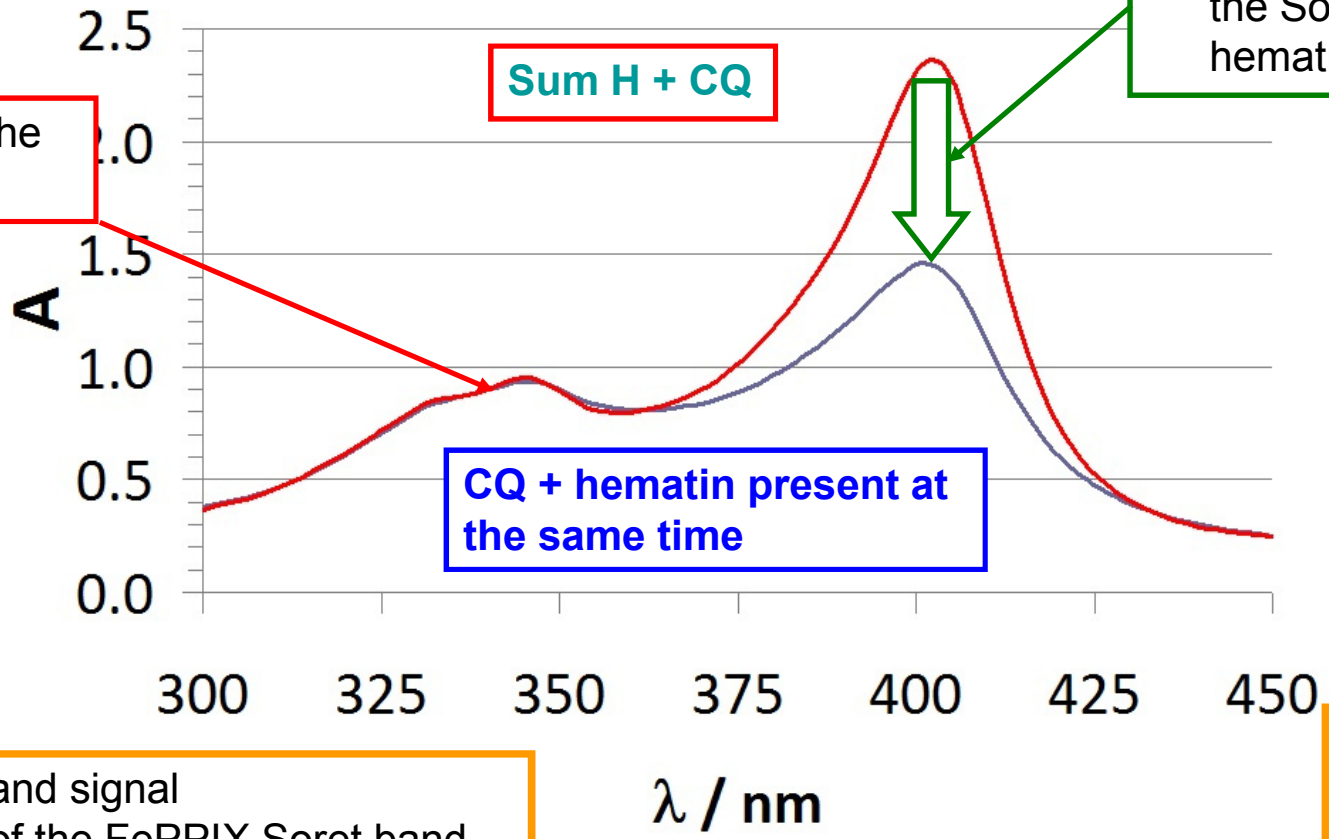

No changes in the CQ signal

Hypochromic shift of the Soret band in hematin

pH = 5.0

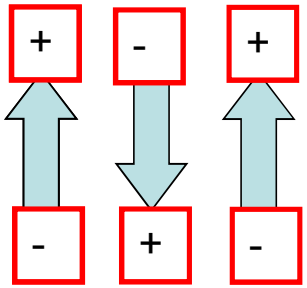

- No shift in the band signal
- Hypochromism of the FePPIX Soret band

Excitonic cupling → **stacking π···π** interactions

Literature models

Molecular mechanics (MM) simulations and spectroscopic data point out that π···π interactions should also play a role in determining the heme:CQ geometry

DFT CQH_2^{2+}

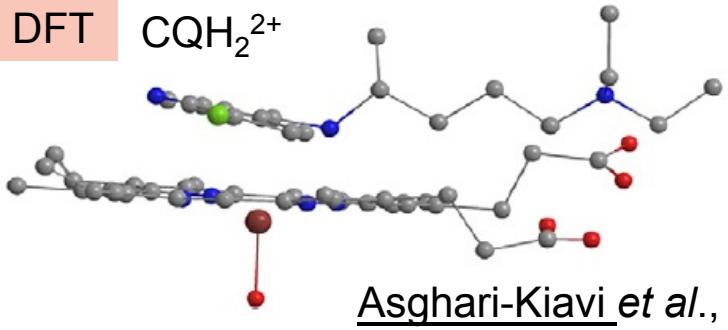

$FePPIX(OH)H_2$

Asghari-Kiavi *et al.*, *J. Inorg. Biochem.* **2011**, *105*, 1662

CQH_2^{2+}

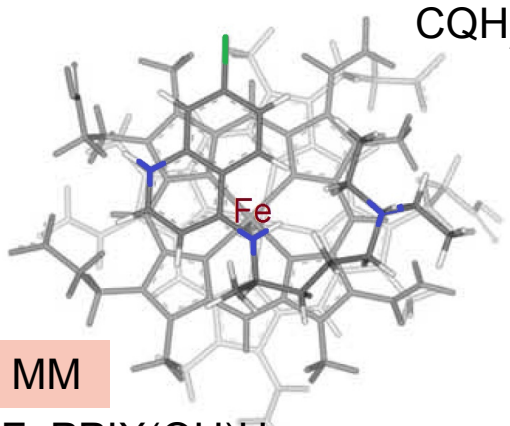

MM

$FePPIX(OH)H_2$

Portela *et al. FEBS Lett.* **2003**, *547*, 217

Mesohematin anhydride

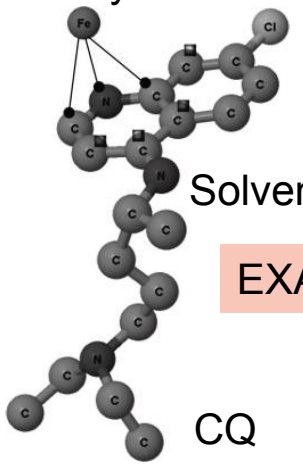

Solvent: DMSO

EXAFS

CQ

Walczak *et al. J. Phys. Chem. B* **2011**, *115*, 1145

CQH_2^{2+}

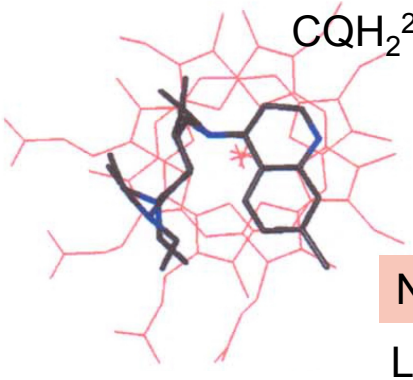

pH > 7

NMR+ constrained MM

Leed *et al. Biochem.* **2002**, *41*, 10245

μ-oxo-$FePPIX(FePPIXH_2)H_2$

The protonation state must be accounted for

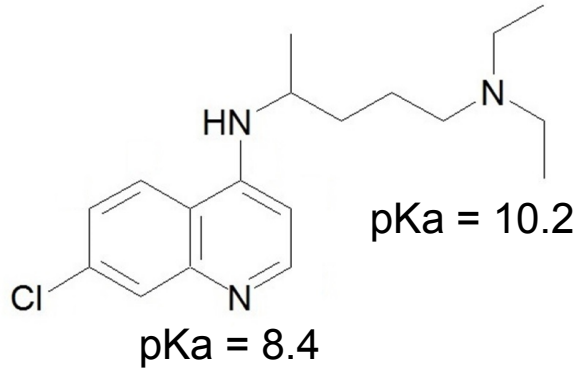

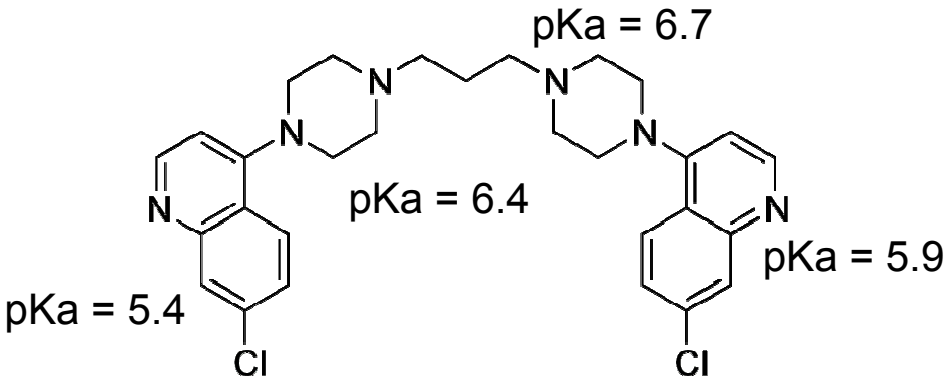

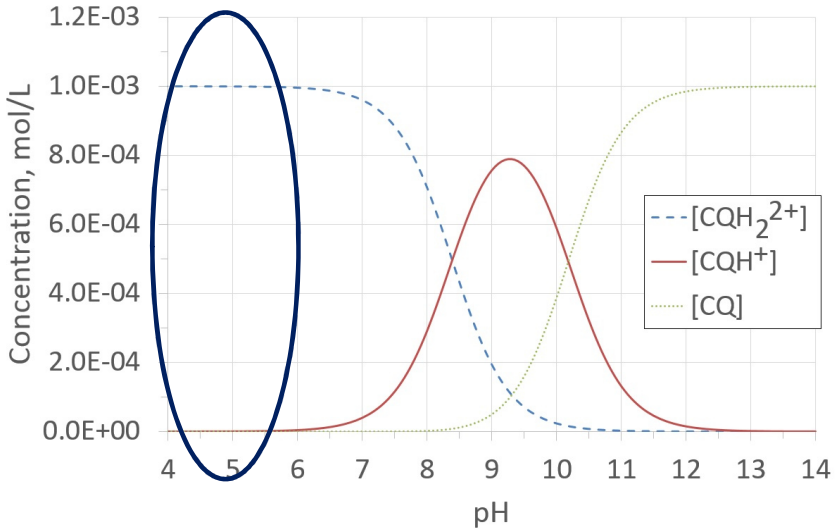

Almost completely protonated in the acidic DV

X-ray results

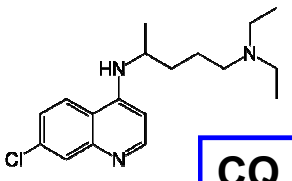

CQ

• $\mathbf{CQH_2^{2+}} \cdot 2(\mathbf{H_2PO_4^-}) \cdot 2(H_2O)$ salt

103 K

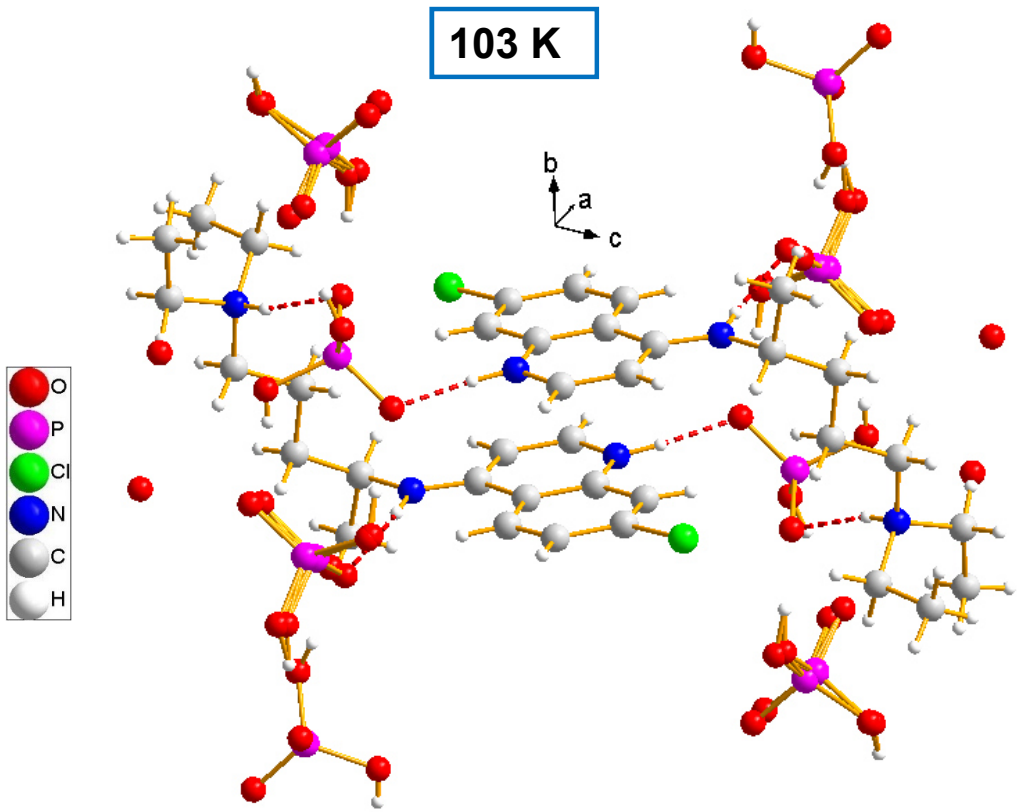

$\sin(\theta/\lambda)_{max}$ = 1.0 Å^{-1}
λ = 0.71073 Å
CCDC number = 1471834

Space Group = $P2_1/c$ (14)
a = 9.7212(1) Å
b = 16.7733(2) Å
c = 15.6966(2) Å
β = 105.1788(2) Å
V = 2470.14(5) Å

X-ray results

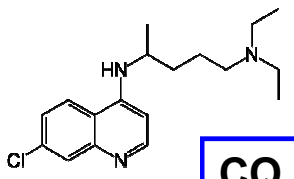

CQ

• **CQH_2^{2+}** · 2(**$H_2PO_4^-$**) · 2(H_2O) salt

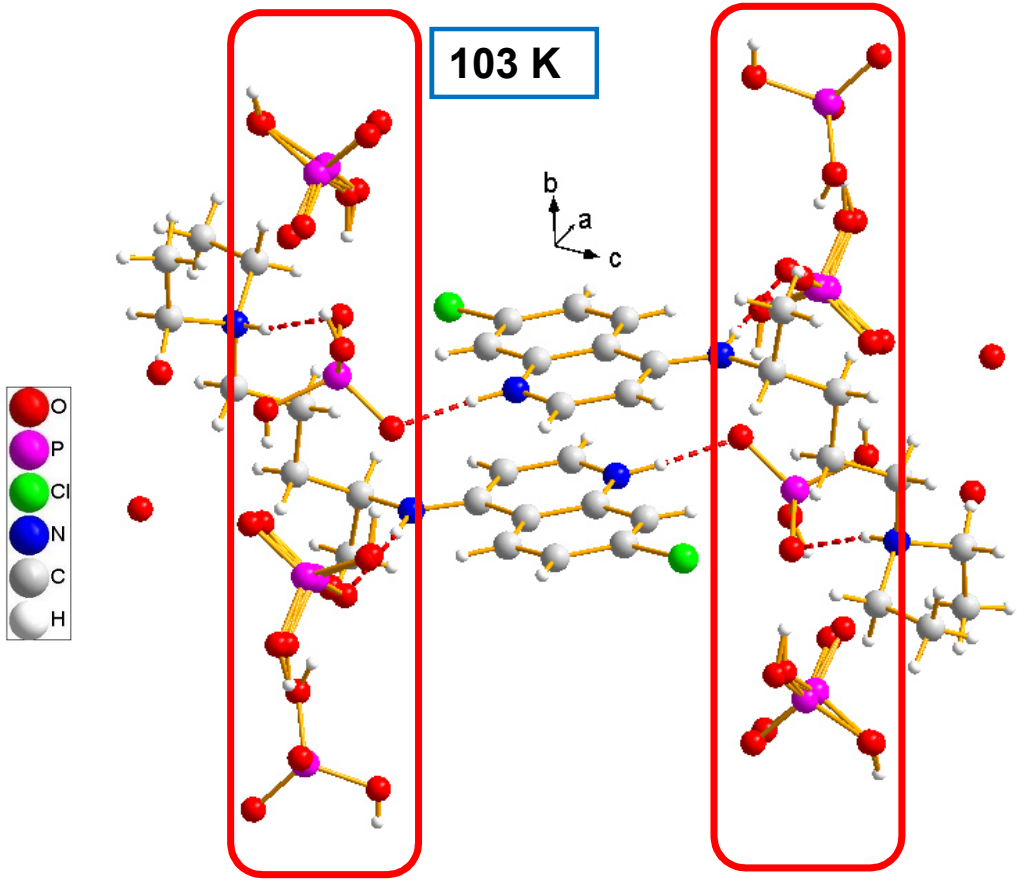

$\sin(\theta/\lambda)_{max}$ = 1.0 Å^{-1}
λ = 0.71073 Å
CCDC number = 1471834

Space Group = $P2_1/c$ (14)
a = 9.7212(1) Å
b = 16.7733(2) Å
c = 15.6966(2) Å
β = 105.1788(2) Å
V = 2470.14(5) Å

Infinite phosphate chains along the b axis

X-ray results

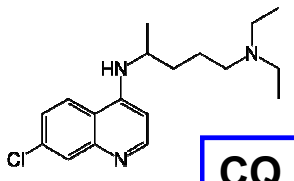

CQ

• **CQH_2^{2+}** · 2(**$H_2PO_4^-$**) · 2(H_2O) salt

103 K

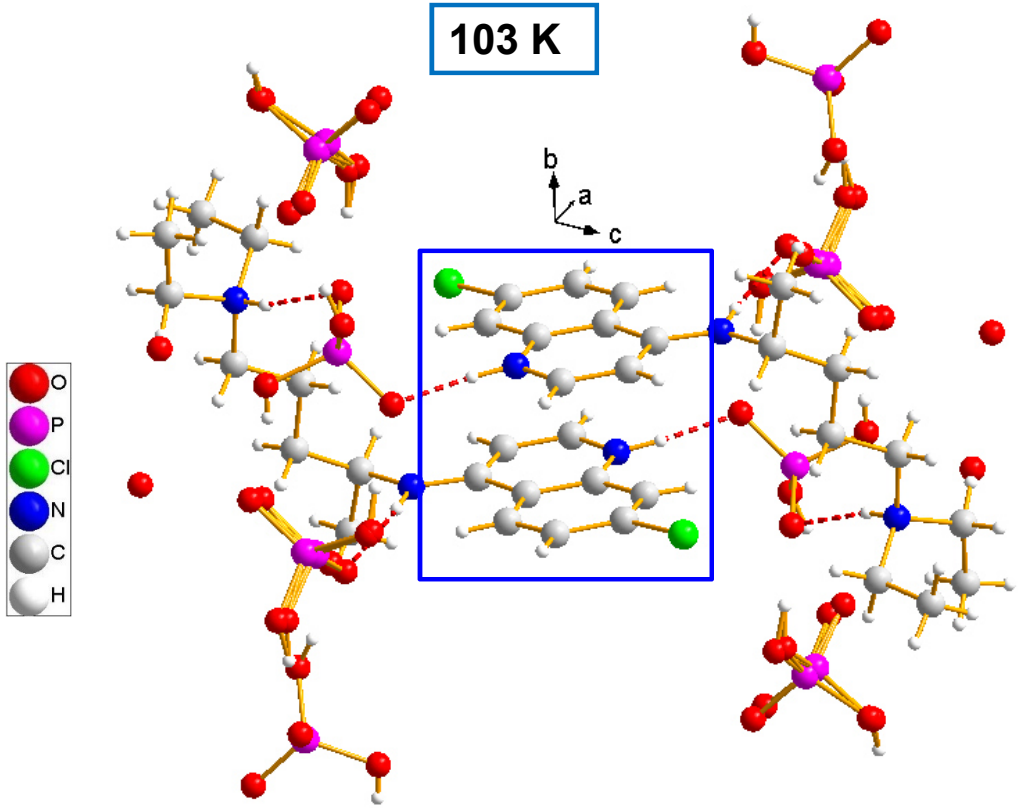

$\sin(\theta/\lambda)_{max}$ = 1.0 Å^{-1}
λ = 0.71073 Å
CCDC number = 1471834

Space Group = $P2_1/c$ (14)
a = 9.7212(1) Å
b = 16.7733(2) Å
c = 15.6966(2) Å
β = 105.1788(2) Å
V = 2470.14(5) Å

CQ perpendicular to phosphate chain

X-ray results

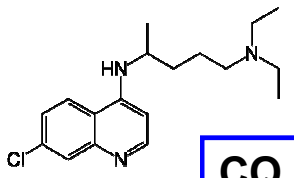

CQ

• $\mathbf{CQH_2^{2+}} \cdot 2(\mathbf{H_2PO_4^-}) \cdot 2(H_2O)$ salt

103 K

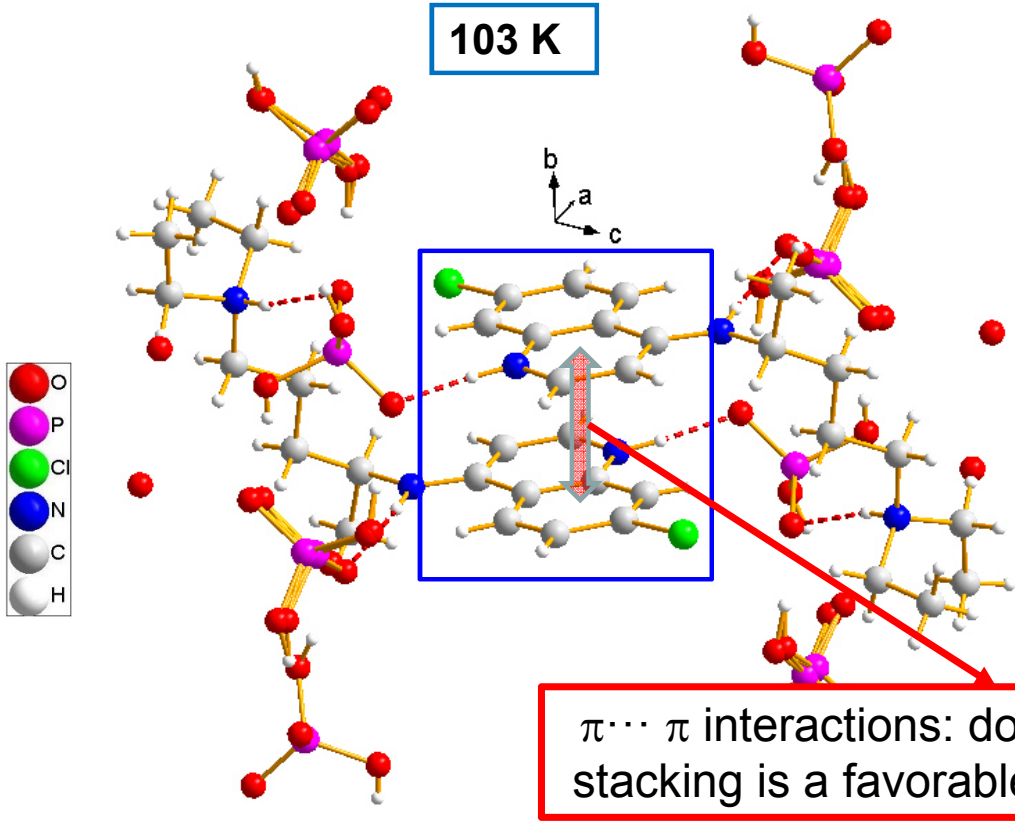

$\pi \cdots \pi$ interactions: does this confirm that stacking is a favorable interaction mode?

$\sin(\theta/\lambda)_{max} = 1.0$ Å^{-1}
$\lambda = 0.71073$ Å
CCDC number = 1471834

Space Group = $P2_1/c$ (14)
a = 9.7212(1) Å
b = 16.7733(2) Å
c = 15.6966(2) Å
β = 105.1788(2) Å
V = 2470.14(5) Å

CQ perpendicular to phosphate chain

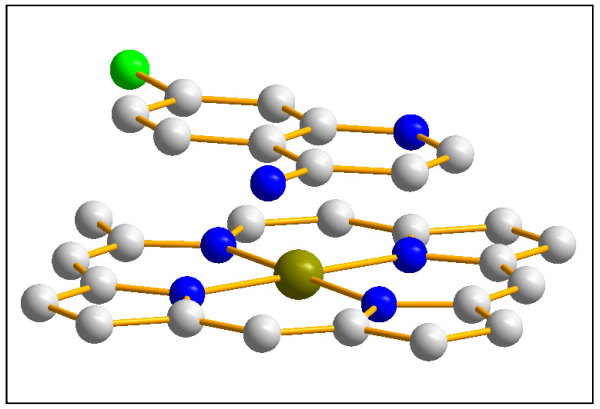

Periodic simulation results

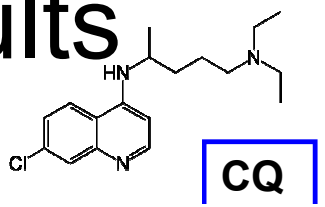

CQ

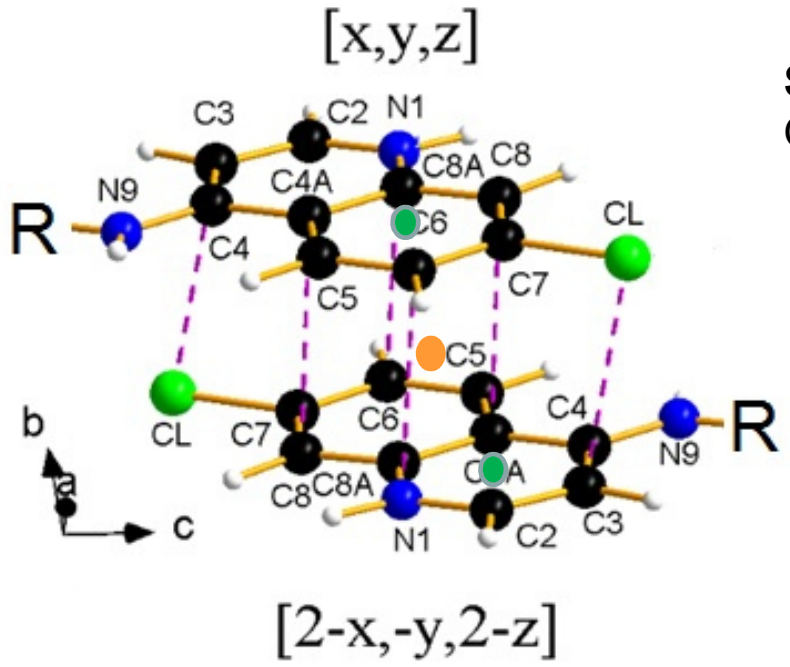

Study of the charge density vector field , $\nabla\rho$, by means of the Quantum Theory of Atoms in Molecules

Bader, Atoms in Molecules: A Quantum Theory, Oxford University Press, 1990

Periodic simulation results

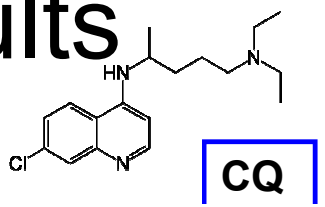

CQ

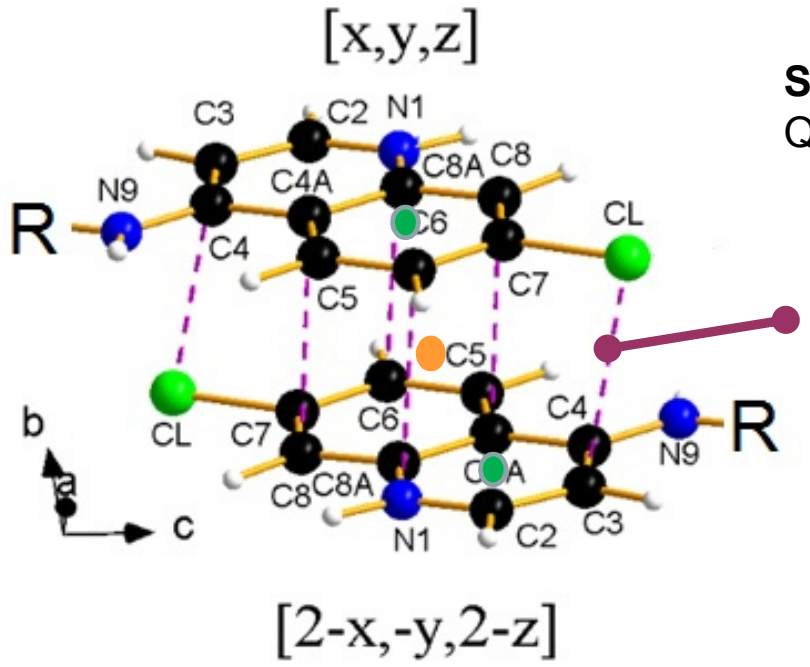

Study of the charge density vector field , $\nabla\rho$, by means of the Quantum Theory of Atoms in Molecules

Atomic interaction lines, indicating some kind of quantum stabilizing interaction between each atom pair

Bader, Atoms in Molecules: A Quantum Theory, Oxford University Press, 1990

Periodic simulation results

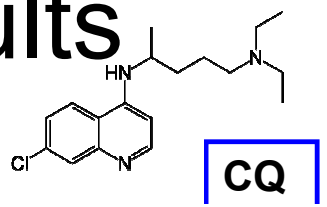

CQ

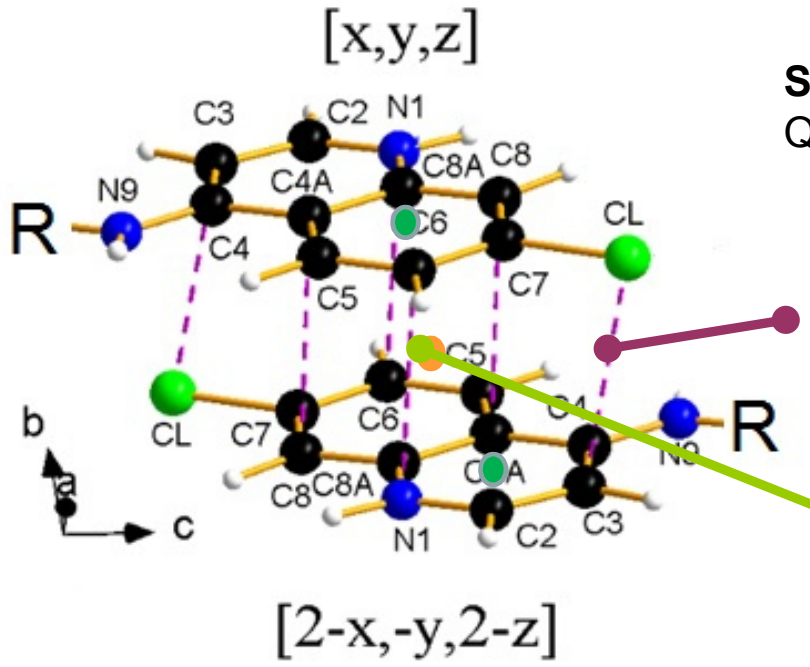

Study of the charge density vector field , $\nabla\rho$, by means of the Quantum Theory of Atoms in Molecules

Atomic interaction lines, indicating some kind of quantum stabilizing interaction between each atom pair

Cage critical point, indicating a minimum in the $\rho(r)$ distribution

Bader, Atoms in Molecules: A Quantum Theory, Oxford University Press, 1990

Periodic simulation results

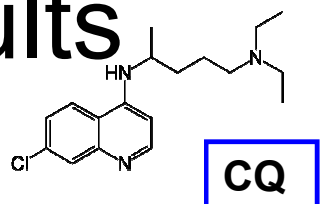

CQ

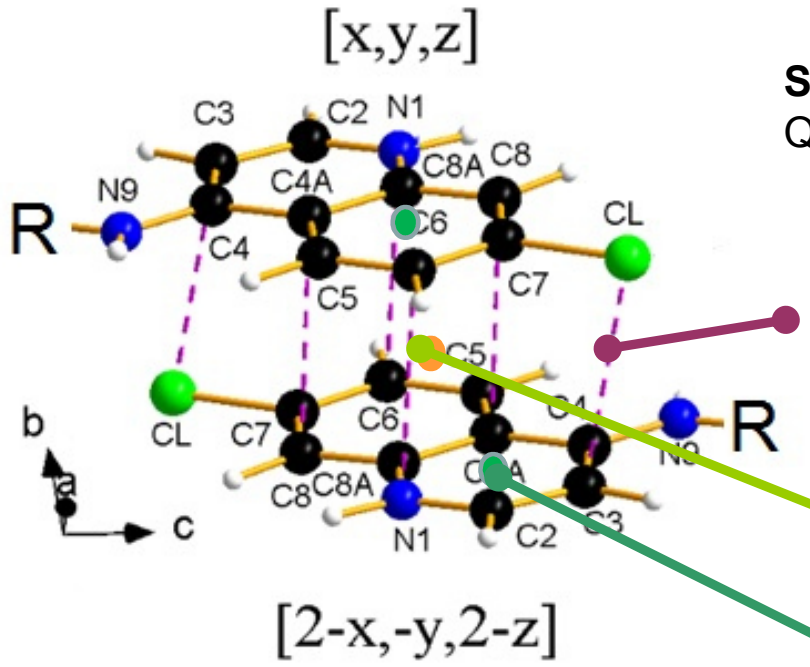

Study of the charge density vector field , $\nabla\rho$, by means of the Quantum Theory of Atoms in Molecules

Atomic interaction lines, indicating some kind of quantum stabilizing interaction between each atom pair

Cage critical point, indicating a minimum in the $\rho(r)$ distribution

Ring critical point, representative of the features of the charge density in the ring

Bader, Atoms in Molecules: A Quantum Theory, Oxford University Press, 1990

Periodic simulation results

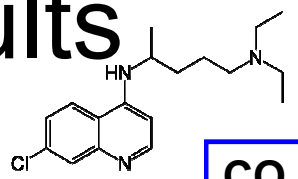

CQ

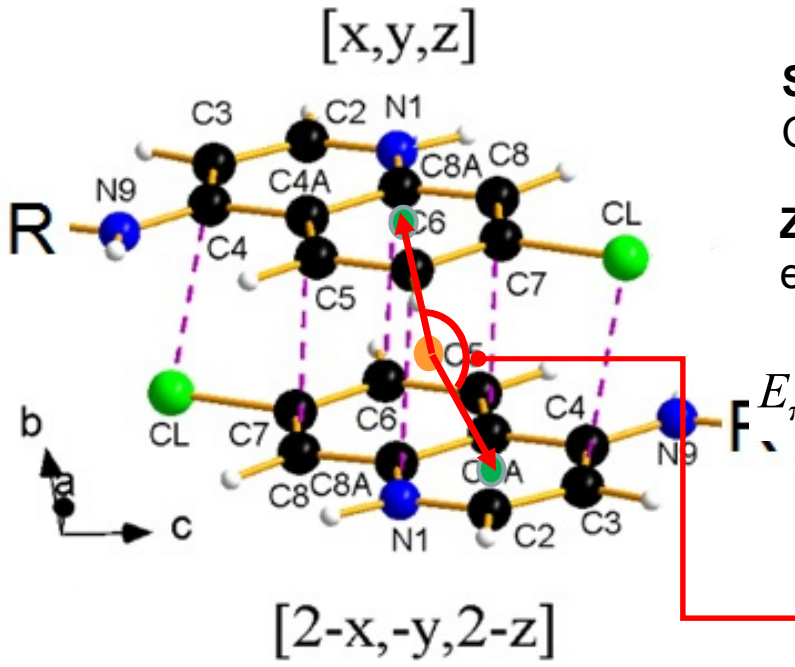

Study of the charge density vector field , $\nabla\rho$, by means of the Quantum Theory of Atoms in Molecules

Zhikol Functional extracts **approximate** $\pi\cdots\pi$ interaction energies from the topological properties of the charge density

$$E_{\pi\cdots\pi} = \sum_i C_i \left\{ 1.214(14)\cdot\nabla^2\rho_i - 131.6(3.9)\cdot\left(\nabla^2\rho_i\right)^2 + 635(84)\rho_i^2 \right\}$$

Sum goes thorugh all the **cage critical points**

C_i is the cosine between the vectors connecting each **cage critical point** with its closest **ring critical points**

$$E_{\pi\cdots\pi} = +4.4(6)\,kcal\cdot mol^{-1}$$

Dispersive contribution to $\pi\cdots\pi$ energy is here weakly repulsive

Zhikol et al. *J. Chem. Phys.* **2005**, *122*, 144104

Periodic simulation results

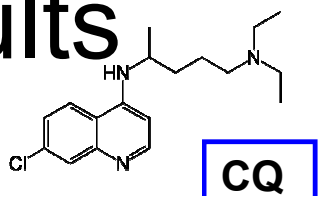

CQ

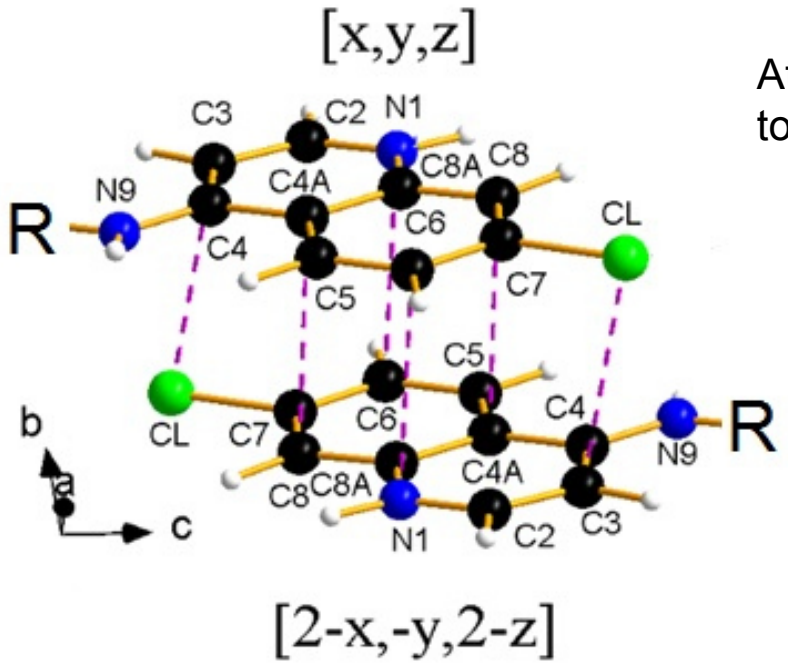

Attractive contributions due to stacking interactions are here due to quadrupolar deformation of the ring charge density (π-hole)

Periodic simulation results

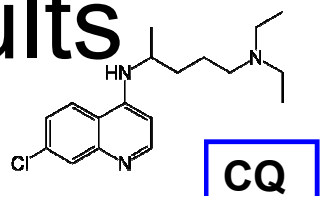

CQ

Attractive contributions due to stacking interactions are here due to quadrupolar deformation of the ring charge density (π-hole)

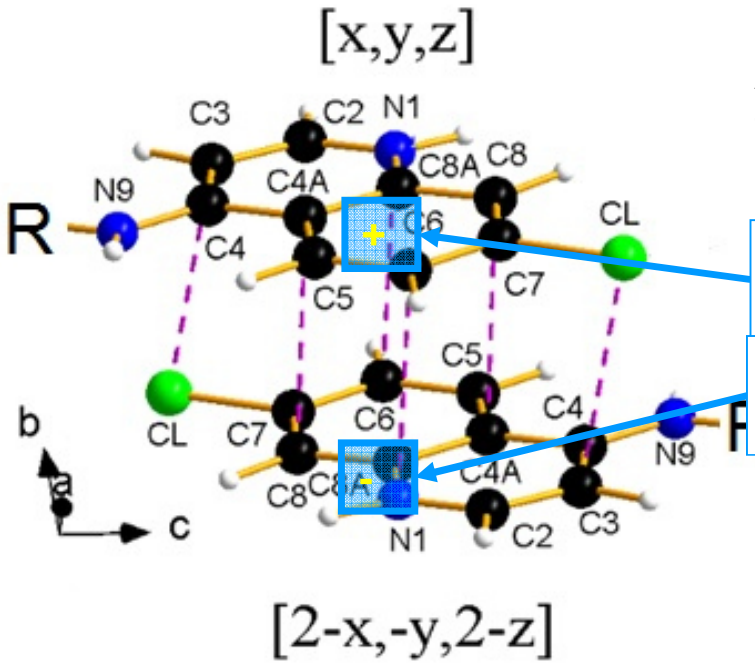

Less charge density at the centre of the rings

More charge density on nuclei

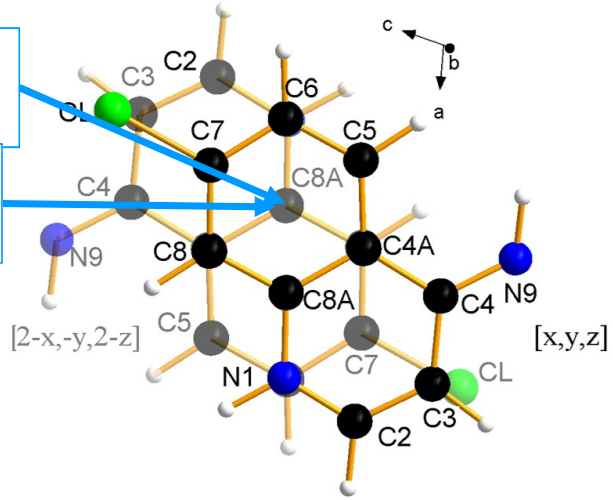

Periodic simulation results

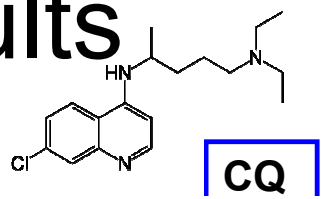

CQ

Attractive contributions due to stacking interactions are here due to quadrupolar deformation of the ring charge density (π-hole)

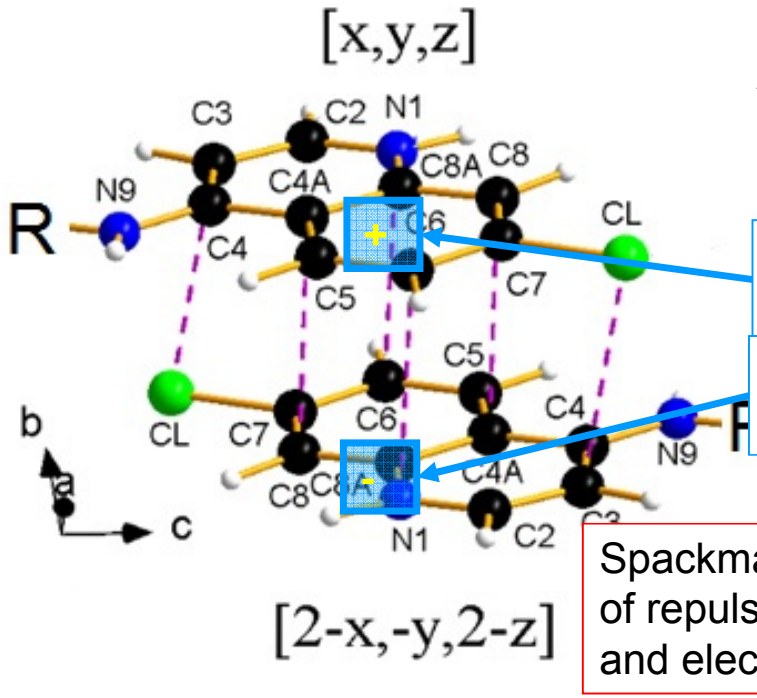

Less charge density at the centre of the rings

More charge density on nuclei

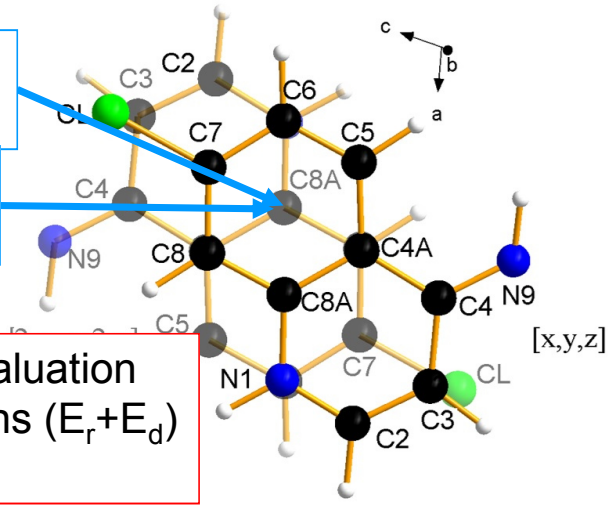

Spackman's model allows the evaluation of repulsive/dispersive contibutions (E_r+E_d) and electrostatics (E_{el})

Spackman et al.. *Am. Chem. Soc*. **1988**, *110*, 775

Periodic simulation results

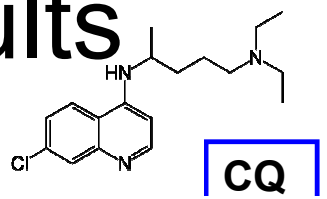

CQ

Attractive contributions due to stacking interactions are here due to quadrupolar deformation of the ring charge density (π-hole)

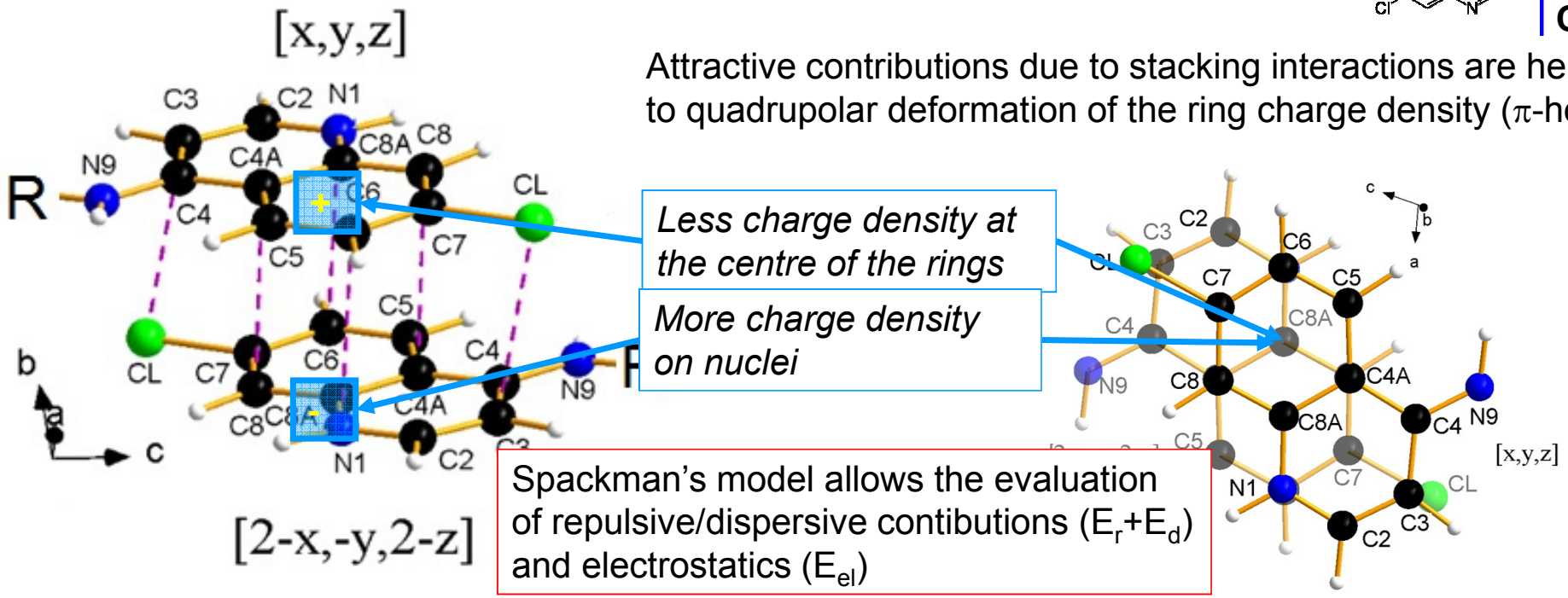

Spackman's model allows the evaluation of repulsive/dispersive contibutions (E_r+E_d) and electrostatics (E_{el})

For **neutral** CQ molecules (kcal·mol^{-1}): E_r+E_d = +0.8; E_{el} = -12.4

Spackman et al.. *Am. Chem. Soc*. **1988**, *110*, 775

Periodic simulation results

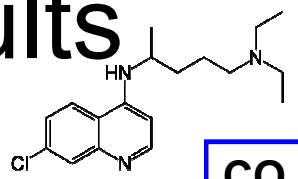

CQ

Attractive contributions due to stacking interactions are here due to quadrupolar deformation of the ring charge density (π-hole)

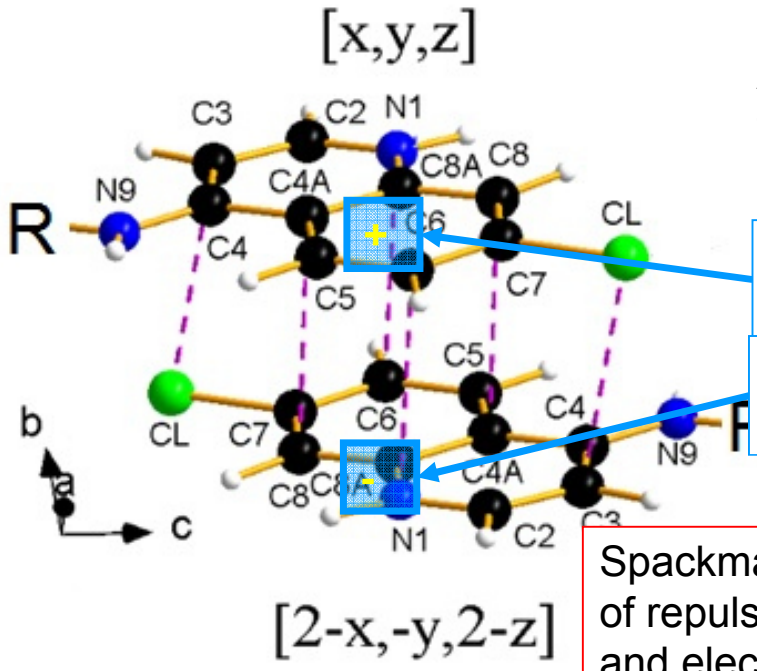

Less charge density at the centre of the rings

More charge density on nuclei

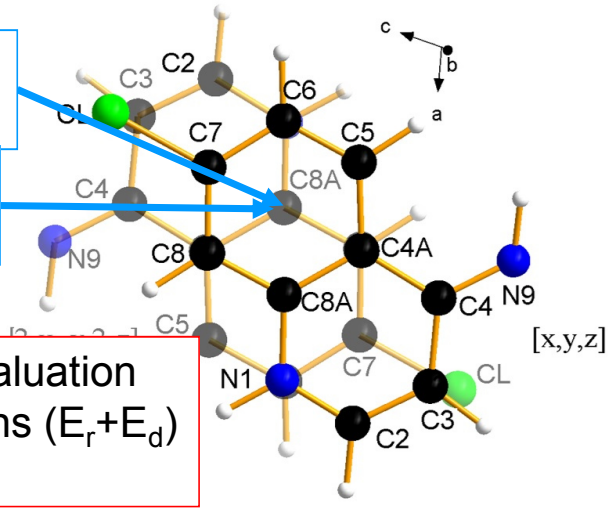

Spackman's model allows the evaluation of repulsive/dispersive contibutions (E_r+E_d) and electrostatics (E_{el})

For **neutral** CQ molecules (kcal·mol^{-1}): E_r+E_d = +0.8; E_{el} = -12.4

For *charged* CQ molecules (kcal·mol^{-1}): E_r+E_d = +0.5; E_{el} = **+136.3**

Spackman et al.. *Am. Chem. Soc*. **1988**, *110*, 775

X-ray results

Analogue π··· π interactions, with similar energies, are found in PQ salts

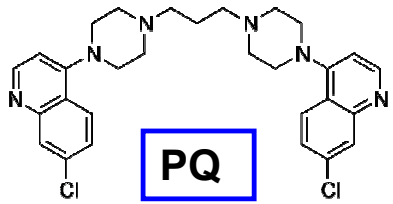

PQ

PQ · 4$\mathbf{H_2PO_4^-}$ · 4(H_2O), 150(2) K

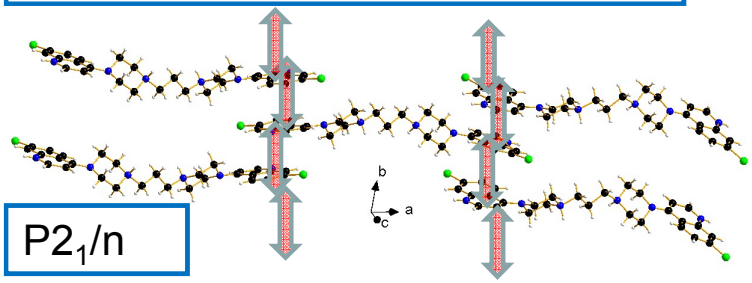

$P2_1/n$

2 [**PQ** · 4($\mathbf{NO_3^-}$)] · 2($H_3O^+ \cdot NO_3^-$) · 2(H_2O), 180(2) K

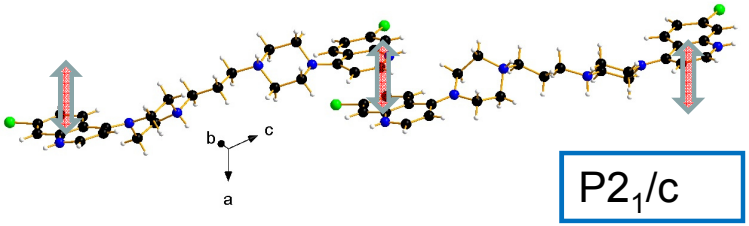

$P2_1/c$

PQ · 4Br^- · ($H_3O^+ \cdot$**Br**$^-$) · 3(H_2O), 120(2) K

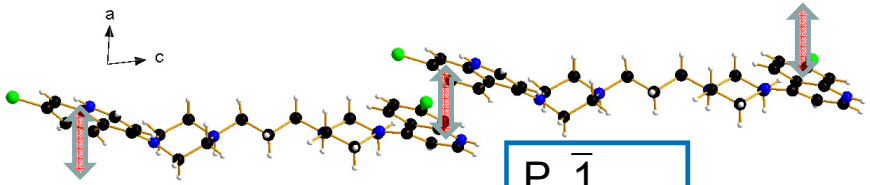

P $\bar{1}$

EXAFS results: fitting model

pH = 5.0, hematin only solution

Fe Kα edge

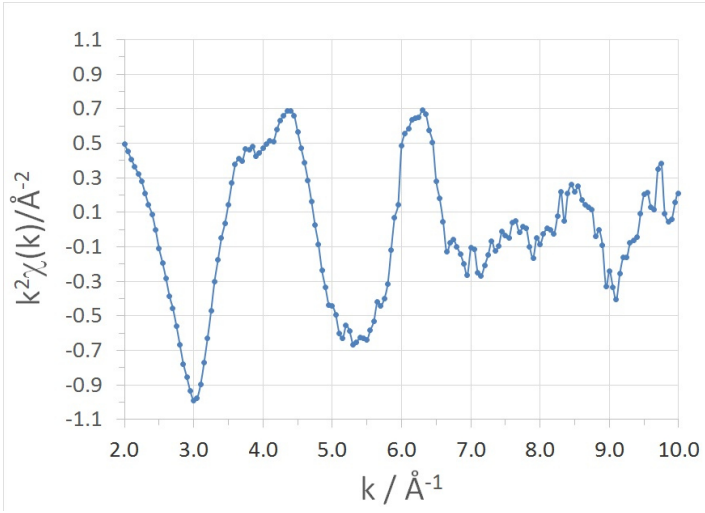

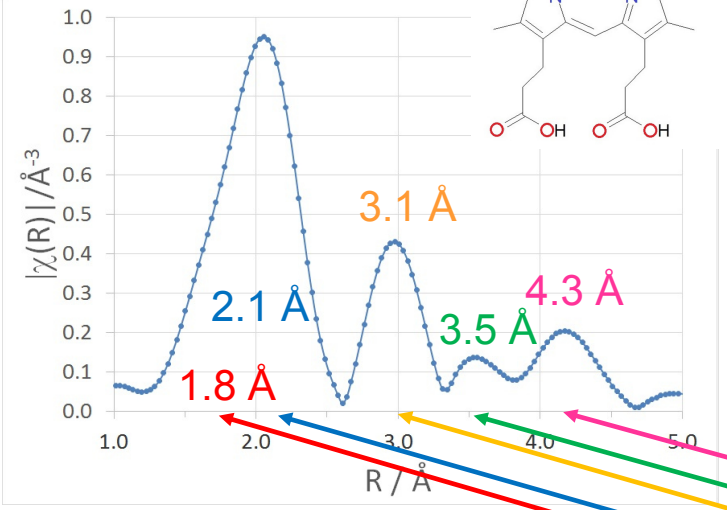

The basic protoporphyrin structural model accounts for the observed FT peaks in the real space.

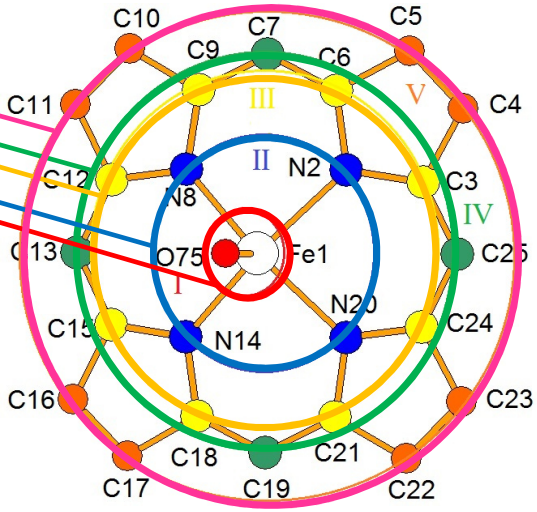

EXAFS results: fitting model

pH = 5.0, hematin only solution

Fe Kα edge

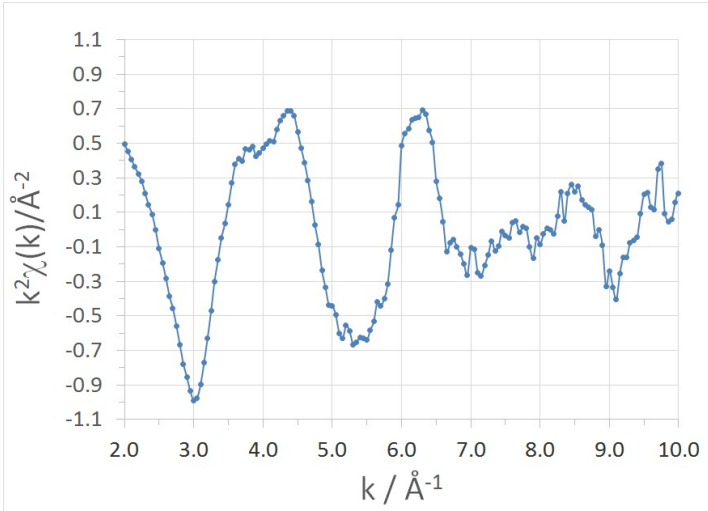

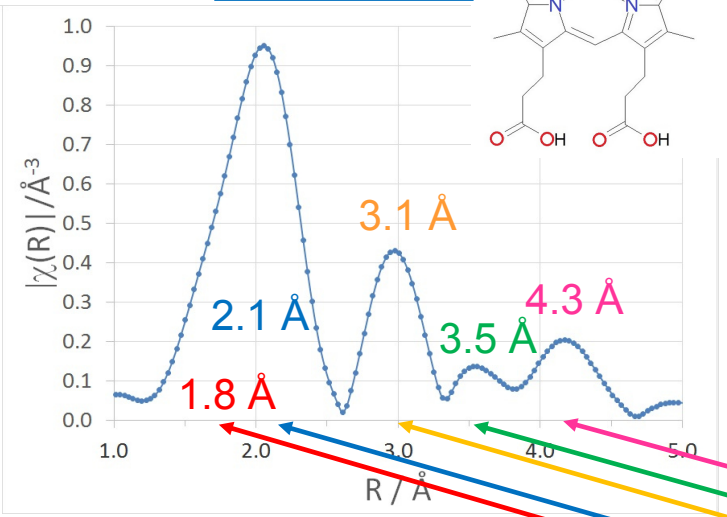

The basic protoporphyrin structural model accounts for the observed FT peaks in the real space.

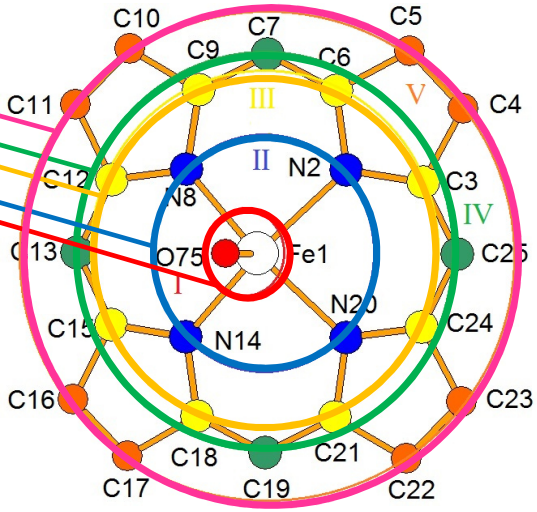

What is the hematin speciation?

- Hematin monomer?
- Hematin dimer?
- Crystalline hemozoin?

EXAFS results: fitting model

pH = 5.0, hematin only solution

Fe Kα edge

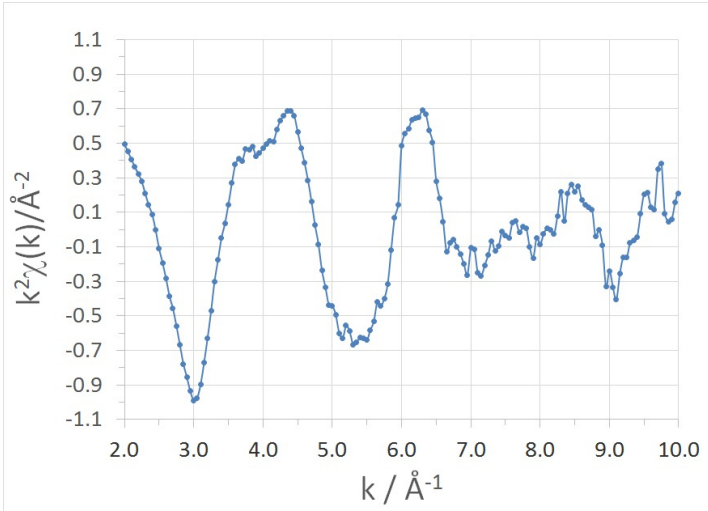

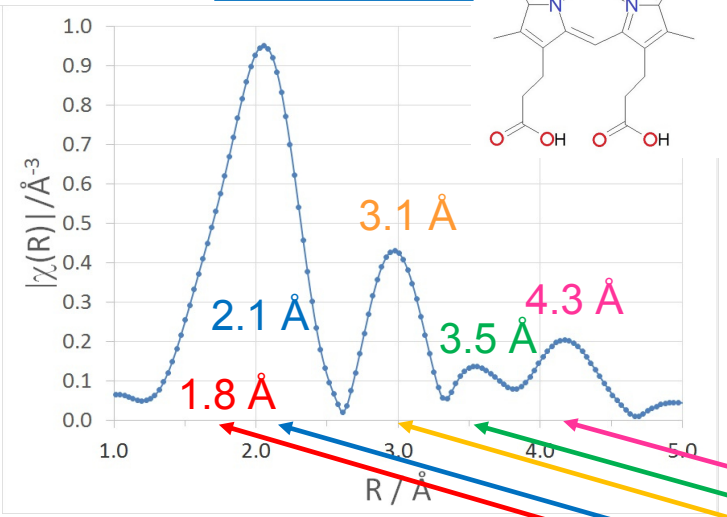

The basic protoporphyrin structural model accounts for the observed FT peaks in the real space.

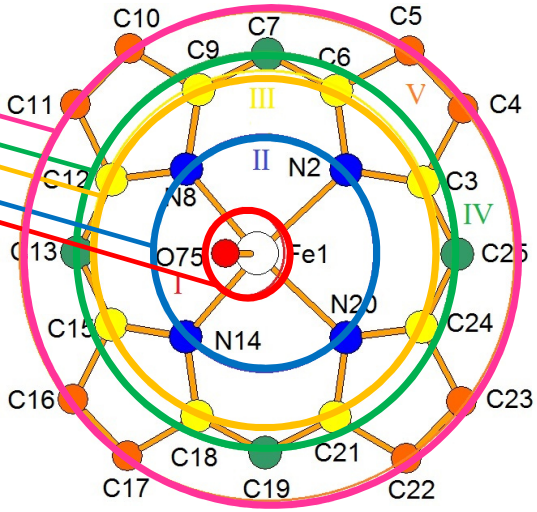

What is the hematin speciation?

- Hematin monomer?
- Hematin dimer?
- Crystalline hemozoin?

Compresence of various species is probable

EXAFS results: fitting model

pH = 5.0, hematin only solution

Fe Kα edge

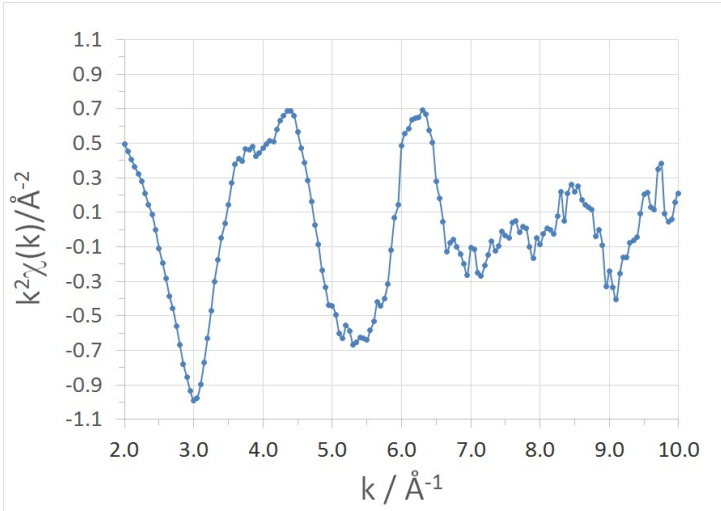

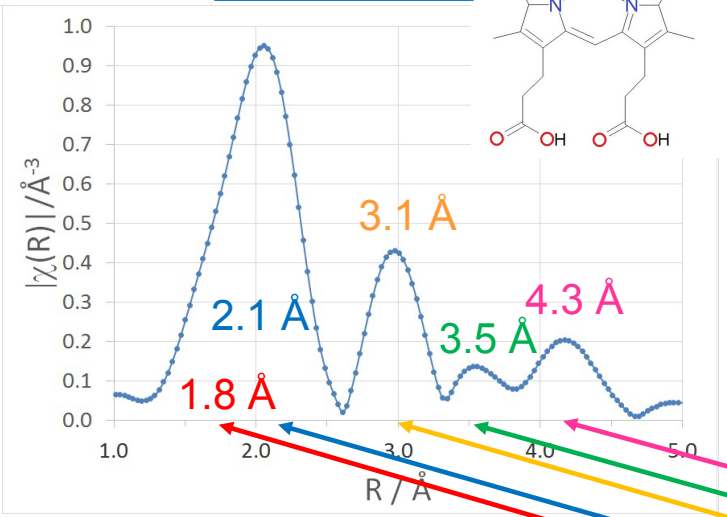

The basic protoporphyrin structural model accounts for the observed FT peaks in the real space.

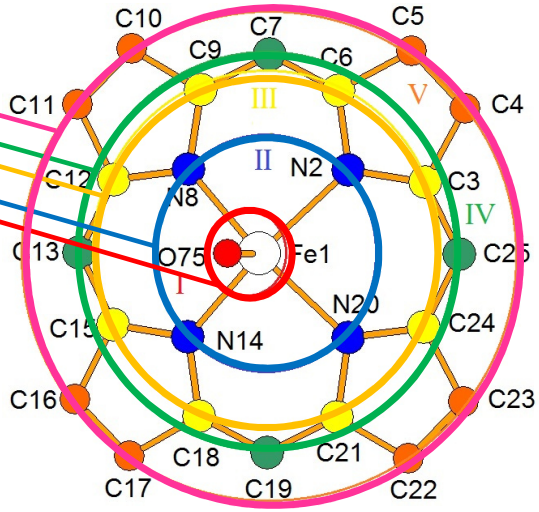

What is the hematin speciation?

- Hematin monomer?
- Hematin dimer?
- Crystalline hemozoin?

Compresence of various species is probable

Interpreting the signal on absolute grounds is difficult

Difference spectrum

pH = 5.0

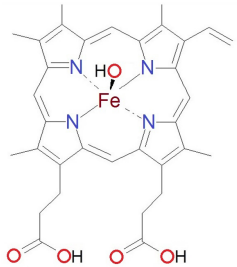

Fe Kα edge

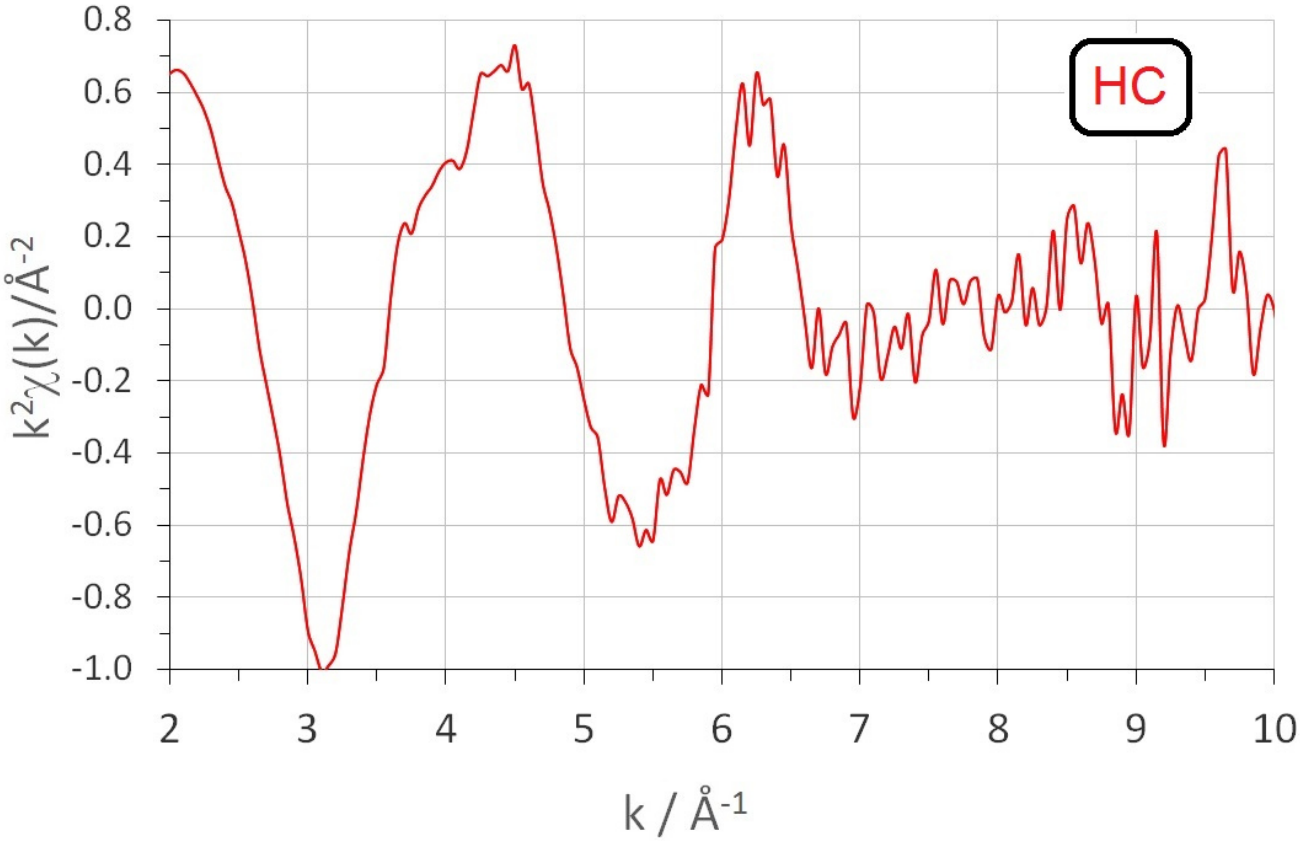

Hematin + CQ solution

Difference spectrum

pH = 5.0

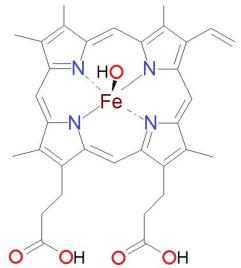

Fe Kα edge

~ - 2 eV shift in the E_0 edge energy

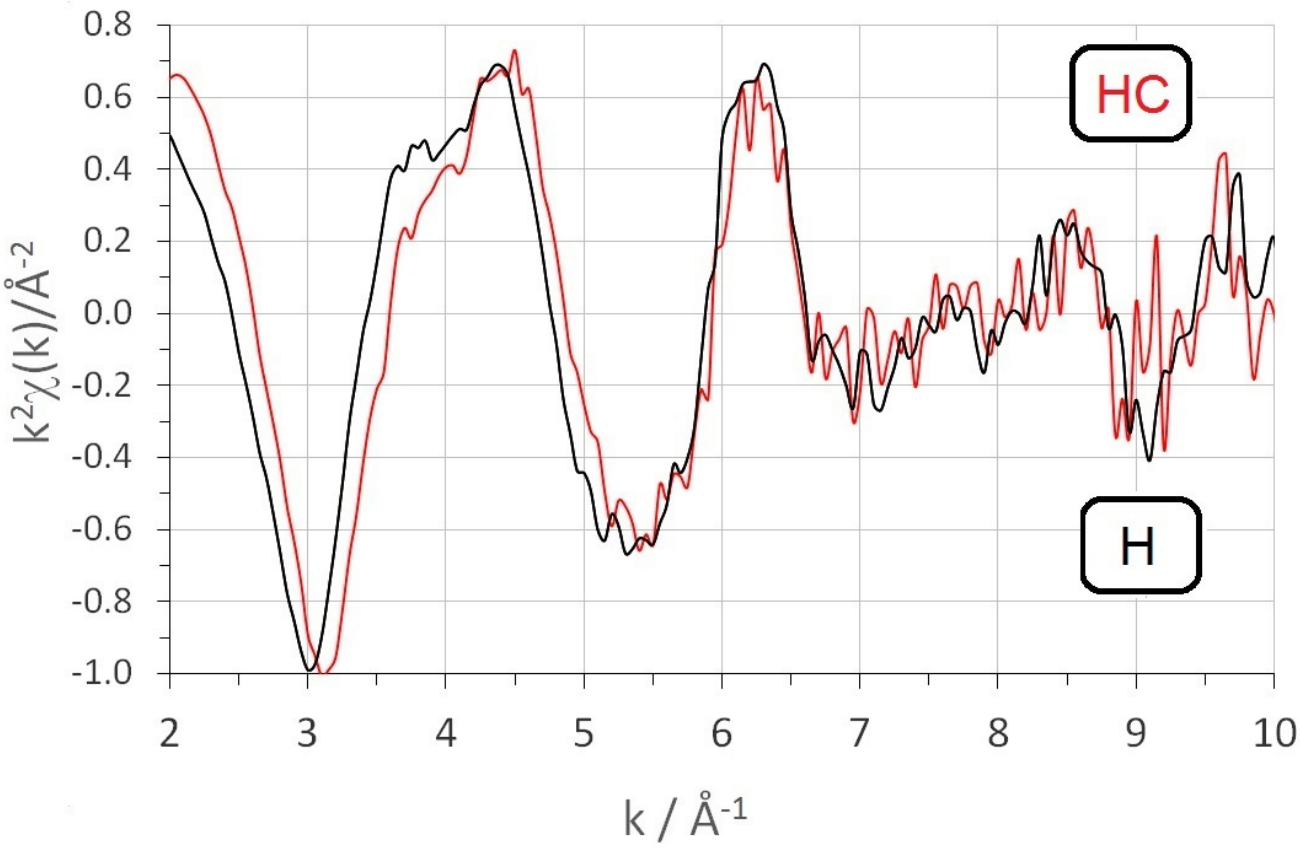

Hematin + CQ solution

Hematin-only solution

Difference spectrum

pH = 5.0

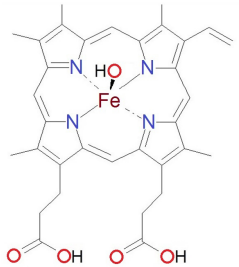

Fe Kα edge

~ - 2 eV shift in the E_0 edge energy

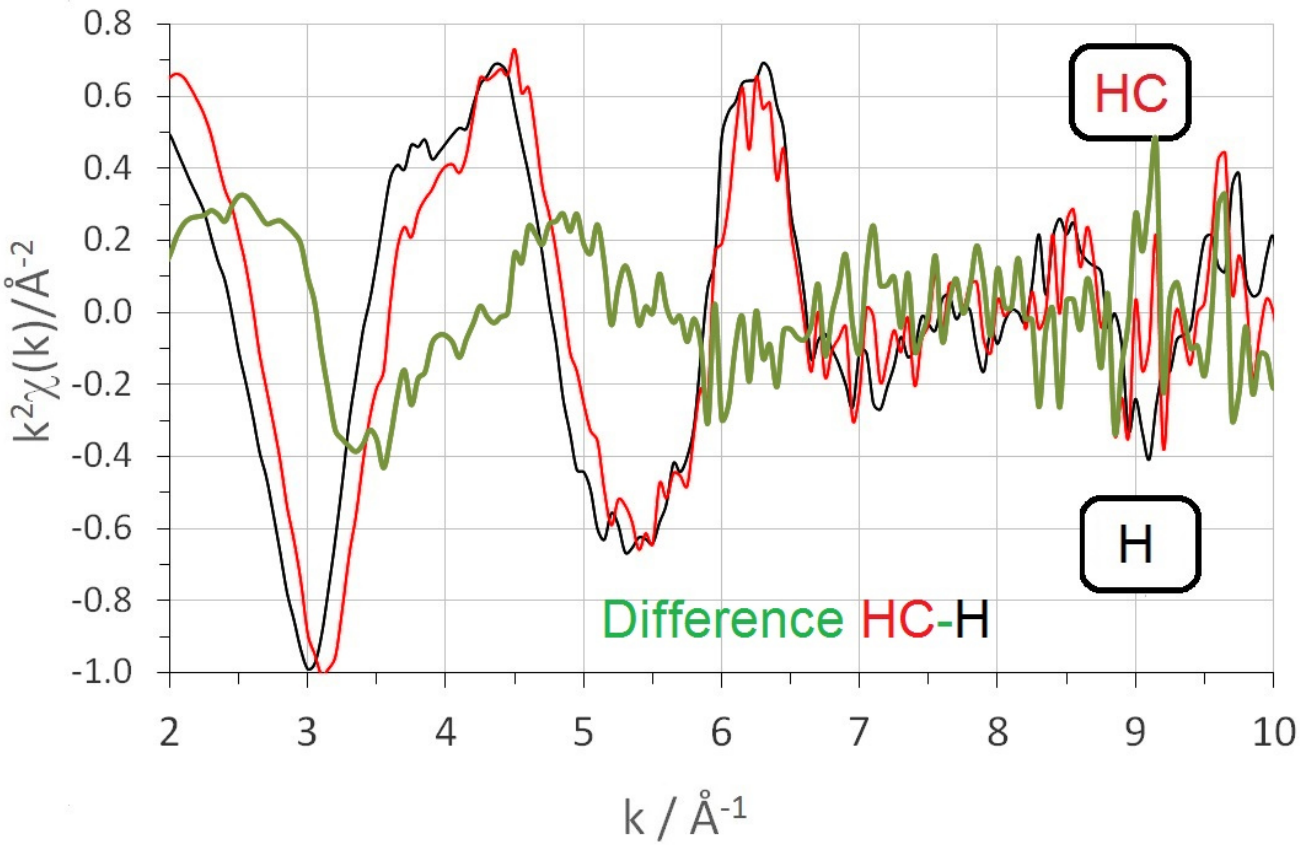

Hematin + CQ solution

Net effect of CQ in the k space

Hematin-only solution

Fitting the difference signal

pH = 5.0

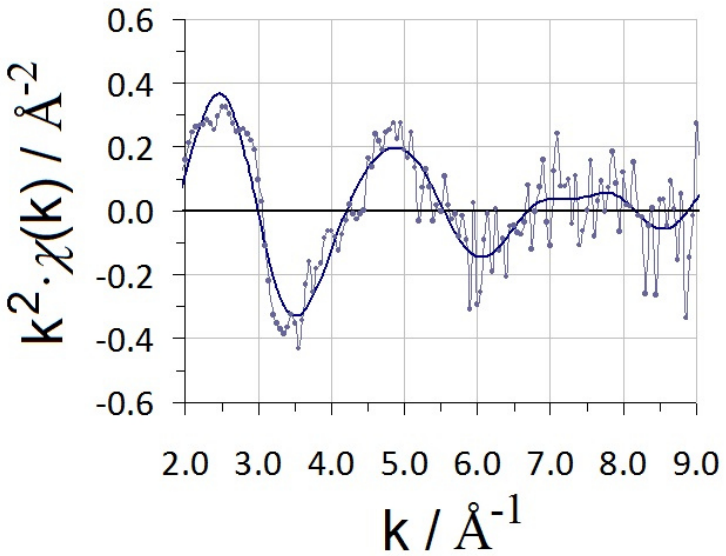

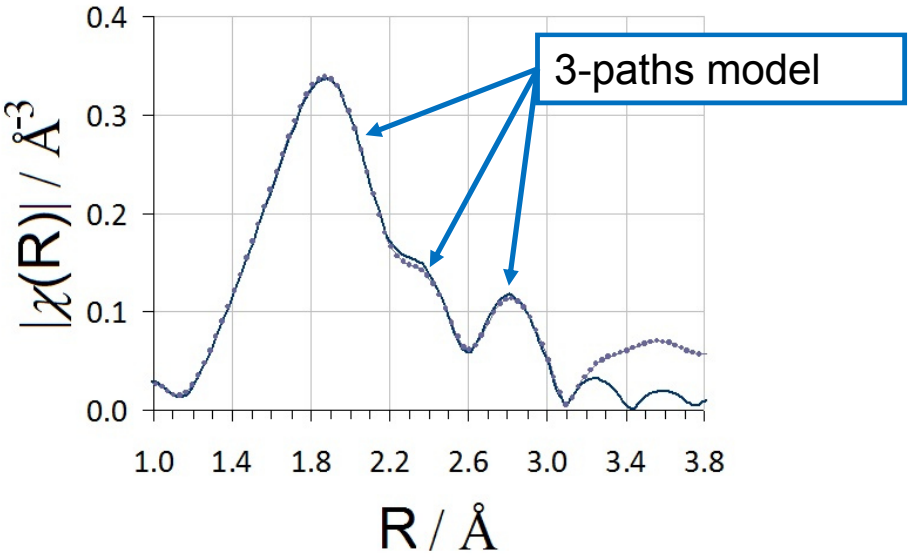

R=0.0699
Reduced χ^2=9.1
DoF=3

Parameter	Path to which it is applied	Value
S_0^2	All	1.1(4)
ΔE_0	All	-6(3) eV
σ^2	All	0.008(6) Å^2
r_1	**Fe-N1**	**1.77(3) Å**
r_2	**Fe-C2**	**2.51(6) Å**
r_2	**Fe-C8**	**2.82(6) Å**

Interpreting the fitting

pH = 5.0

Parameter	Path to which it is applied	Value
r_1	Fe-N1	1.77(3) Å
r_2	Fe-C2	2.51(6) Å
r_2	Fe-C8	2.82(6) Å

A direct Fe-N bond is consistent with previous solid-state NMR findings
de Dios *et al.*, *J. Phys. Chem. A* **2003**, *107*, 5821

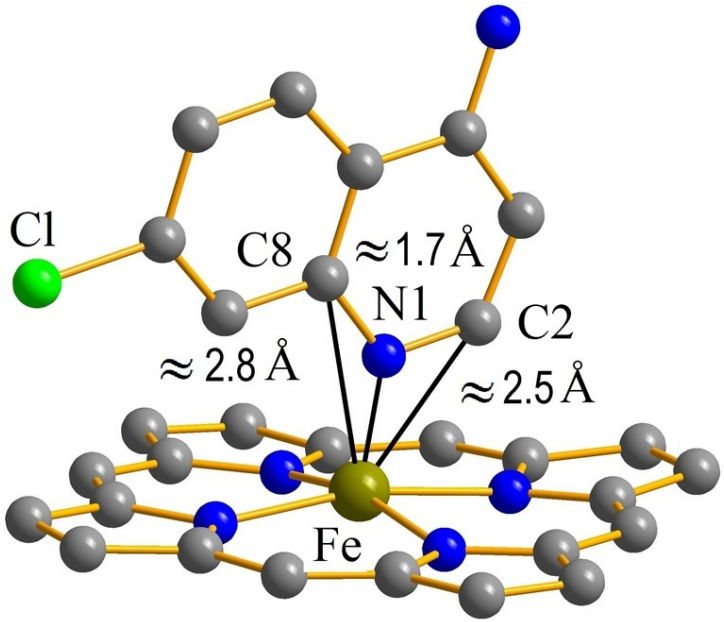

Does such an interaction geometry correspond to a true energy minimum on the PES?

Position of the CQ lateral hydrocarbon chain?

Macetti et al., *Physica Scripta* 2016, **91** 023001

DFT results

UB3LYP 6-311G(p,d), corrected for dispersion

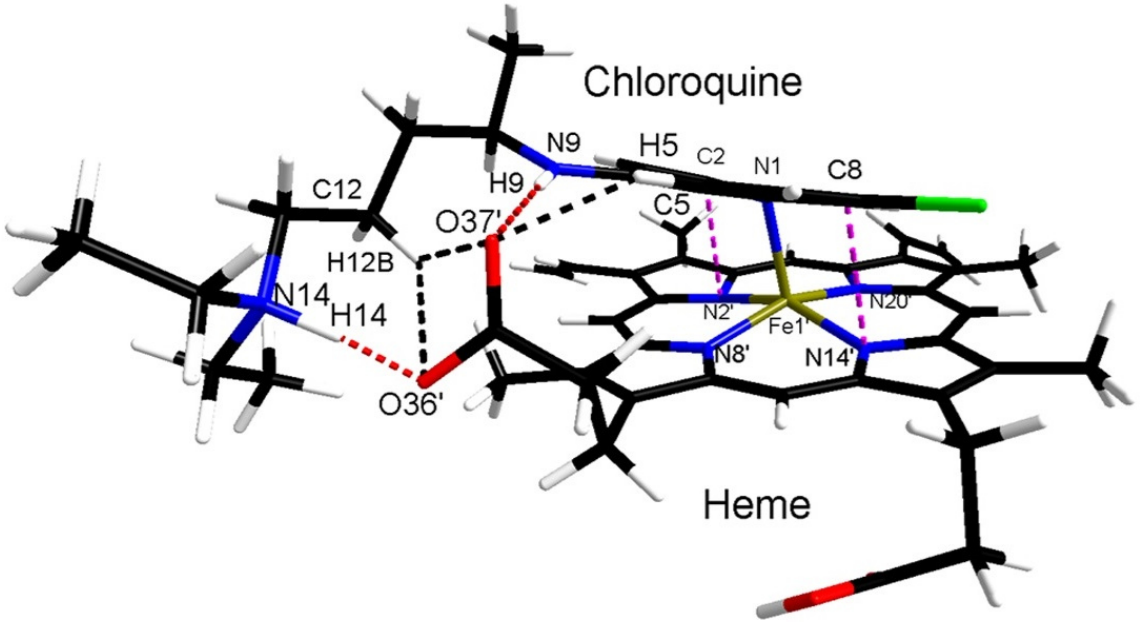

Macetti *et al Crystal Growth Des.* 2016. 16, 6043

DFT results

UB3LYP 6-311G(p,d), corrected for dispersion

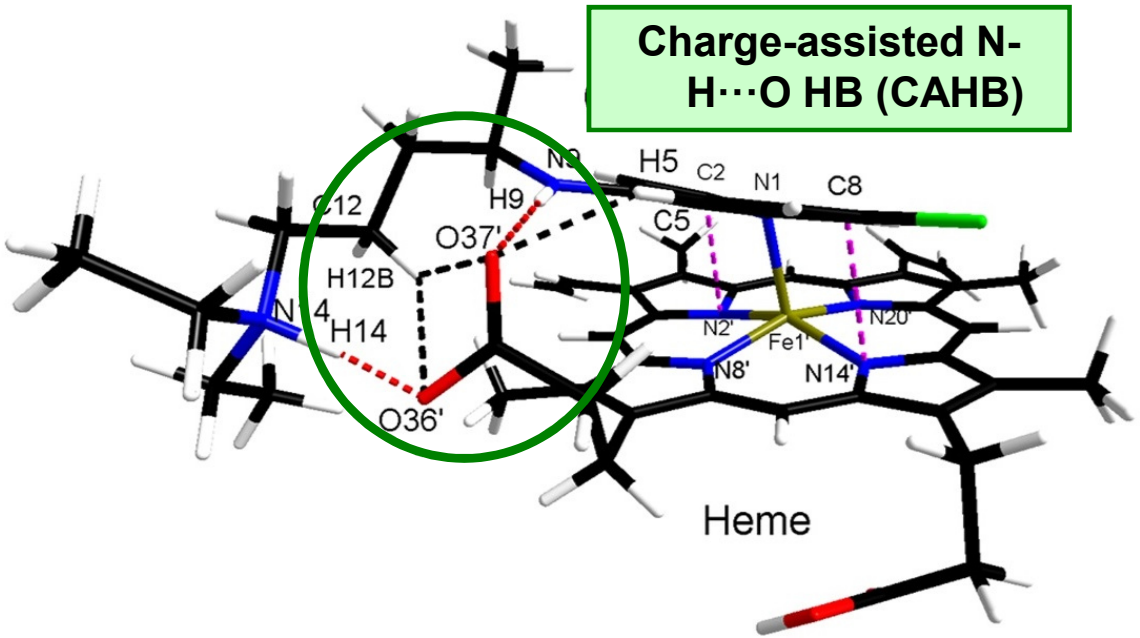

Macetti *et al Crystal Growth Des.* 2016. 16, 6043

DFT results

UB3LYP 6-311G(p,d), corrected for dispersion

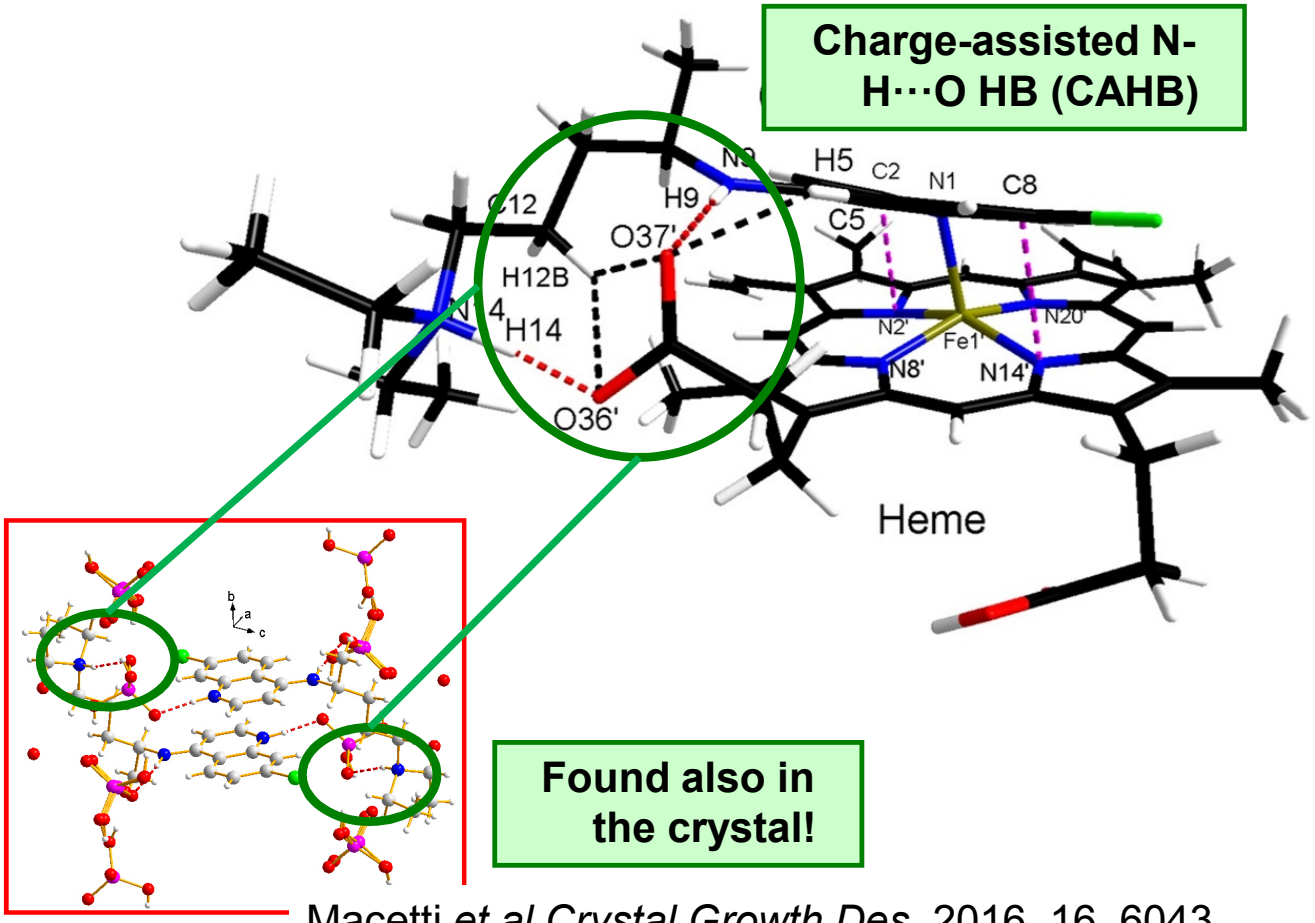

Macetti *et al Crystal Growth Des.* 2016. 16, 6043

DFT Energetics

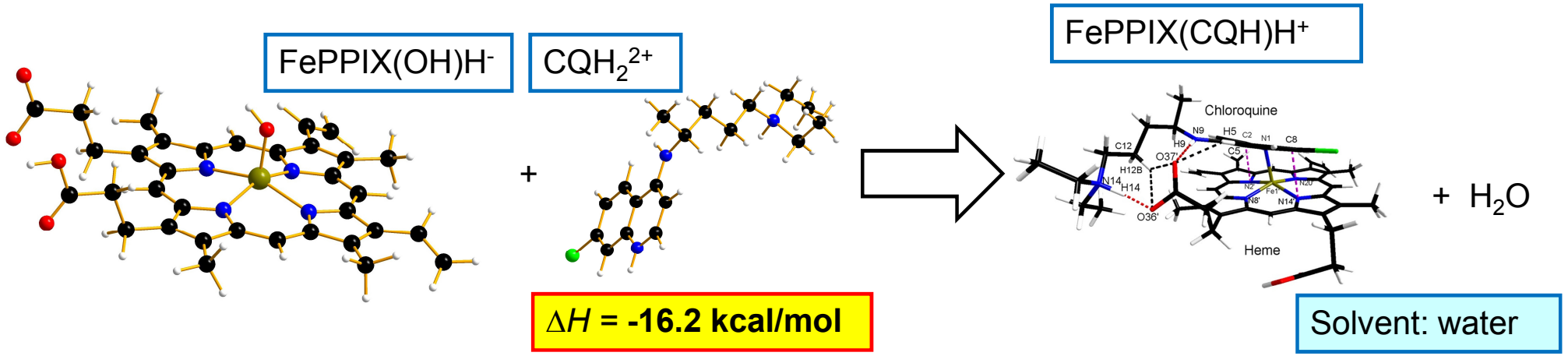

To be compared with **calorimetric results** for the heme:CQ association in water

ΔH = **-10(1) kcal/mol** @ pH = 6.5, T = 37 °C [Dorn *et al., Biochem. Pharmacol*. **1998**, *55*, 727]

ΔH = **-7.9 kcal/mol** @ pH = 5.6, T = 28 °C [Vippagunta *et al., J. Med. Chem*. **1999**, *42*, 4630]

DFT Energetics

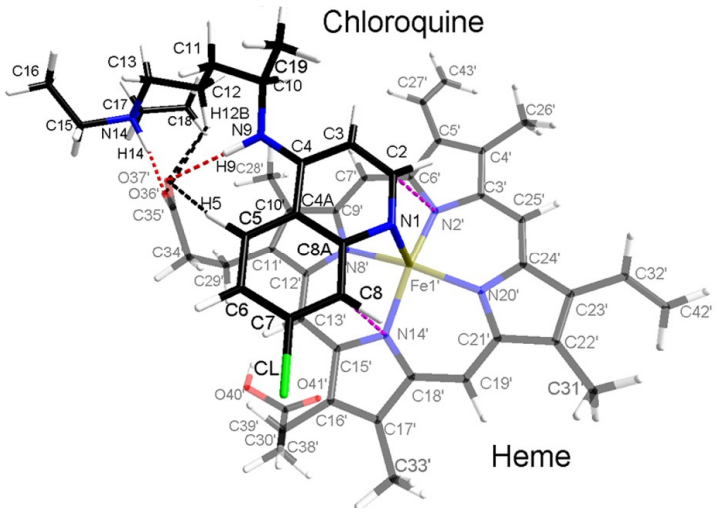

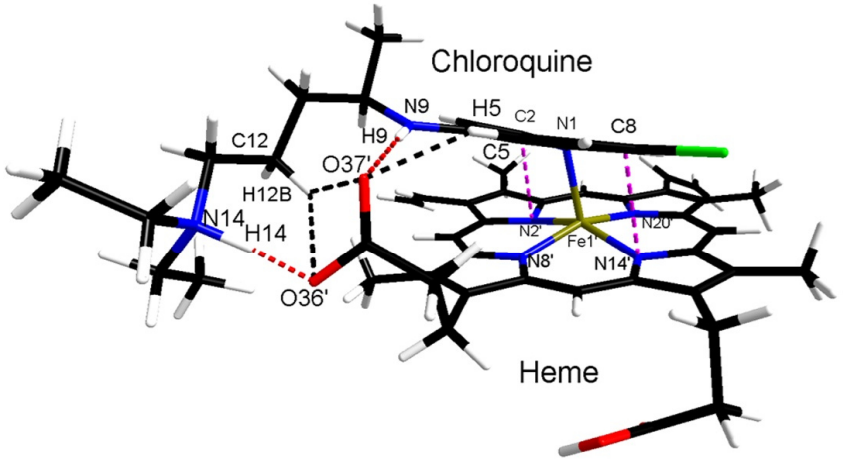

Heme:CQ interaction energy (in vacuo): -106 kcal/mol, $E_{\pi\cdots\pi}$ = -31(2) kcal/mol (Zhikol)

Macetti *et al Crystal Growth Des.* 2016. 16, 6043

DFT Energetics

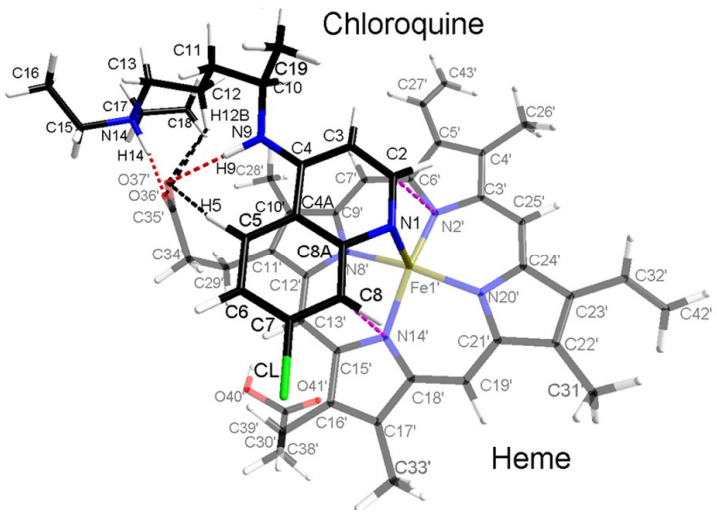

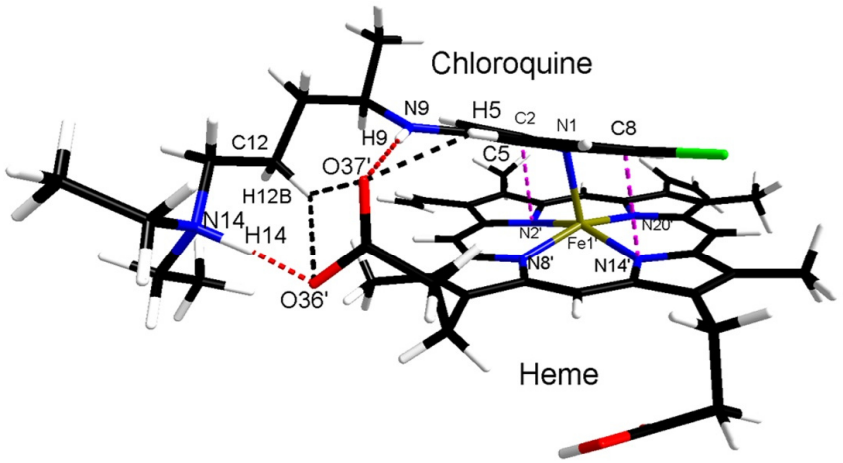

Heme:CQ interaction energy (in vacuo): -106 kcal/mol, $E_{\pi\cdots\pi}$ = -31(2) kcal/mol (Zhikol)

Most of the interaction energy (~ -63 kcal/mol) comes from strong charge-assisted hydrogen bonds, as estimated through the NBO analysis of the first-order density matrix

Macetti *et al Crystal Growth Des.* 2016. 16, 6043

Conclusions

$\pi\cdots\pi$ interactions used to be believed as the main actors of the heme:CQ recognition process

Conclusions

$\pi\cdots\pi$ interactions used to be believed as the main actors of the heme:CQ recognition process

They are indeed found in the solid state, both in chloroquine and in piperaquine, but the interaction between positively charged facing quinoline rings is **strongly repulsive**: and **so should be in solution** between protonated quinoline and Fe(III) in heme

Conclusions

$\pi\cdots\pi$ interactions used to be believed as the main actors of the heme:CQ recognition process

They are indeed found in the solid state, both in chloroquine and in piperaquine, but the interaction between positively charged facing quinoline rings is **strongly repulsive**: and **so should be in solution** between protonated quinoline and Fe(III) in heme

EXAFS and DFT data are consistent with a heme:CQ condensation adduct where a direct Fe-N bond is exploited

Conclusions

$\pi\cdots\pi$ interactions used to be believed as the main actors of the heme:CQ recognition process

They are indeed found in the solid state, both in chloroquine and in piperaquine, but the interaction between positively charged facing quinoline rings is **strongly repulsive**: and **so should be in solution** between protonated quinoline and Fe(III) in heme

EXAFS and DFT data are consistent with a heme:CQ condensation adduct where a direct Fe-N bond is exploited

Charge-assisted hydrogen bonds between heme propionate and lateral CQ hydrocarbon chain are as important as **stacking interactions** to stabilize the adduct: **they are both active part of the drug pharmacophore**

Acknowledgements

Prof. Silvia Rizzato

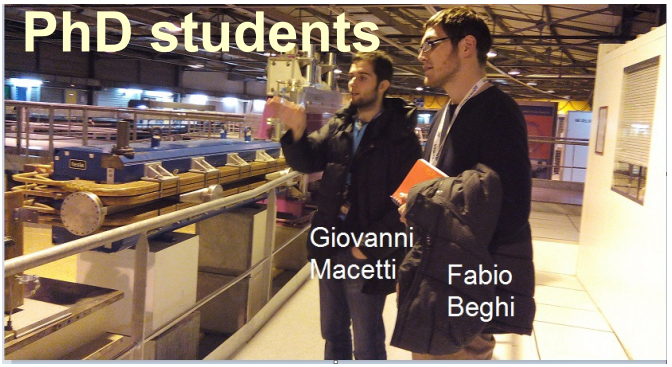

Funding: Development Plan for Athenaeum - Line B – 2016-2017 (project NOVAQ)

BM26A CH-4861 and CH-4370

Funding a PhD bursary

ISCRA C initiative (Project MODELPIP)

Dr. Laura Loconte

Dr. Lucia Silvestrini

Andrea Gionda

Pietro Sacchi

MScstudents

3rd Italian Crystal Growth congress ICG2017

Milano, 20-21 November 2017

Italian Crystal Growth 2017

materials and methods in crystal growth

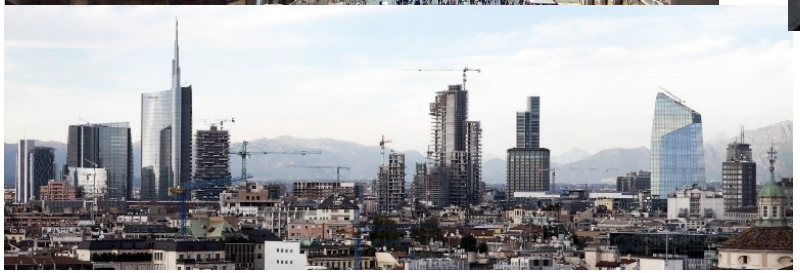

UNIVERSITA' DEGLI STUDI DI MILANO BICOCCA

UNIVERSITAS STUDIORUM MEDIOLANENSIS

... hoping to see you in Milan the next November!

Thank you for your kind attention

Implementing the EXAFS fitting

pH = 5.0

The DFT-predicted adduct was used to generate a novel set of backscattering paths

Rigid translations of the drug with respect to Fe centre were refined:
1 S_0^2 and 1 Δr parameter for the whole CQ molecule (+2 variables)

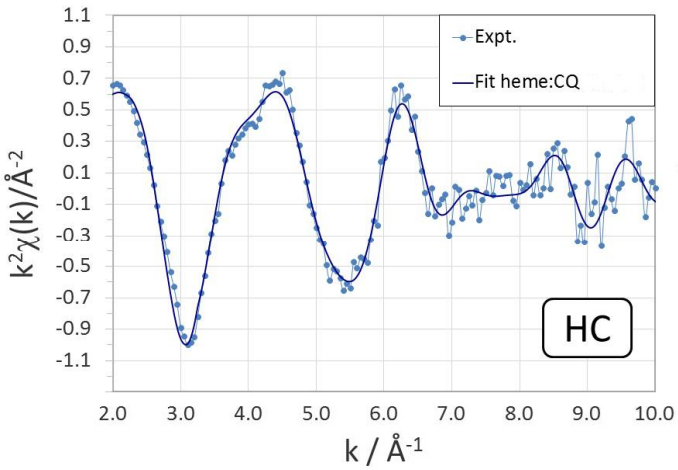

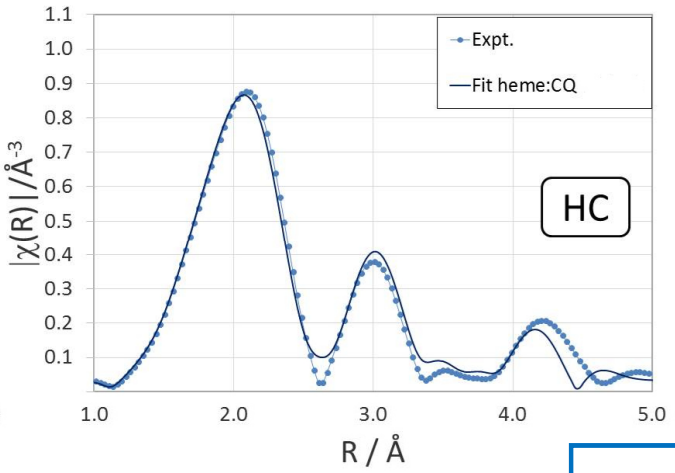

Heme+CQ

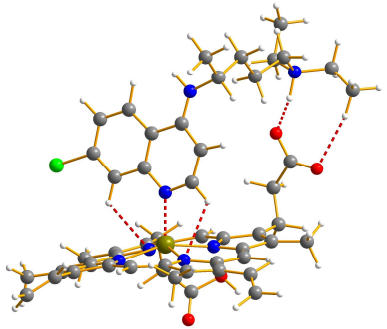

FePPIX(CQH)H⁺

Statistics
Reduced χ^2 = 17.7
R = 0.026
DoF = 5

Hamilton R-test*:
Satisfied (with a confidence level of 75 %) with respect to the model based on monomeric hematin

* Hamilton, *Acta Crystallogr*. **1965,** *A18*, 502

Macetti et al., *Physica Scripta* 2016, **91** 023001

Drug resistance

2001

Cited more than 300 times

Drug resistance in malaria

Peter B. Bloland

World Health Organization

wellcome trust

ing | Managing a grant | Education resources | News | Invest

Drug-resistant malaria has spread to critical border regions of South-east Asia

31 July 2014

2014

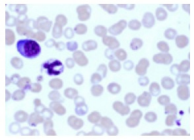

Drug-resistant malaria parasites have spread to critical border regions of South-east Asia, seriously threatening global malaria control and elimination programmes, according to a study published in the 'New England Journal of Medicine'.

Artemisinin Resistance in Cambodia: A Clinical Trial Designed to Address an Emerging Problem in Southeast Asia

Harald Noedl,[1] Youry Se,[2] Sabaithip Sriwichai,[2] Kurt Schaecher,[2] Paktiya Teja-Isavadharm,[2] Bryan Smith,[2] Wiriya Rutvisuttinunt,[2] Delia Bethell,[2] Sittidech Surasri,[2] Mark M. Fukuda,[2] Duong Socheat,[3] and Lon Chan Thap[2]

Noedl *et al. Clinical Infectious Disease*, **2010**, *51*, e82

MALARIA JOURNAL

Lubell *et al. Malaria Journal* **2014**, *13*, 452

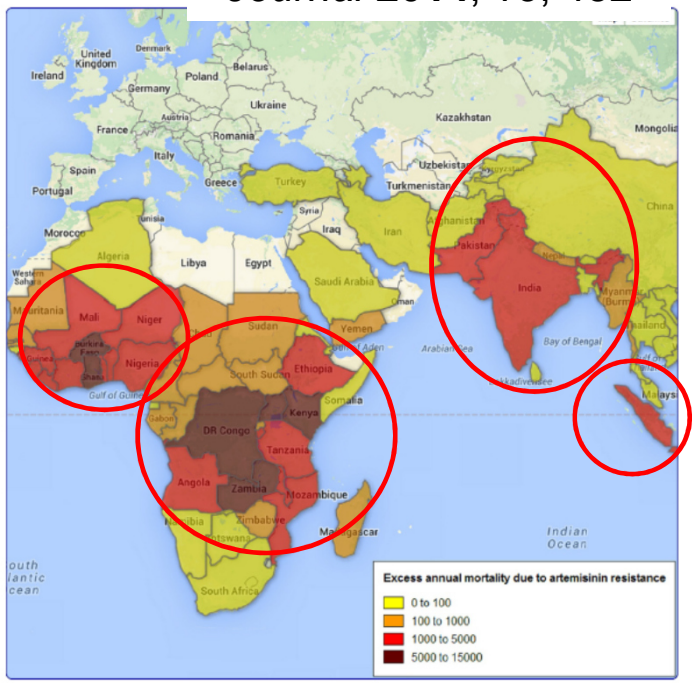

Artemisinin resistance – modelling the potential human and economic costs

Lubell *et al.*

BioMed Central

Lubell *et al. Malaria Journal* 2014, 13:452
http://www.malariajournal.com/content/13/1/452

Other EXAFS results

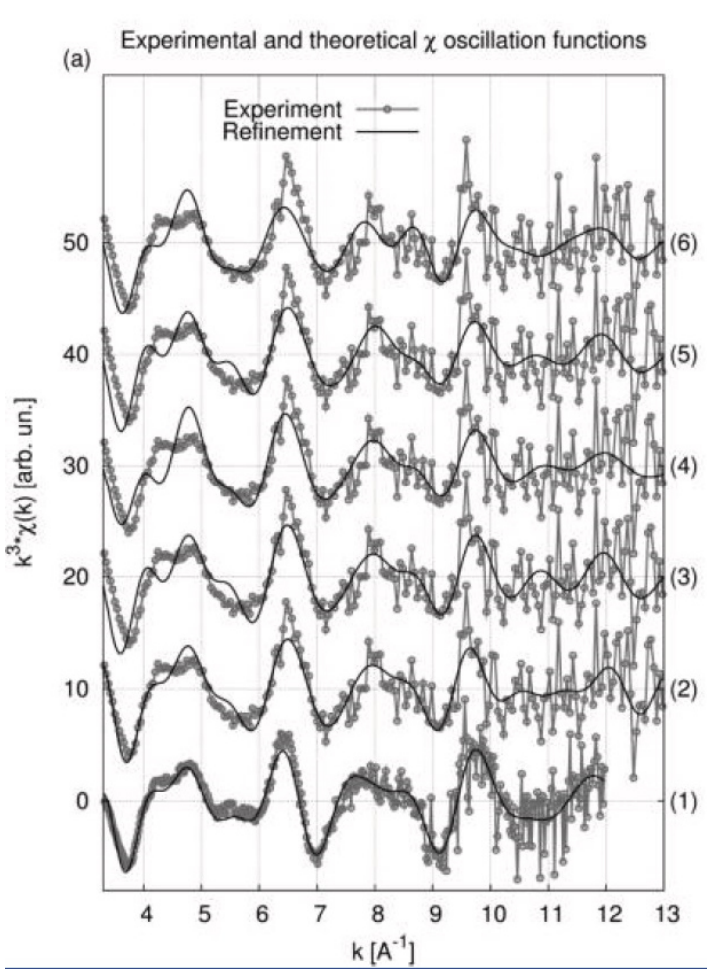

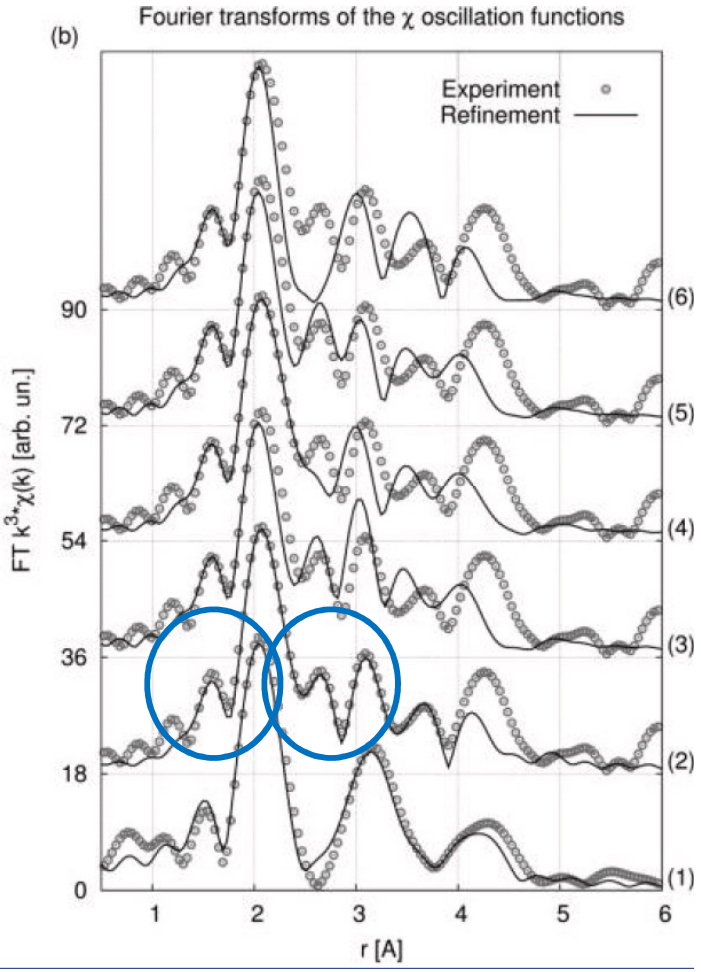

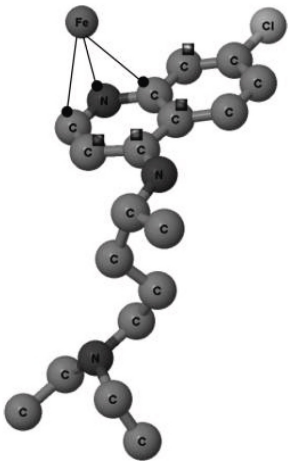

- DMSO as solvent
- Mesohematin anhydride as substrate

Walczak *et al. J. Phys. Chem. B* **2011**, *115*, 1145

DFT Energetics

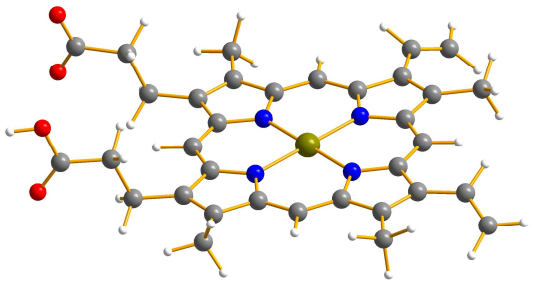

FePPIXH

Solvent: water

+ H_2O

-42.6 kJ/mol

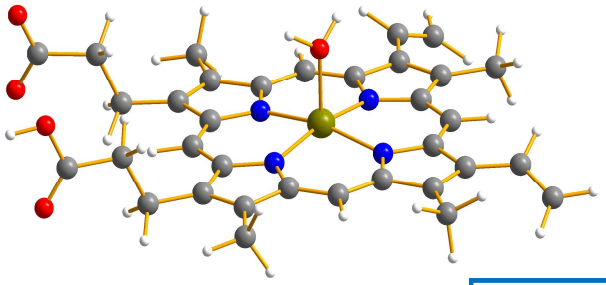

FePPIX(H_2O)H

+ OH^-

-245.6 kJ/mol

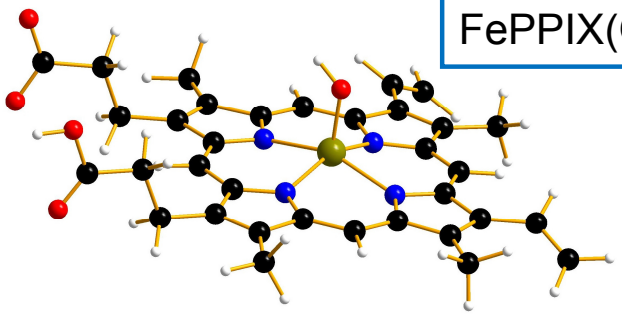

FePPIX(OH)H^-

+ CQH^+

-110.8 kJ/mol

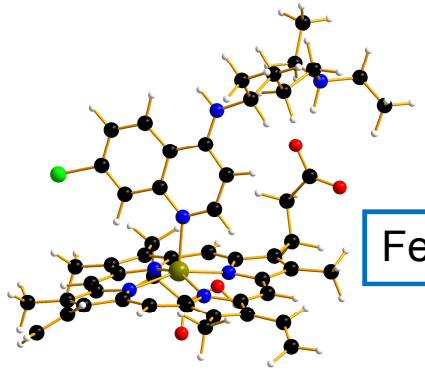

FePPIX(CQH)H^+

Periodic simulation results

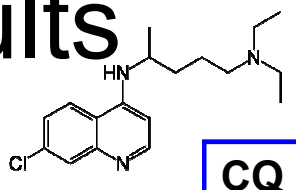

CQ

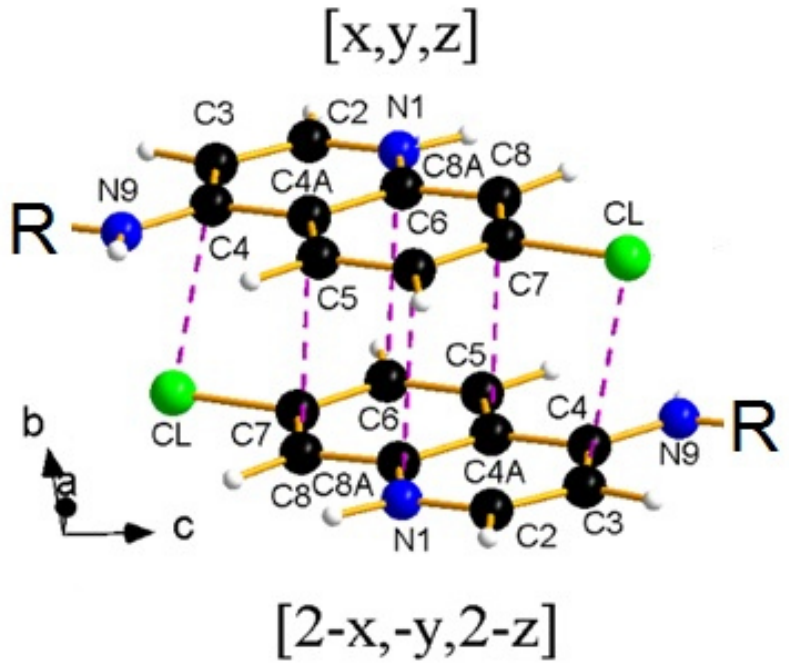

From the topological analysis of the charge density according to the Quantum Theory of Atoms in Molecules, atomic interaction lines (AILs) found between the facing **rings atoms (C,N and Cl)**

. Macetti *et al Crystal Growth Des.* 2016. 16, 6043

Periodic simulation results

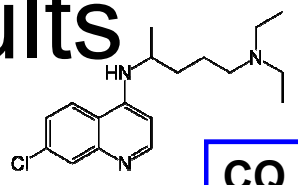

CQ

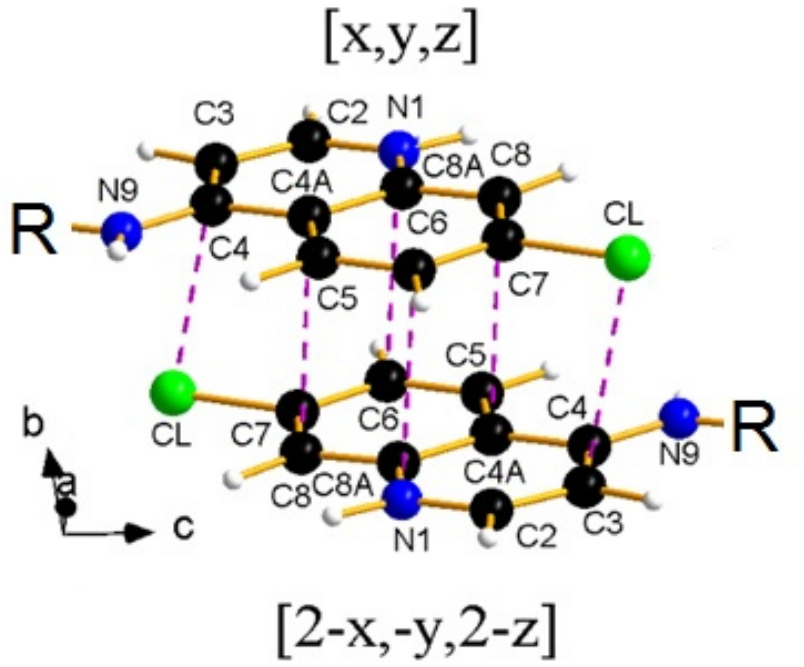

From the topological analysis of the charge density according to the Quantum Theory of Atoms in Molecules, atomic interaction lines (AILs) found between the facing **rings atoms (C,N and Cl)**

The most representative point is the bond critical point (bcp), where $\nabla\rho(\mathbf{r})$ vanishes.

Contact	$d_{A\cdots A}$ / Å	ρ_{bcp} /au	$\nabla^2\rho_{bcp}$ /au	G_{bcp}	V_{bcp}
C3···Cl	3.4497	0.007	0.022	12.4	-10.1
C6···N1	3.4857	0.005	0.021	10.1	-6.6
C4A···C8	3.5204	0.004	0.019	8.6	-5.0

. Macetti *et al Crystal Growth Des.* 2016. 16, 6043

Periodic simulation results

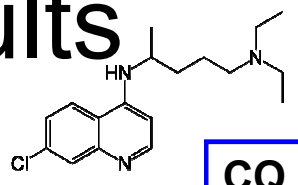

CQ

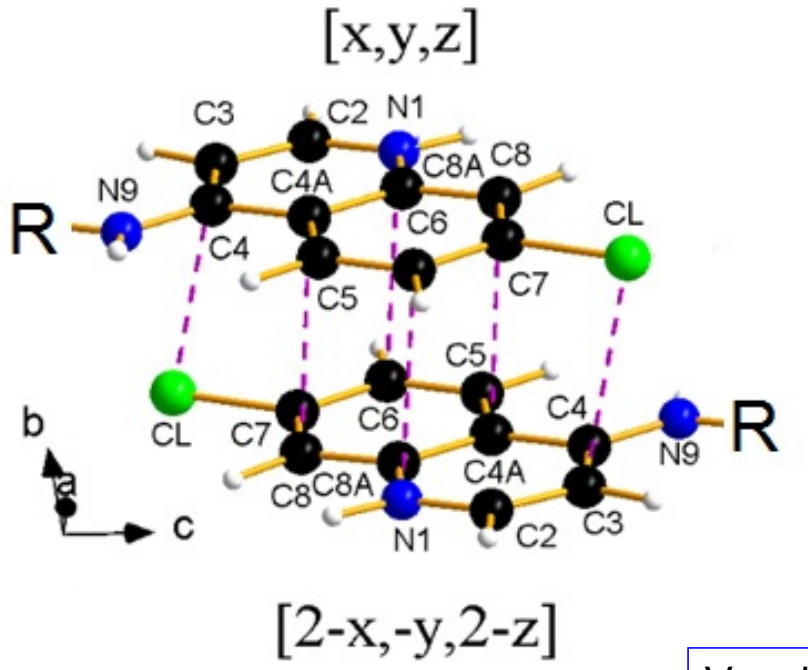

From the topological analysis of the charge density according to the Quantum Theory of Atoms in Molecules, atomic interaction lines (AILs) found between the facing **rings atoms (C,N and Cl)**

The most representative point is the bond critical point (bcp), where $\nabla\rho(\mathbf{r})$ vanishes.

Contact	$d_{A\cdots A}$ / Å	ρ_{bcp} /au	$\nabla^2\rho_{bcp}$ /au	G_{bcp}	V_{bcp}
C3···Cl	3.4497	0.007	0.022	12.4	-10.1
C6···N1	3.4857	0.005	0.021	10.1	-6.6
C4A···C8	3.5204	0.004	0.019	8.6	-5.0

Very low charge density at the bond critical point

. Macetti *et al Crystal Growth Des.* 2016. 16, 6043

Periodic simulation results

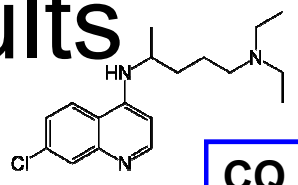

CQ

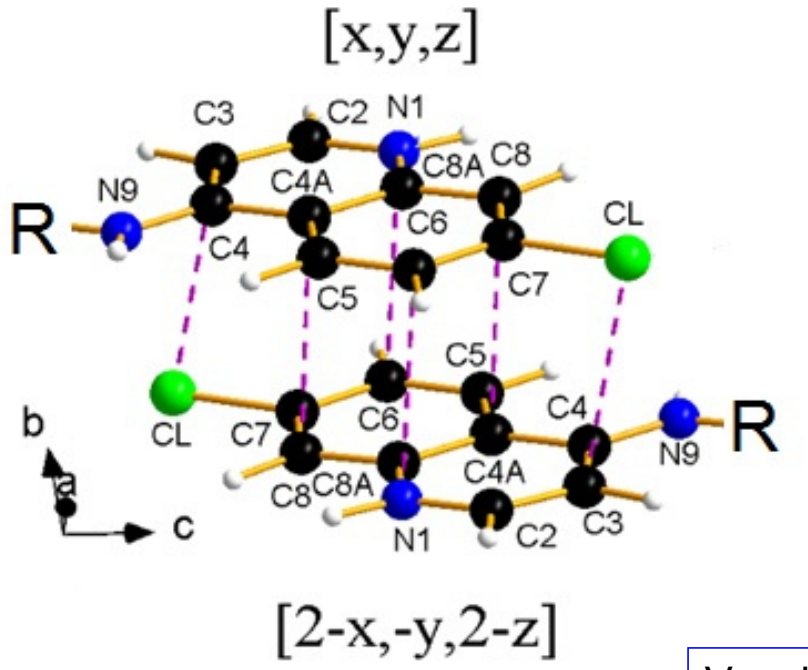

From the topological analysis of the charge density according to the Quantum Theory of Atoms in Molecules, atomic interaction lines (AILs) found between the facing **rings atoms (C,N and Cl)**

The most representative point is the bond critical point (bcp), where $\nabla\rho(\mathbf{r})$ vanishes.

Contact	$d_{A\cdots A}$ / Å	ρ_{bcp} /au	$\nabla^2\rho_{bcp}$ /au	G_{bcp}	V_{bcp}
C3···Cl	3.4497	0.007	0.022	12.4	-10.1
C6···N1	3.4857	0.005	0.021	10.1	-6.6
C4A···C8	3.5204	0.004	0.019	8.6	-5.0

Very low charge density at the bond critical point

Positive Laplacian: local charge depletion

. Macetti *et al Crystal Growth Des.* 2016. 16, 6043

Periodic simulation results

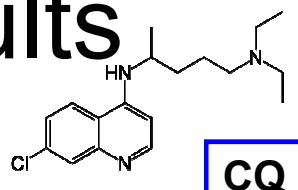

CQ

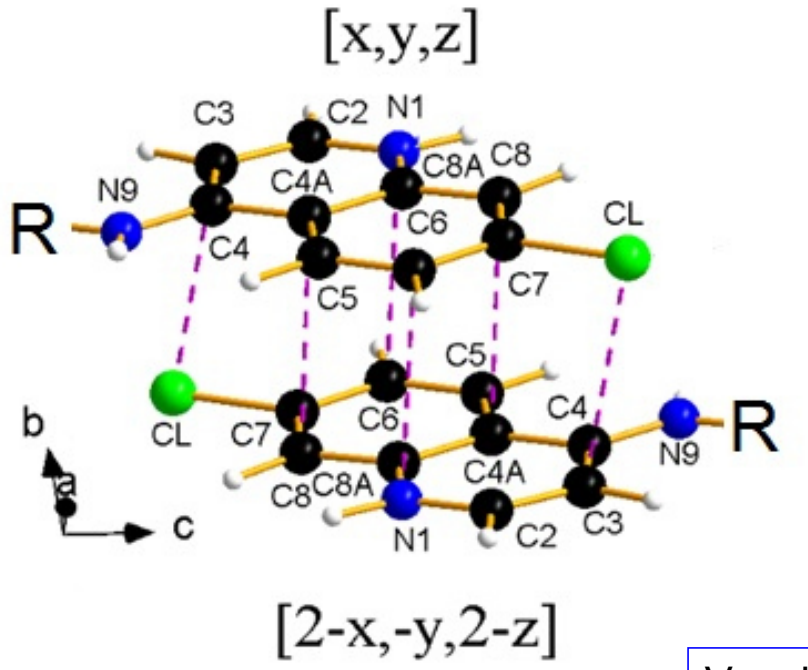

From the topological analysis of the charge density according to the Quantum Theory of Atoms in Molecules, atomic interaction lines (AILs) found between the facing **rings atoms (C,N and Cl)**

The most representative point is the bond critical point (bcp), where $\nabla\rho(\mathbf{r})$ vanishes.

Contact	$d_{A\cdots A}$ / Å	ρ_{bcp} /au	$\nabla^2\rho_{bcp}$ /au	G_{bcp}	V_{bcp}
C3···Cl	3.4497	0.007	0.022	12.4	-10.1
C6···N1	3.4857	0.005	0.021	10.1	-6.6
C4A···C8	3.5204	0.004	0.019	8.6	-5.0

Very low charge density at the bond critical point

Positive Laplacian: local charge depletion

Electronic kinetic energy density dominating over the potential energy density

. Macetti *et al Crystal Growth Des.* 2016. 16, 6043

X-ray results

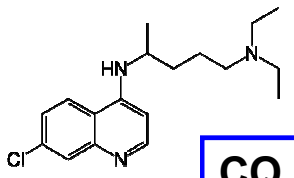

CQ

• **CQ** · 2($H_2PO_4^-$) · 2(H_2O) salt

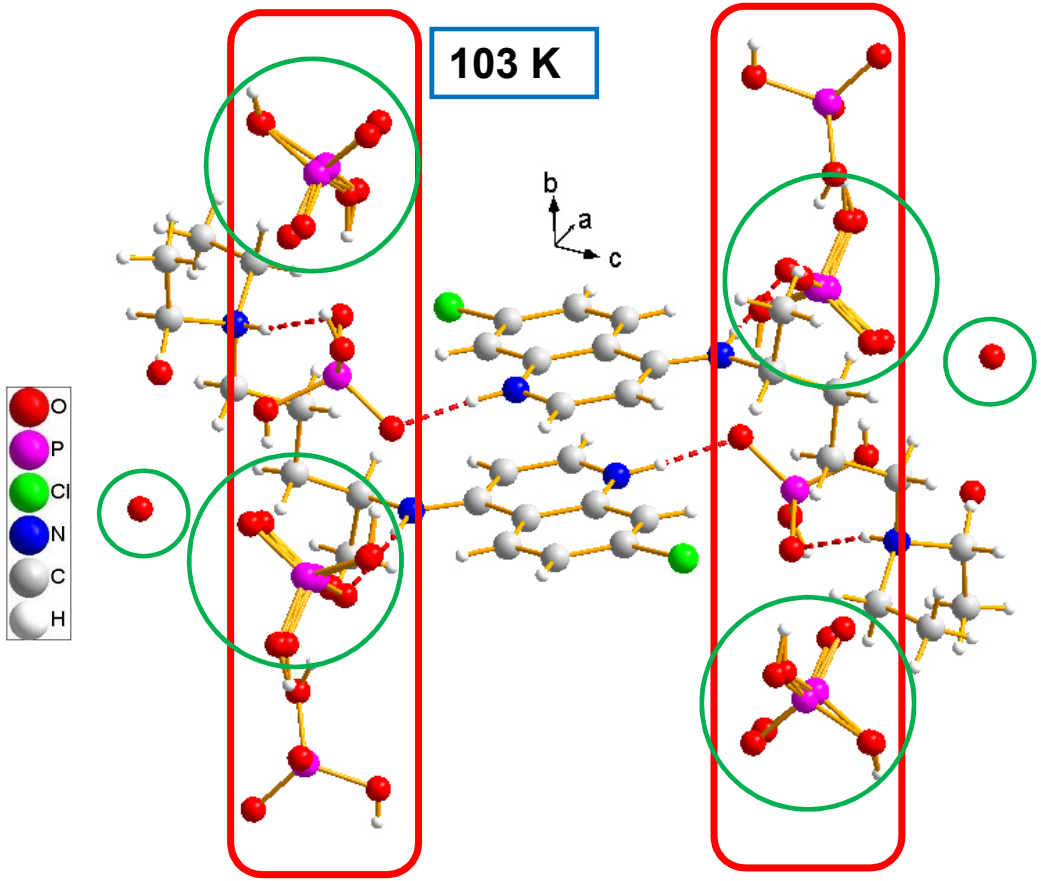

$\sin(\theta/\lambda)_{max}$ = 1.0 Å^{-1}
λ = 0.71073 Å
CCDC number = 1471834

Space Group = $P2_1/c$ (14)
a = 9.7212(1) Å
b = 16.7733(2) Å
c = 15.6966(2) Å
β = 105.1788(2) Å
V = 2470.14(5) Å

Disorder of one $H_2PO_4^-$ ion and water

Infinite phosphate chains along the b axis

X-ray results

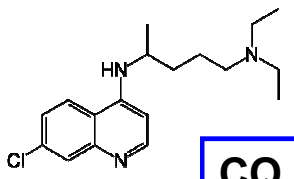

CQ

• **CQ** · 2($H_2PO_4^-$) · 2(H_2O) salt

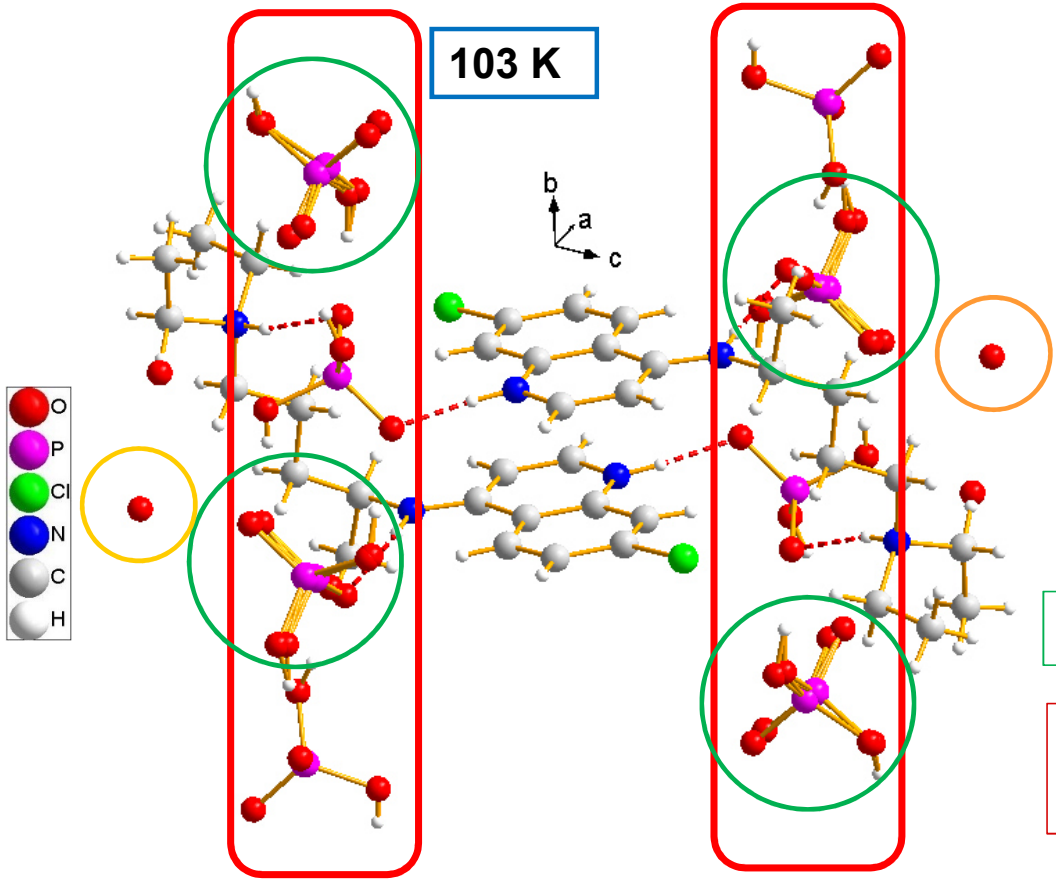

$\sin(\theta/\lambda)_{max}$ = 1.0 Å^{-1}
λ = 0.71073 Å
CCDC number = 1471834

Space Group = $P2_1/c$ (14)
a = 9.7212(1) Å
b = 16.7733(2) Å
c = 15.6966(2) Å
β = 105.1788(2) Å
V = 2470.14(5) Å

Disorder of one $H_2PO_4^-$ ion

Infinite phosphate chains along the b axis

Orientation of co-crystallized water cannot be unequivocally determined

X-ray results

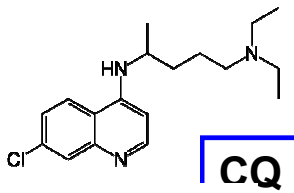

CQ

• **CQ** · 2($\mathbf{H_2PO_4^-}$) · 2(H_2O) salt

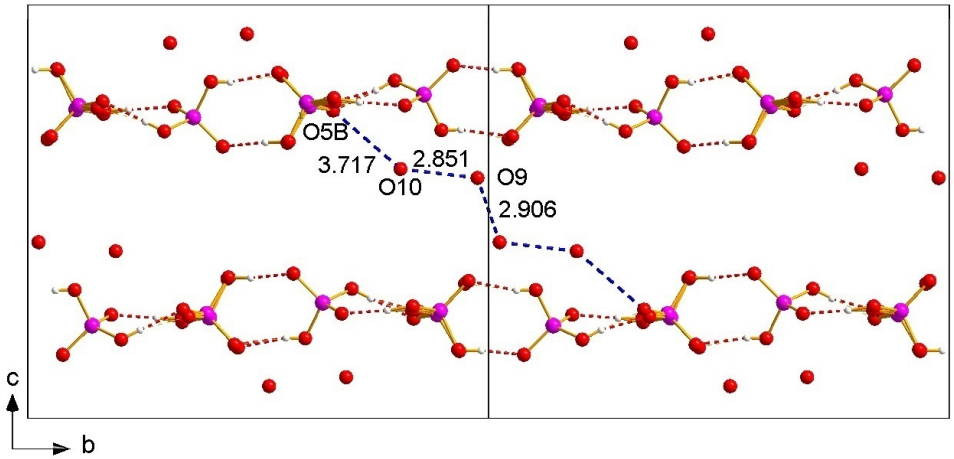

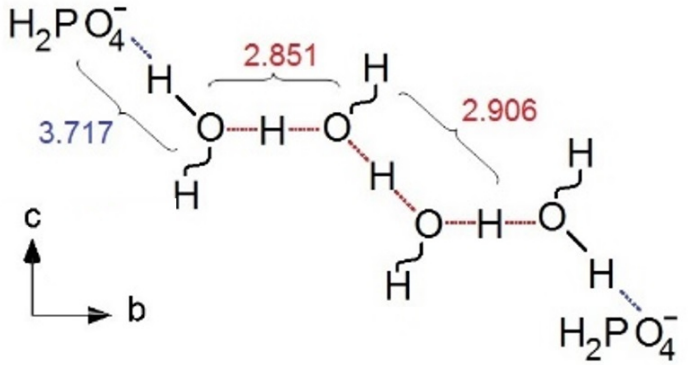

$P2_1/c$ symmetry is not “completely” fulfilled

Very difficult to extract the experimental charge density

X-ray results

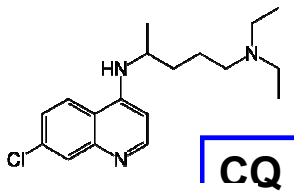

CQ

• **CQ** · 2($\mathbf{H_2PO_4^-}$) · 2(H_2O) salt

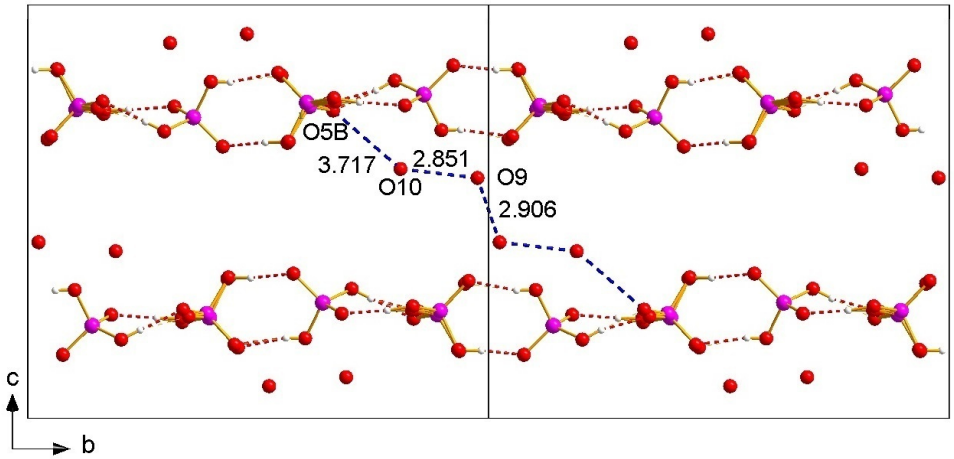

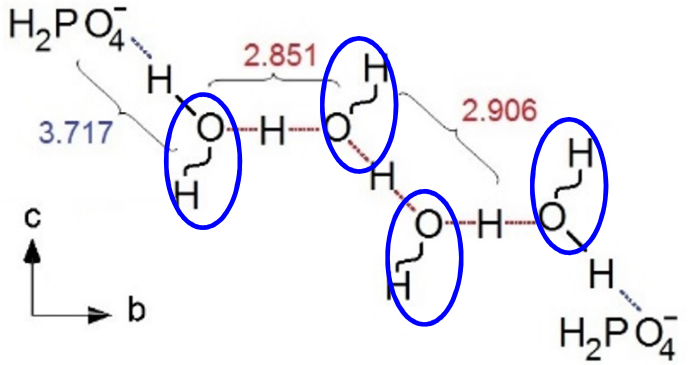

Unknown dihedral

$P2_1/c$ symmetry is not “completely” fulfilled

Very difficult to extract the experimental charge density

X-ray results

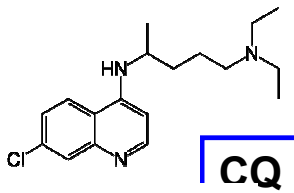

CQ

• **CQ** · 2(**$H_2PO_4^-$**) · 2(H_2O) salt

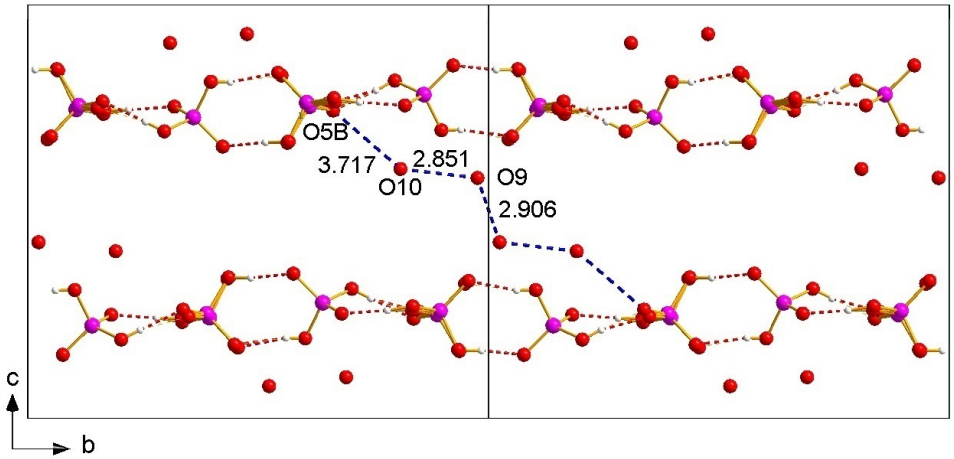

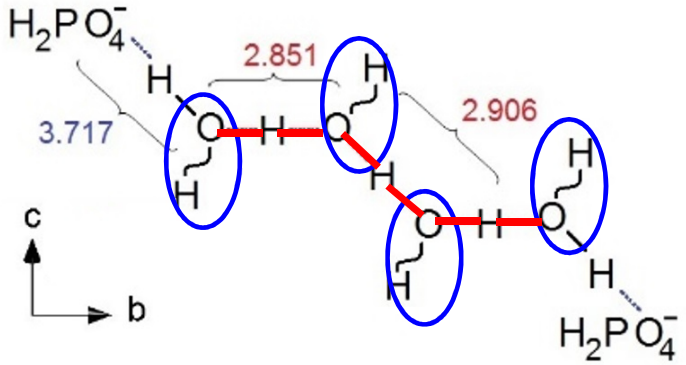

Unknown dihedral

Unknown bond type (covalent or HB?)

$P2_1/c$ symmetry is not “completely” fulfilled

HB frustration

Very difficult to extract the experimental charge density

X-ray results

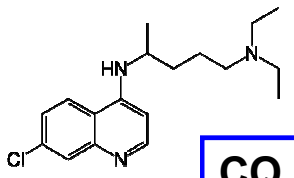

CQ

• **CQ** · 2(**$H_2PO_4^-$**) · 2(H_2O) salt

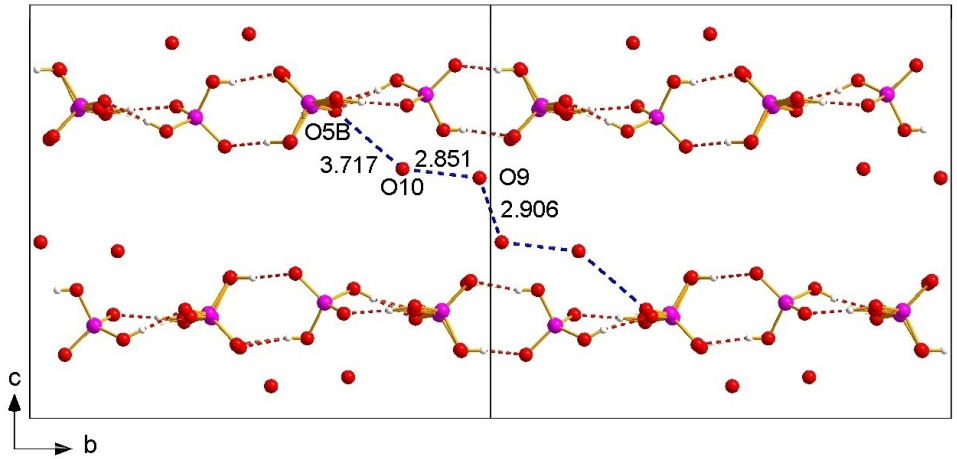

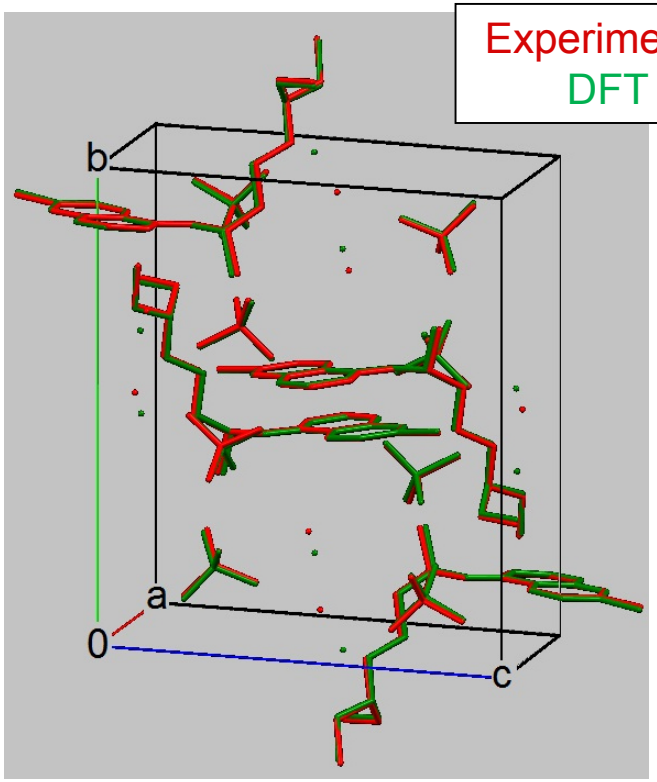

- Bad agreement for the water molecules (shift ≈ 0.8 Å), due to symmetry issues
- Good agreement for the chloroquine and phosphates molecules (RMSD = 0.014)

Water molecules are not significant in determining the intermolecular recognition pattern of CQH_2^{2+}